



U.S. Department  
of Transportation

Federal Railroad  
Administration

# Linear Synchronous Motors For Maglev

National Maglev Initiative  
Washington, DC 20590

Richard D. Thornton  
David Perreault  
Tracy Clark

Massachusetts Institute of Technology  
77 Massachusetts Avenue  
Cambridge, MA 02139

Laboratory for Electromagnetic  
and Electronic Systems

---

DOT/FRA/NMI-92/13

January 1993  
Final Report

This document is available to the  
U.S. public through the National  
Technical Information Service,  
Springfield, Virginia 22161

Technical Report Documentation Page

1. Report No. DOT/FRA/NMI - 92/13	2. Government Accession No. <i>PB93-148559</i>	3. Recipient's Catalog No.
4. Title and Subtitle LINEAR SYNCHRONOUS MOTORS FOR MAGLEV		5. Report Date January 1993
		6. Performing Organization Code
		8. Performing Organization Report No.
7. Author(s) Richard D. Thornton, David Perreault, Tracy Clark		
9. Performing Organization Name and Address Massachusetts Institute of Technology 77 Massachusetts Avenue Cambridge, MA 02139		10. Work Unit No. (TRAIS)
		11. Contract or Grant No. DTFR53-91-C-00070
		13. Type of Report and Period Covered Final Report June, 1991 - January 1993
12. Sponsoring Agency Name and Address U.S. Department of Transportation National Maglev Initiative 400 7th Street, S.W., Room 5106 Washington, D.C. 20590		14. Sponsoring Agency Code 5023
15. Supplementary Notes		
16. Abstract This paper is based in large part on work done in the DOT sponsored study, "Low Cost Linear Synchronous Motor Propulsion for Maglev." The principal objectives are to create a methodology for designing a Linear Synchronous Motor (LSM) with emphasis on new ideas not embodied in existing maglev designs and ideas that contribute to cost reduction. The primary focus is on the propulsion of a high speed vehicle suspended by Electro Dynamic Suspension (EDS), but many of the ideas are applicable to Electro Magnetic Suspension (EMS) designs. We have created models, analytic methods and computation algorithms for predicting performance and estimating cost. There is equal emphasis on simple approximate methods that are suitable for conceptual design studies, and more detailed methods that can be used to refine a design. Also included are descriptions of existing propulsion systems for Maglev and high speed rail because these can be used as a benchmark for comparison with new ideas. There is no attempt to create an "optimum" design because the propulsion system is only a part of a complete maglev system, and many system attributes will affect the LSM design.		
17. Key Words position sensing, maglev, guideways, linear synchronous motor, power electronics electrodynamic suspension, electromagnetic suspension, helical winding, power distribution		18. Distribution Statement Document is available to the U.S. public through the National Technical Information Service, Springfield, VA 22161
19. Security Classif. (of this report) Unclassified	20. Security Classif. (of this page) Unclassified	21. No. of Pages 92
		22. Price

## METRIC/ENGLISH CONVERSION FACTORS

### ENGLISH TO METRIC

#### LENGTH (APPROXIMATE)

1 inch (in.) = 2.5 centimeters (cm)  
 1 foot (ft) = 30 centimeters (cm)  
 1 yard (yd) = 0.9 meter (m)  
 1 mile (mi) = 1.6 kilometers (km)

#### AREA (APPROXIMATE)

1 square inch (sq in, in<sup>2</sup>) = 6.5 square centimeters (cm<sup>2</sup>)  
 1 square foot (sq ft, ft<sup>2</sup>) = 0.09 square meter (m<sup>2</sup>)  
 1 square yard (sq yd, yd<sup>2</sup>) = 0.8 square meter (m<sup>2</sup>)  
 1 square mile (sq mi, mi<sup>2</sup>) = 2.6 square kilometers (km<sup>2</sup>)  
 1 acre = 0.4 hectares (he) = 4,000 square meters (m<sup>2</sup>)

#### MASS - WEIGHT (APPROXIMATE)

1 ounce (oz) = 28 grams (gr)  
 1 pound (lb) = .45 kilogram (kg)  
 1 short ton = 2,000 pounds (lb) = 0.9 tonne (t)

#### VOLUME (APPROXIMATE)

1 teaspoon (tsp) = 5 milliliters (ml)  
 1 tablespoon (tbsp) = 15 milliliters (ml)  
 1 fluid ounce (fl oz) = 30 milliliters (ml)  
 1 cup (c) = 0.24 liter (l)  
 1 pint (pt) = 0.47 liter (l)  
 1 quart (qt) = 0.96 liter (l)  
 1 gallon (gal) = 3.8 liters (l)  
 1 cubic foot (cu ft, ft<sup>3</sup>) = 0.03 cubic meter (m<sup>3</sup>)  
 1 cubic yard (cu yd, yd<sup>3</sup>) = 0.76 cubic meter (m<sup>3</sup>)

#### TEMPERATURE (EXACT)

$$[(x - 32)(5/9)]^{\circ}\text{F} = y^{\circ}\text{C}$$

### METRIC TO ENGLISH

#### LENGTH (APPROXIMATE)

1 millimeter (mm) = 0.04 inch (in)  
 1 centimeter (cm) = 0.4 inch (in)  
 1 meter (m) = 3.3 feet (ft)  
 1 meter (m) = 1.1 yards (yd)  
 1 kilometer (km) = 0.6 mile (mi)

#### AREA (APPROXIMATE)

1 square centimeter (cm<sup>2</sup>) = 0.16 square inch (sq in, in<sup>2</sup>)  
 1 square meter (m<sup>2</sup>) = 1.2 square yards (sq yd, yd<sup>2</sup>)  
 1 square kilometer (km<sup>2</sup>) = 0.4 square mile (sq mi, mi<sup>2</sup>)  
 1 hectare (he) = 10,000 square meters (m<sup>2</sup>) = 2.5 acres

#### MASS - WEIGHT (APPROXIMATE)

1 gram (gr) = 0.036 ounce (oz)  
 1 kilogram (kg) = 2.2 pounds (lb)  
 1 tonne (t) = 1,000 kilograms (kg) = 1.1 short tons

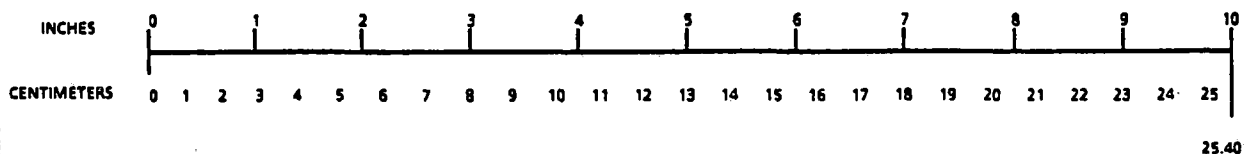
#### VOLUME (APPROXIMATE)

1 milliliter (ml) = 0.03 fluid ounce (fl oz)  
 1 liter (l) = 2.1 pints (pt)  
 1 liter (l) = 1.06 quarts (qt)  
 1 liter (l) = 0.26 gallon (gal)  
 1 cubic meter (m<sup>3</sup>) = 36 cubic feet (cu ft, ft<sup>3</sup>)  
 1 cubic meter (m<sup>3</sup>) = 1.3 cubic yards (cu yd, yd<sup>3</sup>)

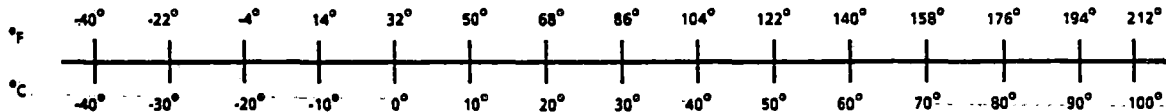
#### TEMPERATURE (EXACT)

$$[(9/5)y + 32]^{\circ}\text{F} = x^{\circ}\text{C}$$

### QUICK INCH-CENTIMETER LENGTH CONVERSION



### QUICK FAHRENHEIT-CELSIUS TEMPERATURE CONVERSION



For more exact and or other conversion factors, see NBS Miscellaneous Publication 286, Units of Weights and Measures. Price \$2.50. SD Catalog No. C13 10286.

## Contents

Contents .....	2
Outline.....	3
1 Maglev Propulsion System Overview.....	5
1.1 Basic concepts .....	5
1.2 Vehicle attributes .....	7
1.3 Motor attributes .....	9
1.4 Block switching.....	15
1.5 Power electronics .....	16
1.6 Power distribution .....	17
1.7 Position sensing and propulsion control .....	18
References and Bibliography .....	20
2 Motor Analysis and Design.....	21
2.1 Motor models and performance characteristics .....	21
2.2 Vehicle field .....	24
2.3 Guideway winding .....	28
2.4 Voltage and current waveforms .....	37
2.5 End effects.....	39
2.6 Helical winding .....	39
References and Bibliography .....	42
3 Electronic Power Conversion.....	43
3.1 Propulsion power requirements .....	43
3.2 Semiconductor power switching devices .....	45
3.3 Passive components .....	49
3.4 Inverter and converter modules.....	51
3.5 Commutation .....	57
3.6 Chopper control.....	60
3.7 Cost analysis .....	61
References and Bibliography .....	64
4 Power Distribution .....	67
4.1 Overview .....	67
4.2 Utility issues.....	68
4.3 Power distribution examples .....	72
4.4 A dc distribution system .....	74
4.5 Cost analysis .....	75
References and Bibliography .....	78
5 Control .....	79
5.1 Overview .....	79
5.2 Position Sensing .....	79
5.3 Observer based control.....	82
References .....	84
6 Far Fields and Shielding .....	85
6.1 Far field analysis .....	85
6.2 End effects.....	88
6.3 Mitigation techniques.....	90
References .....	92

## **Outline**

### **1 Maglev System Overview**

A Linear Synchronous Motor (LSM) is a complex system with many interacting subsystems. This section is an overview of the system requirements for a motor that is suitable for propelling a maglev vehicle. It also describes the key components of a complete propulsion system in anticipation of the more detailed discussions in the remaining sections.

### **2 Motor Analysis**

An active guideway LSM consists of a number of vehicle magnets that create a constant magnetic field, and a guideway winding that creates a traveling magnetic field. The interaction of these two magnetic fields produces the propulsive force. In addition, there must be a means of connecting the electronic inverter to the particular block of the guideway winding that contains the vehicle. This section discusses the analysis and design of all of these components of the motor. The nature of the active guideway linear motor makes the winding inductance an important factor, and methods of minimizing winding inductance are discussed. The "helical winding" is presented as an alternative which shows promise of reducing cost and improving performance.

### **3 Electronic Power Conversion**

The LSM requires high power electronics for converting fixed voltage and fixed frequency power from the utilities to variable voltage and frequency power for exciting the motor windings. It is preferable, though not essential, that the conversion be reversible in order to allow recovery of braking energy. The cost of the power conversion equipment is on the order of 10% of the guideway capital cost, so any design must make cost reduction a major issue. But reliability and fault tolerance are equally important. This section addresses these issues and describes the alternatives that seem most appropriate for maglev applications. A major focus is on methods of estimating and reducing cost.

### **4 Power Distribution**

The power distribution system accepts power from electric utility operated high voltage transmission lines and distributes this power at lower voltages to the electronic power inverters. This section describes both ac and dc power distribution alternatives, including the option of distributing energy that is regenerated from braking vehicles. Among the issues discussed are reliability, flicker, harmonic power generation, and fault

tolerant design. This section also discusses methods of estimating the cost of delivered energy and some of the ownership issues.

## **5 Control**

The control system is a critical part of the LSM because it affects many system attributes, including safety, reliability, fault tolerance, efficiency, and passenger comfort. Control of a synchronous motor depends critically on position sensing, and multiple position sensing schemes are mandatory. This section discusses these issues and describes a novel position sensing scheme that shows promise for high accuracy and reliability and low cost. There is also a discussion of observer based control, the preferred scheme for enhancing performance and improving efficiency.

## **6 Far Fields and Shielding**

The vehicle magnets for an LSM will create magnetic fields that extend significant distances from the vehicle. These remote fields can create a number of problems, particularly for designs with large magnetic gaps and no ferromagnetic path for the flux to follow. This section develops approximate models that provide a good understanding of how the design can be adapted to minimize the impact of the far field and to provide shielding.

## 1 Maglev Propulsion System Overview

A Linear Synchronous Motor (LSM) is a complex system with many interacting subsystems. This section is an overview of the system requirements for a motor that is suitable for propelling a maglev vehicle. It also describes the key components of a complete propulsion system in anticipation of the more detailed discussions in the remaining sections.

### 1.1 Basic concepts

#### Types of linear motors

Two types of linear motors are suitable for maglev propulsion: the Linear Induction Motor (LIM) and the Linear Synchronous Motor (LSM). For each type, multiphase electric power can be supplied in either of two ways: to windings on the guideway, called "active guideway" or "long primary" or "long stator"; or to windings on the vehicle, called "active vehicle" or "short primary" and sometimes called "short stator," but since it isn't stationary, stator is an inappropriate term. The use of the term "primary," analogous to a transformer primary, will be used in this report.

In the case of the LIM, the unpowered portion is called the secondary. It can consist of a conducting sheet by itself or a sheet mounted on the surface of a steel plate. Sometimes the secondary consists of conducting material mounted in slots in laminated steel plates. The primary induces currents in the secondary, and these currents create a magnetic field that reacts with the primary currents to produce thrust.

In the case of the LSM, the unpowered section is called the field and consists of an array of magnets with constant field strength. These magnets can be normal electromagnets, superconducting magnets, or permanent magnets. Unfavorable scaling laws make permanent magnets inappropriate at the power levels required for high speed transportation, but they are suitable for lower power applications. An electromagnetic field can be used if the air gap is modest, but for wide gaps there are fundamental material properties that would necessitate very large power dissipation in the field magnet windings. Virtually all Electro Dynamic Suspension (EDS) and wide gap Electro Magnetic Suspension (EMS) designs use superconducting field magnets and an active guideway linear synchronous motor. Some EMS designs, including the German Transrapid vehicle TR07, use electromagnetic field magnets with the guideway winding embedded in slots in the laminated steel rails of the guideway.

This report is focused exclusively on the long primary LSM with an emphasis on EDS, but with some discussion of EMS issues.

### Existing designs

All versions of Japanese HSST vehicles and German Transrapid TR1 through TR4 used active vehicle LIM propulsion. German TR5 through TR7 and Japanese MLU001 and MLU002 used active guideway LSM propulsion. For an EDS system with the optimal air gap—probably in the range 15 to 150 mm—there is little choice except to use an active-guideway Linear Synchronous Motor. One key problem with alternatives is the lack of a known, reliable way to transfer several megawatts of power to a vehicle moving at a speed of 150 m/s. Additionally, even if such a power transfer scheme were possible it is unlikely that the cost of guideway electrification, on board power conversion equipment, and guideway mounted conductors would be less than the cost of the long primary LSM alternative. A short primary for EDS would require the guideway to have a very massive electromagnetic structure or superconducting coils, and a short primary LIM would be prohibitively heavy and inefficient with a large air gap.

Many designs for both EMS and EDS use the magnets that create lift to also create the reaction field for the LSM. This is true for the original MIT Magneplane, German TR5 through TR7, Japanese MLU001 and MLU002, and for most new U.S. designs being proposed today. If one set of magnets provide both suspension and propulsion fields, then there are usually two motors, which will be designated the port and starboard motors. An exception is the New Magneplane design which uses magnets in the middle of the vehicle for propulsion and separate bogey-mounted magnets for suspension.

### Attributes of a long primary LSM

For an active guideway LSM the currents in the winding are controlled so as to make the vehicle move at the same speed as the traveling field, and hence the term *synchronous* motor. A synchronous motor system includes:

- Windings in the guideway which produce the traveling magnetic field;
- A wayside power distribution system that connects an electronic power inverter to motor windings in a block of guideway in which a vehicle is located;
- Electronic power conversion equipment that converts fixed voltage and frequency utility power into variable voltage, variable frequency power that is applied to the windings;
- A power transmission system that accepts utility generated power and distributes it to electronic power converters located at regular intervals along the guideway;
- A control system that provides the correct current waveforms in the guideway windings according to vehicle force and speed requirements, and also provides various protection and failure monitoring facilities.

### Propulsion differences between EDS and EMS

For an EDS system the magnetic field produced by the vehicle is assumed to be created by superconducting magnets with no iron in the magnetic path. Thus there is virtually no limit to the size of the motor winding, and the area of the conductors can be tailored to the need. For example, acceleration near terminals or climbing a steep grade more than doubles the required force, so the winding size and inverter power ratings could be correspondingly increased. The penalties for too large a winding are a reduced field for the portions of the winding more distant from the field source and a higher cost for the winding.

For an EMS system there is a limited area in the slots of the iron core that carries the magnetic flux. Thus the EMS winding size is fixed and particular attention must be paid to the space limitations on the conductors and their insulation. The winding resistance and inductance are necessarily larger than for EDS, because of the limited area and proximity to high permeability material. The block lengths of the EMS guideway must be reduced to limit the winding resistance and inductance. This creates a requirement for feeder cables and wayside switching components.

Another important difference is the electrical excitation frequency. EMS designs have a shorter pole length and thus a higher frequency. Examples are the Transrapid design with a pole pitch of 0.258 meters and the Grumman Team superconducting EMS design with a pole pitch of 0.6 meters. For comparison, the Japanese EDS design uses a 2 meter pole pitch, the Bechtel Team's US1 design uses a 1 meter pole pitch, and the New Magneplane design uses a 0.75 meter pole pitch. Thus the electrical frequency for EMS can be several times larger than the frequency for EDS. This increases the impact of winding inductance and affects other system design parameters.

### 1.2 Vehicle attributes

In a maglev system people and freight are carried in a vehicle or train of vehicles that are coupled into a single unit that is aerodynamically streamlined. In this paper the term vehicle is used to mean either a single rigid structure or a tightly coupled set of cars that are not intended to be decoupled. For U.S. applications most researchers have assumed that the vehicles will have the size of short haul commercial aircraft and carry between 100 and 200 passengers. The systems being developed in Germany and Japan have focused on designs suitable for longer vehicles that carry 600 to 1000 passengers. The reason for this difference is that most proposals for U.S. maglev envision point-to-point travel with off-line loading or unloading and relatively few stops for a typical trip. Hence the focus of this paper is on smaller vehicles that operate with short headway.

However, the system design should provide the flexibility to allow intermixing various size vehicles. As traffic density increases it may be desirable to allow larger vehicles, so this report discusses methods of upgrading the system to provide increased power for longer vehicles.

We assume a maximum safe operating speed of 150 m/s (336 mph) and a maximum normal operating speed of 125 to 135 m/s (280 to 302 mph). For these speeds we can estimate the vehicle propulsion requirements for different sizes of vehicles for level travel. The following table gives probable values for minimum and maximum size vehicles as well as for TR07 and a hypothetical vehicle, designated X1.

Table 1.1. Typical vehicle attributes.

<i>Parameter</i>		<i>EDS min</i>	<i>EDS max</i>	<i>TR07</i>	<i>X1</i>	<i>units</i>
Vehicle size	length	26	51	51	36	m
	width	3.0	4.1	3.7	4.0	m
	height	4.0	4.1	4.1	4.1	m
	sections	1	3	2	2	
	rows of seats	18	36	36	24	
	coach seats	72	216	180	144	
Vehicle mass	empty	30	60	90	50	tonnes
	loaded	38	82	105	65	tonnes
Prop. magnets	number	2	4	15	3	
	total length	20	40	46	24	m
Air gap	mechanical	50	50	8	50	mm
	magnetic	120	120	8	120	
Aerodyn. drag	@ 135 m/s	18	48	53	28	kN

In Table 1.1 the vehicle dimensions are overall and the aerodynamic drag could vary substantially with details of vehicle shape. The number of passengers for TR07 is reduced 10% from published values for second class seating in order to allow for baggage and be more comparable to values given for the EDS designs. The numerical values are based on ranges of parameters in some of the recently completed System Concept Design Studies.

The motor force for a given motor current is proportional to the length of the magnet assembly which provides the field for the motor. Some vehicle designs, such as the EDS designs proposed by the Japanese, Foster-Miller, and Magneplane teams place the superconducting propulsion field magnets over only about 25% of the vehicle length. Other designs, such as Transrapid and those proposed by the Grumman and Bechtel

Teams, assume the propulsion magnets run nearly the full length of the vehicle. The motor specification must indicate the maximum required force per field magnet.

### 1.3 Motor attributes

The power is specified by the mechanical requirements, but there are possible tradeoffs between voltage, current, number of phases, electrical frequency, and method of winding. This tailoring is constrained by a number of practical realities:

- The motor winding can have almost any number of phases but most practical designs will have between 3 and 6 phases. The number of phases need not be the same everywhere, so more phases might be used where higher acceleration is required. The Transrapid and all Japanese EDS designs use 3 phases, but there are very good reasons to consider the use of more phases for an EDS design.
- The lower limit on motor voltage is determined by the length of the propulsion field magnets, the motor width, and the average magnetic field. In most designs it appears that 1 or 2 turns per "slot" is about all that is practical, and with long vehicles even 1 turn per slot can require phase voltages over 10 kV. Problems of insulation suggest that the instantaneous voltage from a winding to earth ground should not exceed about 15 kV.
- With separate port and starboard motors it is possible to use two inverters, or the windings may be connected in series or parallel so as to use only a single inverter. In some cases it has been proposed to interconnect port and starboard motors so as to provide guidance. For this guidance to work the interconnection must be done on a scale of a few meters, not on the scale of an entire block. In a guideway turn it is necessary to increase the pole pitch on the outside of the turn and decrease the pole pitch on the inside of the turn. This change in pole pitch limits the radius of turn that is acceptable, and poses problems for long vehicles on a short radius turn through a large arc angle.

#### Winding

The guideway has several phases of meander windings, each carrying the same frequency current, but phased such that the winding currents create a traveling magnetic field that moves at the same speed as the vehicle. The winding can have any number of phases, and a simplified winding diagram for a 3-phase motor is shown in Figure 1.1. The wavelength  $\lambda$  is the distance between equivalent points in the periodic magnetic wave, and is equal to twice the pole pitch, which is the distance between successive magnetic poles. The winding width  $w$  is defined to be an effective width that is somewhat longer than the straight section to account for the flux linking the end turns; this part of the winding produces the propulsive force. The three phase currents are  $i_1$ ,  $i_2$  and  $i_3$ ; the control of these currents is the key to controlling the propulsive force for the vehicle.

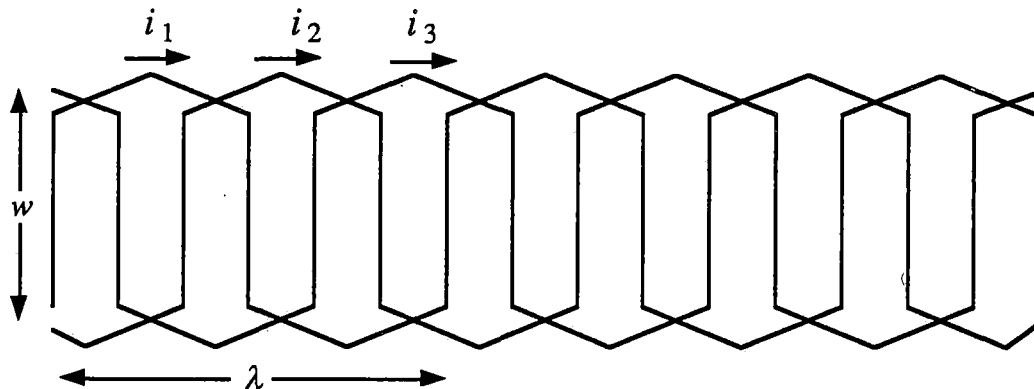


Figure 1.1. Example of a 3-phase guideway winding.

### Waveforms

The current waveforms in Figure 1.2 are indicative of what might be expected. They resemble sine waves but can have substantial harmonic content. For optimum motor efficiency the current waveform should have the same shape as the waveform of the induced voltage in the propulsion winding, and this shape depends on many details of the motor design.

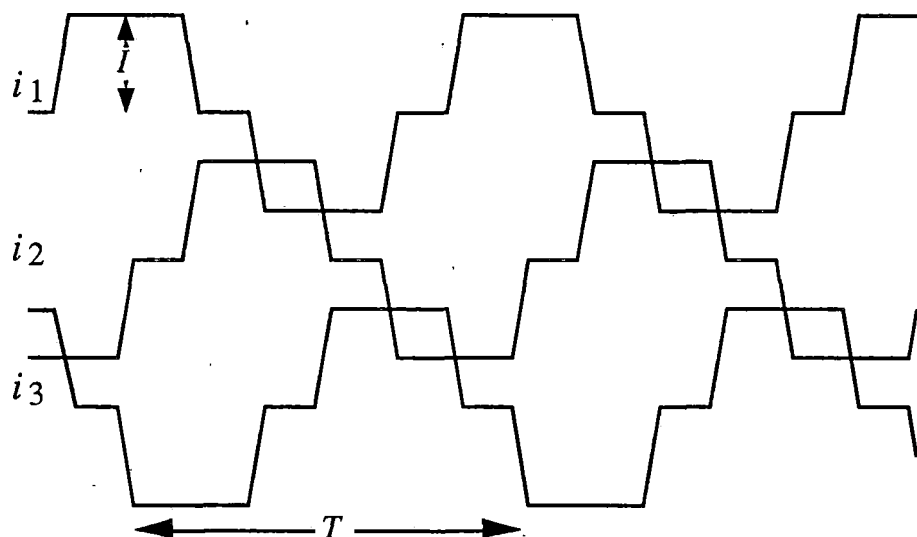


Figure 1.2. Typical currents for excitation of one 3-phase group.

### Acceleration and deceleration

Acceleration is limited by the thrust available from the linear motor, but it is also limited by requirements of providing passenger comfort. For U.S. applications it is expected that major sections of the guideway will follow Interstate Highway Rights of Way, and vehicles will thus be subject to relatively frequent speed changes in order to negotiate turns with acceptable banking angles. This makes it necessary to limit vehicle

acceleration to values that are compatible with passengers standing and walking. There is some debate as to how high this can be, but a value of 0.15 to 0.25 g appears to be acceptable and even higher values have been proposed. Although still higher acceleration is possible with seated and belted passengers, the cost of increasing motor thrust to achieve greater acceleration is almost prohibitive.

Figure 1.3 shows typical acceleration and deceleration for a typical vehicle as a function of the motor thrust. Note that for a wide range of speeds the vehicle drag is on the order of 0.3 to 0.5 g, so quick estimates can be made by assuming the net propulsive force for acceleration is 0.04 g less than the motor thrust.

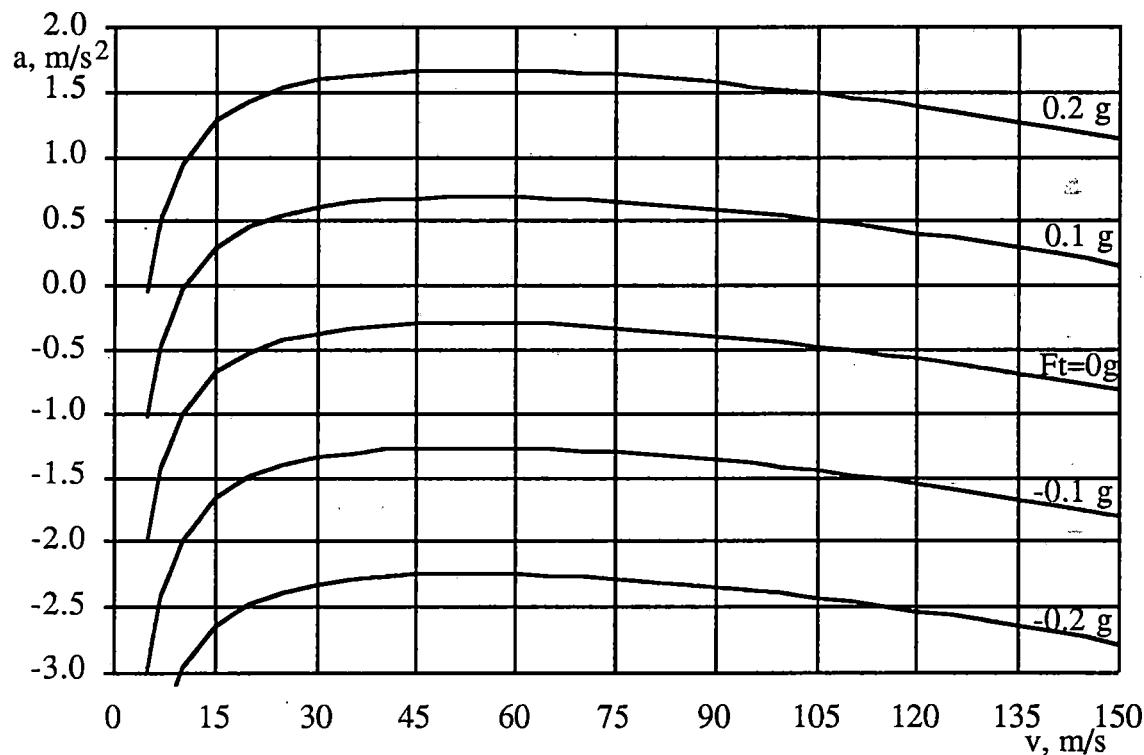


Figure 1.3. Typical acceleration vs. speed for different motor thrusts for EDS.

Under normal conditions the desire to achieve high ride quality imposes both deceleration and acceleration limits, and these limits are usually equal in magnitude. Normal braking can be regenerative with most of the vehicle's kinetic energy being converted to electric power that is made available for propulsion of nearby vehicles or, with some designs, inserted back into the utility grid.

### Normal emergency braking

Normal emergency braking will occur when the vehicle is required to stop unexpectedly because of an unexpected fault condition, but the fault condition is within design limits. For example, if a vehicle switches off of the main line but the switch then fails, all trailing vehicles must slow down more rapidly than normal. Since the headway has been chosen to allow for this type of failure, normal regenerative braking would be employed and the electronic inverter would provide speed control. For this mode the linear motor should be capable of providing at least 0.25 g reverse thrust and, when the aerodynamic and magnetic drag are added, the total deceleration will be on the order of 0.3 g. Where possible the passengers would be given a few seconds warning before being subjected to this level of deceleration, but 0.3 g deceleration is commonly experienced in other travel modes and is assumed to be acceptable where necessary to avoid accidents. For this scenario, and assuming typical aerodynamic and magnetic drag, the vehicle can be stopped in about 3 kilometers.

### Severe emergency braking

For severe and very rare events, such as an unexpected and major earthquake, braking rates in excess of 0.5 g may be desirable. Conventional high speed trains do not have the ability to brake this rapidly, so some system designs do not include fast braking as a feature. However, the use of an active guideway LSM offers "dynamic braking" as an option that should be carefully considered by system designers.

With dynamic braking there are resistors connected across the motor winding so that the voltage generated by the moving vehicle creates current and hence power loss in these resistors. This induced current does not have to flow through the inverter or any power limiting component so very high braking forces are possible. The only limits on braking force are the resistance and inductance of the winding and the mechanical strength of the winding and guideway structural members. This mode can be made fail safe because it does not require active control or a source of power. The power resistors and winding must not overheat during the deceleration, but this is a one time process so there is plenty of time for these components to cool down after the braking event.

A typical plot of dynamic braking force vs. vehicle velocity is shown in Figure 1.4. The shape of the curve is the same for any design, and is given by Equation 1.1.

$$F_{brake} = \frac{a_1 u}{1 + a_2 u^2} \text{ where } u \text{ is the vehicle velocity} \quad (1.1)$$

The value of the force and velocity at the drag peak will depend on design details, such as winding resistance and inductance and the pole pitch. Note that the optimum resistor for

high speed braking is typically greater than 0, so ideally an unexcited block should be shunted with a resistor value chosen to provide minimum stopping distance with no other action by the controller. For a vehicle with typical drag coefficients the stopping distance could be on the order of 2 km with dynamic braking.

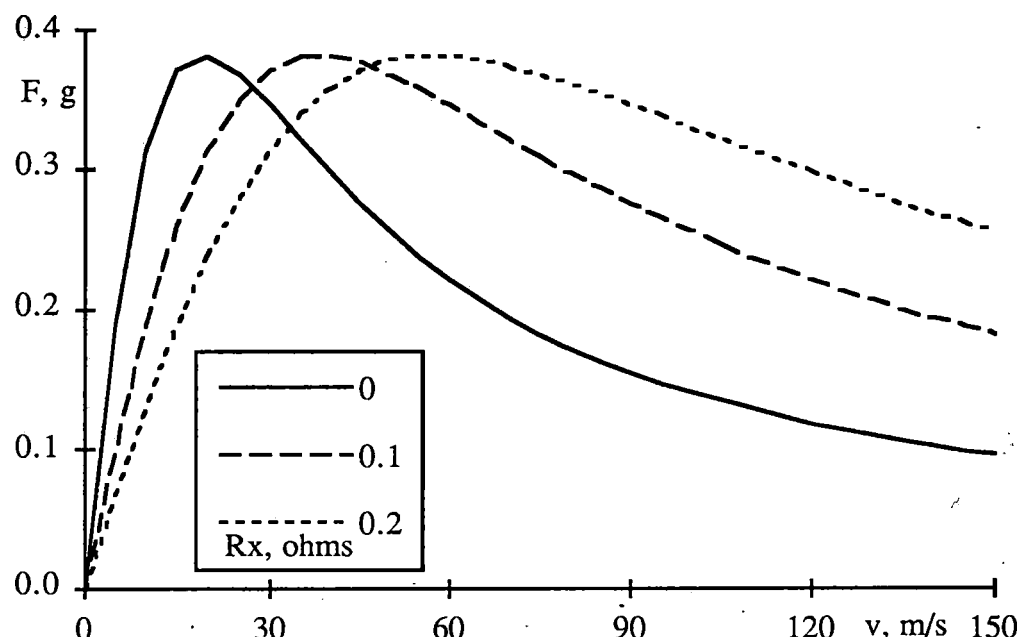


Figure 1.4. Dynamic braking force vs. velocity for different external resistors.

A better scenario is to use a passive resistor until the vehicle slows down somewhat, and then place a short circuit across the winding, and at a still lower speed activate normal regenerative braking. This scenario requires the use of an active control but can reduce the stopping distance to under 2 km and the stopping time to less than 30 seconds for an initial speed of 135 m/s.

An LSM for an EMS system can not achieve enough force for rapid braking, so other mechanisms must be used. In the case of TR07 there are eddy current brakes which induce currents in the solid steel guidance rails. These eddy current brakes are used for all deceleration greater than about  $0.5 \text{ m/s}^2$ . High speed trains have also been fitted with eddy current brakes that induce currents in the rails, and this braking method can be very reliable and not dependent on a friction force. Concerns about rail overheating have impeded the application of rail eddy current brakes, but it has been proven to give faster stopping in all weather conditions.

Some maglev vehicle designs have proposed the use of aerodynamic braking, such as a parachute that would be deployed for fast emergency stops. This braking method

should not be necessary if the dynamic braking option can provide a short enough stopping distance.

The most important issue to reconcile is the possible advantage of rapid braking versus the cost of building a stronger guideway and the risk of a faulty control system producing unnecessary rapid braking. An unnecessary application of dynamic braking could, itself, cause accidents. A cure can be worse than a disease!

### Fault tolerance

For any high speed guided transportation system it is imperative that the system have a high degree of fault tolerance. This means:

- In the event of a minor failure it should be possible to operate almost indefinitely with, at most, some modest reduction in power. Thus the motor might have a multiplicity of phases but be able to operate at nearly full speed and power with one phase disabled.
- More serious failures should be extremely rare, and it should be possible for a person or team of people to effect the repair in a very short time, preferably under 1 hour.
- More common failures that can not be avoided by good design should have redundancy or automatic repair capabilities so that the system can operate at full power in spite of a failure.
- No failure that can be reasonably expected should be allowed to compromise the safety of operation.
- Some components can be expected to fail after several years of service. For these components there should be automatic monitoring to try and anticipate the failure, and replacement should be relatively rapid. For example, the motor winding in the guideway will probably have a shorter life than the concrete portion of the guideway. There is a high probability that there will be precursors to winding failure so scheduled replacement can be done if the design allows sections of winding to be replaced without major disruption of service.

### Redundancy and maintainability

Redundancy is related to fault tolerance, but not all systems with redundancy are fault tolerant, and vice versa. A requirement for redundancy can lead to very high cost. For example, in some cases it has been proposed to have a complete spare inverter that can be automatically substituted for one that fails. This solution is unacceptably expensive and it is almost certainly better to try to find other approaches. For example, if there are separate half-power inverters for port and starboard motors, and if inverters are always installed in pairs for two way travel on adjacent guideways, then a fifth inverter may be all that is needed. In this case the cost is only 25% higher than without redundancy. Even better, if it is economical to have a separate inverter for each phase, then the cost of redundancy may be very low.

## Capability to be upgraded

In spite of the best efforts to design a propulsion system that will meet needs for several years, it is inevitable that at some time in the future it will be necessary to upgrade the system in order to handle changes such as higher capacity, larger vehicles, higher speeds, etc. There should be a plan for dealing with future demands for handling shorter headways and/or longer vehicles.

### 1.4 Block switching

A generic block switching scheme is shown in Figure 1.5. The guideway is divided into zones with one or more inverter modules for each zone and for each direction of travel. The zone is then divided into blocks which are excited in sequence as the vehicle moves down the guideway. Switching devices, either mechanical or solid state, are used to connect the inverter to the appropriate block as the vehicle moves along the guideway. Feeder cables are used to transfer power from an inverter to an active block.

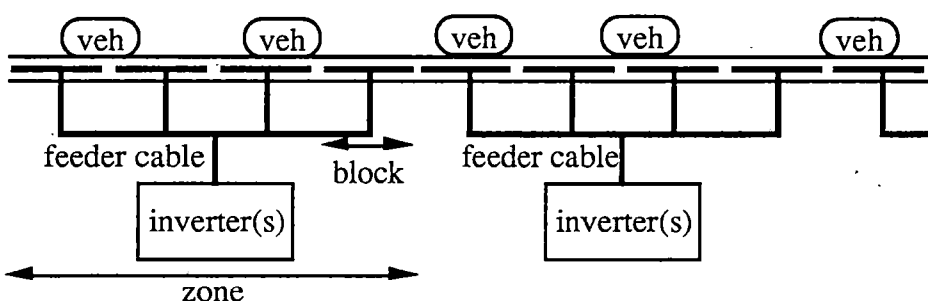


Figure 1.5. Zone control system.

The zone length is determined by the minimum vehicle headway and the assumption that there will be an upper limit to the number of vehicles per zone. The zone is then divided into blocks with the restriction that no more than one vehicle may be in a block at a given time. There must be at least one inverter, or inverter pair in the case of a dual motor system, for each vehicle in a zone at any time.

The block length is determined by a number of factors. For an EMS system the winding resistance and inductance would be excessive for block lengths greater than about 0.5 or 1 km, and this implies the use of several blocks for each zone. For EDS it is possible to use block lengths of 2 to 3 km so one could make the zone length equal to the switching block length. For a high capacity systems this may be a good design, but with today's estimated traffic and for most U.S. locations the headway requirement will be greater than 4 km. Thus the block length is usually less than a full zone, and some sort of block switching is required.

In addition to block switching, there must be some way to effect the gradual transfer of a vehicle from one block to the next. Some designs have used "leap frog" designs in which one inverter powers one block and a different inverter powers the next block. Other designs have used a staggered arrangement in which a port motor is used to transfer the vehicle across a gap in the starboard motor, and vice versa. Whatever the method, it is imperative that ride quality is not degraded by having discontinuities in propulsive force at each block boundary.

The determination of optimum block length is an important system design decision and many factors must be considered. For example, one reason to have short block length is to allow for short vehicle headway distances when the vehicles are operating at reduced speed. There will be occasions when some malfunction or weather condition requires vehicles to proceed at lower than normal speed along a portion of the guideway. If the vehicle spacing is forced to be more than about 2 km, then the guideway capacity will be reduced at speeds below about 100 m/s, and the entire guideway system will be disrupted by a slowdown in a small section of guideway. A preferred mode is to allow reduced speed operation with vehicles spaced as close as 2 km and this can be done by methods that are discussed in Section 5.

## 1.5 Power electronics

Since the propulsion power source must produce a variable voltage at a variable frequency, it is necessary to use power electronic systems to provide the conversion from electric utility power to LSM power. This is done with a combination of a "rectifier" that converts ac power from the utilities to dc power, and then an "inverter" that converts the dc power to the correct voltage, current, and frequency needed for propulsion. Each inverter must be capable of delivering 5 to 50 megawatts. The cost of the power conversion system is likely to be on the order of 10% to 15% of the guideway cost, so careful design is imperative.

In the case of rotary motors it is possible to operate many synchronous motors from the same power source. This is possible because there is usually an induction start mechanism and once the motor reaches synchronous speed there are damper windings that help maintain synchronism in spite of load changes. For maglev systems there are no damper windings that can maintain stability of synchronization. Additionally, the vehicles may be accelerating and decelerating for turns so that two nearby vehicles may require different speeds. Thus we assume there is only one vehicle powered from a single inverter or inverter pair.

The fact that inverters are on the guideway instead of on the vehicle means there is no weight penalty on the inverter design, thus the cost can be lower. Additionally, the vehicle is smaller and lighter so the propulsion requirements are reduced. Since the total number of inverters required for a guideway is roughly equal to the number that would be required if they were on the vehicles, there is a cost advantage in having guideway mounted units. The only significant disadvantage is a reliability requirement that is much more severe for a guideway installation, which must always operate, versus a vehicle installation, which can be taken out of service for repair.

## 1.6 Power distribution

The power distribution will normally have the generic form shown in Figure 1.6. Substations located every 20 to 50 km convert 3-phase, high voltage utility power to lower voltages suitable for distribution. The power distribution can be either dc or 3 phase ac with line to ground voltages in the 15 to 25 kV range. Power is distributed along the guideway to wayside inverters which generate variable voltage, variable frequency power for the LSM. This power system is similar to ones used for conventional electrified rail and does not pose any problems that have not been addressed in that context.

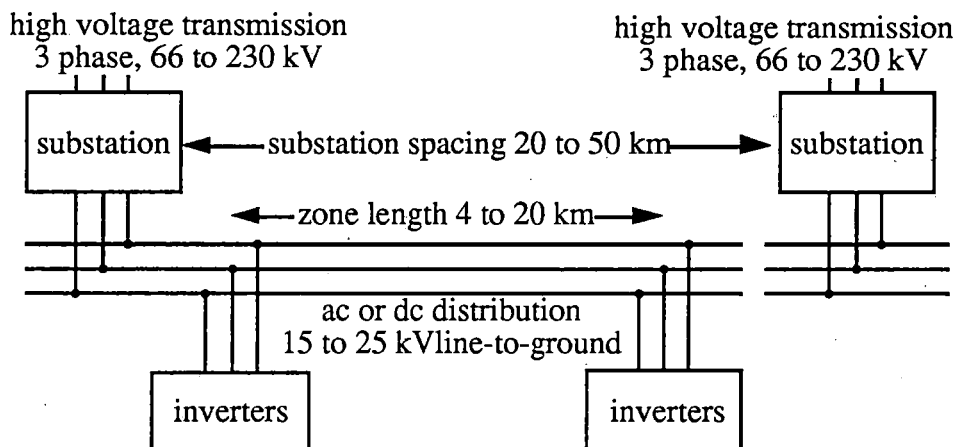


Figure 1.6. Generic power distribution system.

The choice of transmission line voltage is based on availability and power requirements. Lower transmission voltages are preferable because they lead to lower cost substations. Transmission voltages less than 66 kV will not normally have enough capacity for a high speed maglev system, and even 66 kV systems may be inadequate for reasons to be discussed. Voltages over 230 kV will lead to very high substation cost and should be avoided unless the maglev substation can share facilities with other power users.

The choice of distribution voltage is based on power levels and distribution distances. Most high speed rail systems use 25 kV, the exception being the German ICE

which uses 15 kV. The German Transrapid maglev design is based on a 20 kV, 3 phase distribution system that is common in Germany. Studies have also arrived at line to ground voltages in the 15 to 25 kV range as the best choice for U.S. maglev.

The substations contain transformers and equipment for protection and control. For dc distribution the substations also include a rectifier. There are options as to whether regenerated power can be fed back into the transmission line system and whether there is a voltage control capability for the distribution circuit.

The required power levels depend upon speed, vehicle size and headway distances. As an example, if the vehicles can operate with headways as short as 5 km and each vehicle carries 144 people and requires 7 MW average power, then a 2-way system will require 2.8 MW per km (i.e.  $2 \times (7 \text{ MW} / 5 \text{ km})$ ). A simpler way to estimate power requirements is in terms of guideway capacity. A fully loaded maglev vehicle averaging 125 m/s will require about 100 Wh per passenger km. If the guideway capacity is 12,000 passengers per hour, then the power demand is  $100 \times 12,000 = 1.2 \text{ MW}$  per km for each direction of travel, or 2.4 MW/km for a dual guideway. Note that this calculation is independent of vehicle size and indicates that power system cost is more closely related to guideway capacity than to any other design parameter.

Assuming an average demand of 2.5 MW/km and a substation spacing of 30 km, at times of maximum demand the average power per substation is 75 MW. Because of statistical fluctuations in headway and power levels, the maximum power averaged over several minutes will probably be less than this value, but the instantaneous peak power will be significantly larger. Because power consumption depends strongly on speed, at times of maximum demand it is possible to reduce the system speed somewhat, thus decreasing maximum demand. This type of power consumption management could easily reduce average demand to about 2 MW/km.

## 1.7 Position sensing and propulsion control

It is not possible to simply excite the guideway with the desired electrical frequency and hope that the vehicle stays in synchronism with the traveling field. The vehicle must be maintained in synchronism by electronic feedback control. The method used in all existing maglev designs is to sense vehicle position relative to the traveling field, and vary the winding current to maintain the desired relative vehicle position. There are several means to determine vehicle position and following is a partial list of proposed schemes.

- The vehicle carries an electronically readable "tag" that is read by a guideway detector every time the vehicle enters a new zone or block. This type of block sensing is almost mandatory and is a part of most proposed designs.

- A special signal can be superimposed on the motor winding by the vehicle, and the inverter controller can then sense the relative position of the vehicle within a one wavelength span of the LSM. This short distance sensor is then combined with a cycle counter to locate the vehicle within a block. This type of sensing can be so accurate that the sensor can detect perturbations in guideway uniformity.
- The motion of the vehicle causes voltage to be induced in the winding, and this voltage can be used to identify vehicle position quite accurately once the vehicle reaches some threshold speed.
- The vehicle can detect some suitable guideway signal to determine position, and this information can be "radioed" back to ground controllers.

Most designs use a combination of these four sensor types to provide continuous and fault tolerant monitoring of the exact vehicle position. With knowledge of the exact vehicle position, the controller supplies the correct voltage and current waveforms to follow the desired velocity profile while also satisfying some other criteria. In some designs, such as TR07, the other criteria is the optimization of motor efficiency. In other designs, such as the Magneplane, the LSM is used to help control ride quality by virtue of lateral and vertical forces. In this case the controller will sacrifice efficiency as necessary in order to provide this control of ride quality.

The control system must also monitor the behavior of the vehicle with an intent to identify component degradation or malfunction. Parameters such as winding resistance, winding irregularities, power distribution voltages, and vehicle drag can be monitored in order to help achieve this objective. The vehicle can also monitor it's own acceleration and velocity in all directions, and send this information back to the zone controller to help monitor guideway parameters.

## References and Bibliography

### Books

- 1 Rhodes, R. G. & Mulhall, B. E., *Magnetic Levitation for Rail Transport*, Clarendon Press, Oxford, 1981.
- 2 Heinrich, Klaus & Kretzschmar, Rolf, Editors, *Transrapid Maglev System*, Hestra-Verlag Darmstadt, 1989 (ISBN 3-7771-0209-1).

### Special reports

- 3 Atherton, David L., Ed., *Study of Magnetic Levitation and Linear Synchronous Motor Propulsion*, Canadian Institute of Guided Ground Transport, Queens University, Kingston, Ontario, Annual Report for 1972.
- 4 The Maglev Technology Advisory Committee, *Benefits of Magnetically Levitated High-Speed Transportation for the United States, Volume 2 - Technical Report*, prepared for the U.S. Senate Committee on Environment and Public Works, March 1992.

### Papers

- 5 Powell, J. R. & Danby, G. T., "High speed transport by magnetically suspended trains," presented at the ASME Winter Meeting, N.Y., Tech. Rep. 66-WA/RR-5, Nov. 1966.
- 6 Kolm, H. H., & Thornton, R. D., "The magneplane: guided electromagnetic flight," *Proceedings of the 1972 Applied Superconductivity Conference*, May 1-3, 1972.
- 7 Danby, G. & Powell, J., "Integrated systems for magnetic suspension and propulsion of vehicles," pp. 120-126, *Proceedings of the 1972 Applied Superconductivity Conference*, May 1-3, 1972.
- 8 Powell, J. R. & Danby, G. T., "The linear synchronous motor and high speed ground transport," presented at the 6th Intersoc. Energy Conversion Engineering Conf., Boston, Mass., 1971.
- 8 Thornton, R. D., "Flying Low with Maglev," *IEEE Spectrum*, pp. 47-54, April 1973.
- 9 Kolm, H. H., & Thornton, R. D., "Electromagnetic flight," *Scientific American*, Vol. 229, No. 4, pp. 17-25, October 1973.
- 10 Slemon, G. R., Turton, R. A., Burke, P. E., & Dewan, S. B., "Analysis and Control of a Linear Synchronous Motor for High-Speed Ground Transport," *Linear Electric Machines*, Proceedings of Conference at London, England, Oct. 21-23, 1974, pp. 143-148.
- 11 Thornton, R. D., "The Magneplane Linear Synchronous Motor Propulsion System" *Linear Electric Machines*, Proceedings of Conference at London, England, Oct. 21-23, 1974, pp. 230-235.

## 2 Motor Analysis and Design

An active guideway LSM consists of a number of vehicle magnets that create a constant magnetic field, and a guideway winding that creates a traveling magnetic field. The interaction of these two magnetic fields produces the propulsive force. In addition, there must be a means of connecting the electronic inverter to the particular block of the guideway winding that contains the vehicle. This section discusses the analysis and design of these components of the motor. The nature of the active guideway linear motor makes the winding inductance an important factor, and methods of minimizing winding inductance are discussed. The "helical winding" is presented as an alternative which shows promise of reducing cost and improving performance.

### 2.1 Motor models and performance characteristics

#### DC model

The combination of motor and electronic inverter can be thought of as a dc motor that can be modeled as shown in Figure 2.1. This simplified dc motor model consists of a winding resistance  $R_w$  and an electromechanical transducer that is modeled as two dependent sources,  $F_e$  and  $v_m$ . The force is modeled by dependent current source  $F_e$ , which is proportional to the motor current, and the induced voltage is modeled by dependent voltage source  $v_m$ , which is proportional to vehicle velocity. This transducer is lossless and represents the transfer of electric power to mechanical power and vice versa. The load is modeled as a set of three current sources representing the drag. The values of the current sources have the following velocity dependence: aerodynamic power loss varies as the cube of the speed so it is represented by a current proportional to the square of velocity; suspension related drag is modeled by a constant power term so the current is inversely proportional to velocity; and the eddy current losses vary as the square of the speed so the current is proportional to the speed. Although it is not usually possible to identify voltages and currents directly related to the model quantities, the model is very useful in portraying the major motor performance limitations.

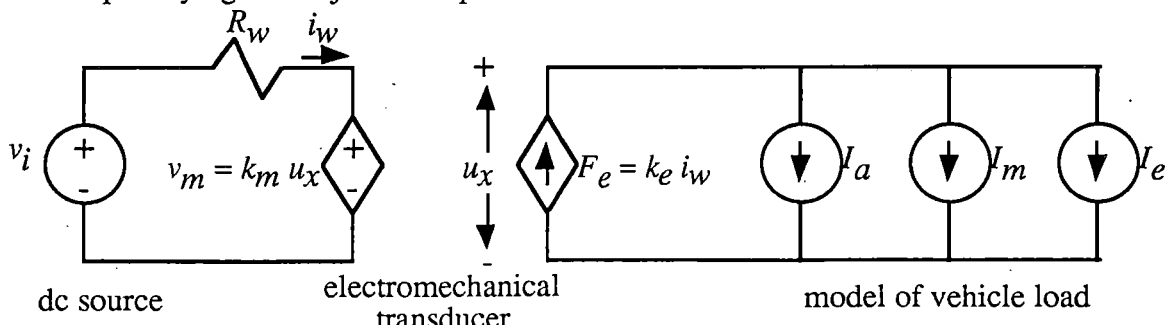


Figure 2.1. DC motor model.

The dc model leads to the generic representation of the motor characteristics shown in Figure 2.2. This plot is a superposition of force vs. velocity and current vs. voltage with the model parameter  $k_e$  and  $k_m$  used to scale the two plots so that they overlap. It is then possible to show mechanical attributes, such as force vs. velocity for level travel, superimposed on a plot that shows the required motor output voltage and current implied by the force and velocity. Note that the maximum available voltage and the voltage drop in the motor winding resistance limit the thrust at any given speed. The model of Figure 2.2 does not include loss in the inverter or power distribution system.

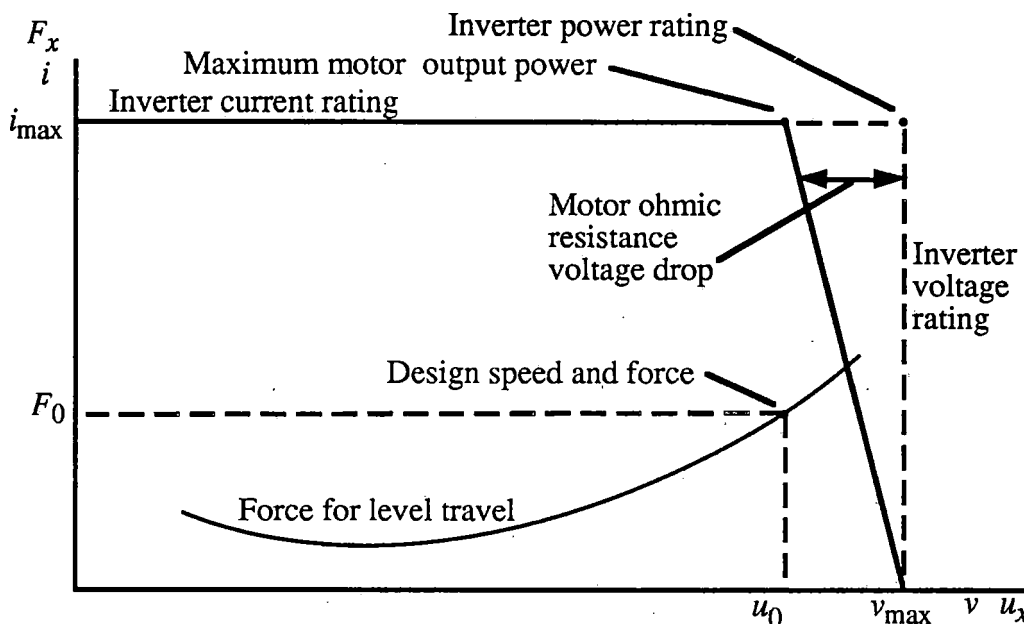


Figure 2.2. Generic representation of motor performance based on dc circuit model.

The generic motor characteristics depicted in Figure 2.2 can be converted to specific performance attributes, such as the curves shown in Figure 2.3. This Figure shows the thrust limit and speed limit as horizontal and vertical lines. For this example the maximum motor power output is 15.9 MW and the maximum inverter power output is 20.5 MW. The contours of constant acceleration of 0 and 0.1 g are shown superimposed on this plot, and the nominal cruise power of 6.05 MW is the intersection of 0 g acceleration and 135 m/s velocity. The curve of constant motor power output is shown as a hyperbola and in some designs there may be a power limit in addition to voltage and current limits. The voltage and current scales are not shown since they will depend on the details of motor design. As an example, if the motor requires 20 amps per kN of thrust, then conservation of power demands that there be 50 volts per m/s of velocity for the motor back voltage.

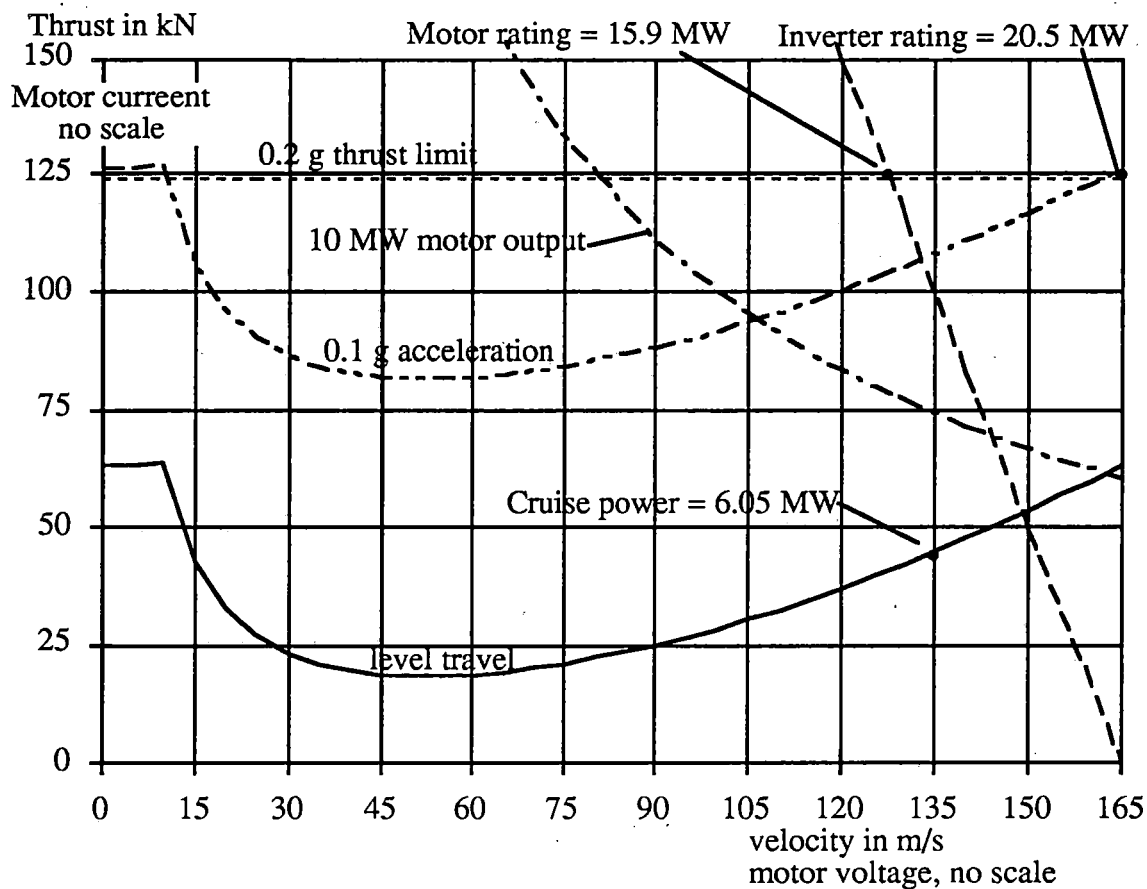


Figure 2.3. Performance requirements for an typical design.

An inverter may have only voltage and current limits, but in some cases it may be necessary to impose power output limits as well. For example:

- If the inverter is powered from a utility transformer or drives an output transformer, the rating of the transformer may be less than the peak Volt-Amp output for the inverter.
- In case of a failure in a utility substation, if there are many vehicles in operation it may be necessary to impose power limits on all vehicles traveling in a given area.
- The commutation circuitry for the power switches may create lower current limits at high voltage, and thereby provide the equivalent of a power limit.

Figure 2.3 shows the effect of a 10 MW limit; note that this 50% reduction in maximum motor output power does not limit top speed, but it does limit acceleration at higher speeds.

### AC model

The dc model shown in Figure 2.1 is a good representation of how the motor performs, but in order to design an inverter we need a more complete ac model. For EDS designs the lack of steel makes a linear model suitable for virtually all analysis. Even for an EMS design it may be possible to use a linear model because of the large air gap. A simple linear model is shown in Figure 2.4.

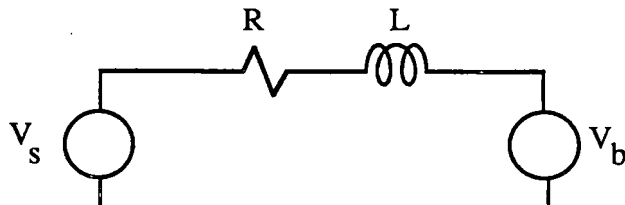


Figure 2.4. Single line circuit model for LSM.

$V_s$  is a multiphase source,  $\mathbf{R}$  represents the winding resistance matrix,  $\mathbf{L}$  is an inductance matrix, and  $\mathbf{V}_b$  is the back voltage produced by the interaction with the vehicle magnets. Just as with the dc model, the force is proportional to the motor current and the back voltage is proportional to the vehicle speed. Here each winding has the same resistance,  $R_w$ , and the inductances are described by an inductance matrix. For example, the winding impedance of a three phase winding is described by

$$\begin{aligned} \mathbf{Z} = \mathbf{R} + s\mathbf{L} &= \begin{bmatrix} R_w & & \\ & R_w & \\ & & R_w \end{bmatrix} + s \begin{bmatrix} L_s & L_m & -L_m \\ L_m & L_s & L_m \\ -L_m & L_m & L_s \end{bmatrix} \\ \mathbf{I} &= [I_1 \quad I_2 \quad I_3]^T \\ \mathbf{V}_b &= [V_{b1} \quad V_{b2} \quad V_{b3}]^T \end{aligned} \quad (2.1)$$

where  $R_w$  is the resistance of each phase,  $L_s$  is the self inductance of each phase, and  $L_m$  is the mutual inductance between adjacent phases. The calculation of  $\mathbf{R}$  and  $\mathbf{L}$  are considered later.

## 2.2 Vehicle field

### Field calculations

The magnetic field produced in the plane of the motor windings by the superconducting vehicle magnets can be calculated by using the Biot-Savart Law, Equation 2.2. To compute the field produced by a loop we integrate Equation 2.2 around the loop.

$$d\mathbf{H} = \frac{1}{4\pi} \frac{\hat{s} \times \hat{r}}{r^2} I \, ds \quad (2.2)$$

where  $\hat{s}$  and  $\hat{r}$  are unit vectors in the  $s$  and  $r$  directions.

If the loop is composed of straight sections, then we start by integrating Equation 2.2 over the length of a straight section of conductor, as modeled in Figure 2.5. The result is shown in Equation 2.3.

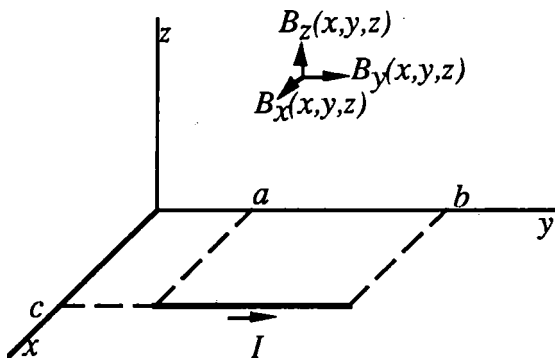


Figure 2.5. Model for field contribution due to a straight current element.

$$\begin{aligned}
 B_x &= \frac{\mu_0 I}{4\pi} \frac{z}{d^2} \left( \frac{(y-a)}{\sqrt{(y-a)^2 + d^2}} - \frac{(y-b)}{\sqrt{(y-b)^2 + d^2}} \right) \\
 B_y &= 0 \\
 B_z &= \frac{\mu_0 I}{4\pi} \frac{x-c}{d^2} \left( \frac{(y-a)}{\sqrt{(y-a)^2 + d^2}} - \frac{(y-b)}{\sqrt{(y-b)^2 + d^2}} \right)
 \end{aligned} \tag{2.3}$$

where  $d^2 = (x-c)^2 + z^2$

The motor field magnets, located on the vehicle, are modeled as a linear array of rectangular coils as shown in Figure 2.6. We compute  $\mathbf{B}(x, y, z)$  by summing the contributions of all coils.

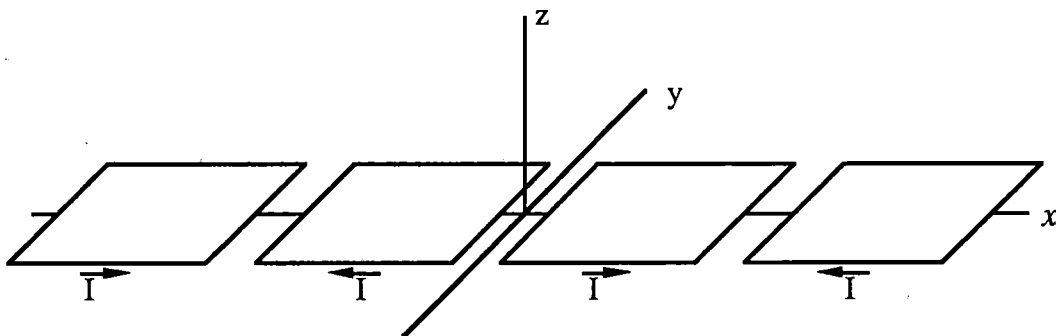


Figure 2.6. Model of vehicle magnet for field calculation.

### Field calculation example

In order to illustrate the calculation and interpretation of the field produced by the vehicle magnets, consider an example with the parameters given in Table 2.1. The pole pitch is chosen as 1 meter not only because this is a practical value, but also because it facilitates scaling to estimate the field for other dimensions. For example, if all dimensions are multiplied by  $k_d$  and all currents are multiplied by  $k_i$ , then all values of  $\mathbf{B}$  are multiplied by  $k_i/k_d$ .

**Table 2.1.** Typical coil parameters for vehicle magnets.

Pole pitch	$p$	1.0 m
Length	$l_c$	0.8 m
Width	$w_c$	0.8 m
Current	$I_f$	500,000 A-turns

In practice the coil conductors will occupy a finite volume and the coil dimensions are assumed to be an average of all the turns in the actual coil. For simplicity, the coils are assumed to be square with dimension 80% of the pole pitch. The choice of 80% is consistent with practical designs and has the added benefit of eliminating the fifth harmonic component of back voltage, for reasons that will be discussed. The same methodology will work with other coil shapes, and the conclusions are similar. In typical designs the distance between the planes of the vehicle coils and the LSM windings is on the order of 20% of the pole pitch, so for this example we assume  $h = 0.2$  m. The resulting components of the magnetic field are shown in the three 3 dimensional plots of Figures 2.7-8.

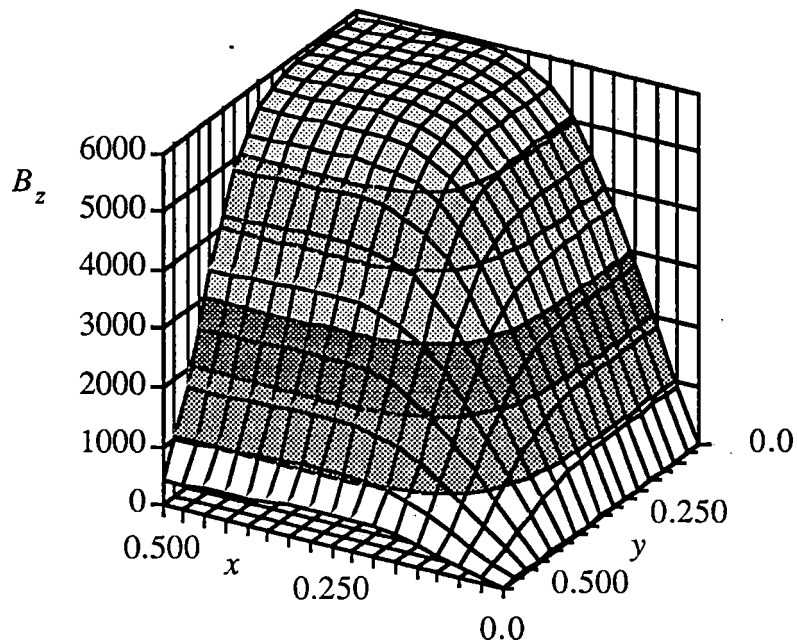
**Figure 2.7.**  $B_z$  produced by vehicle coils with parameters given by Table 2.1.

Figure 2.7 is a plot of  $B_z$  for a quarter section of one pole of an infinitely long array of vehicle coils and for a separation between coils and windings of  $h = 0.2$  meters.  $B_z$  is the only field component that produces a net propulsive force. Unless  $h$  is exceptionally small, the  $z$  component can be approximated as:

$$B_z = B_{z0} \sin(\pi x / p) \cos(4\pi y / (w + h)) e^{-k_z \pi z / p} \quad (2.4)$$

$|y| < (w + h) / 2, z < p / 2$

The parameter  $k_z$  is an empirical, dimensionless constant to account for the fact that the field falls off more rapidly than it would if the coil width were infinite; a typical value is  $k_z = 1.25$ . This approximation neglects higher space harmonic terms so, for more precise analysis, the third and, possibly, fifth harmonics should be added. Note that the presence of a significant third harmonic term is not necessarily undesirable because it can reduce the peak motor voltage while simultaneously contributing additional thrust.

There can also be guidance forces produced by  $B_z$  if the vehicle is not centered over the windings. The longitudinal component of the LSM windings, i.e. the "end turns," produce these guidance forces and they are usually small because the end turns are usually located in regions where  $B_z$  is small. But currents in a "helical" winding, which will be discussed later, can interact with  $B_z$  to produce strong guidance forces. Alternatively, the propulsion windings can be specifically designed to provide for guidance forces.

The  $x$  and  $y$  components of  $\mathbf{B}$  are also important, and are shown in Figure 2.8 for direct comparison with  $B_z$  in Figure 2.7.

$B_x$  can not produce a net propulsive force, but it can produce lift forces by interaction with the  $y$ -directed sections of the LSM winding.  $B_y$  can not produce a net propulsive force, but it can produce lift forces by interaction with the  $x$  directed sections of the LSM winding.  $B_x$  and  $B_y$  are important if the linear motor is being used for heave damping as well as for propulsion.

$B_x$  is produced only by the transverse components of the vehicle coils and  $B_y$  is produced only by the longitudinal components of the coils. These fields can be estimated using Equation 2.5, the field near a long, current carrying wire.

$$B = \pm \frac{\mu_0 I_f}{2\pi r},$$

$r$  is distance to current element,  $x$  not near the wire end; (2.5)

e.g. if  $I = 500,000\text{A}$ ,  $z = 0.2\text{ m}$ , then  $B = \pm 0.5\text{ Tesla} = \pm 5,000\text{ gauss}$ .

The end turns of the winding can be located in the region where  $B_y$  is large, so by proper choice of the LSM winding currents a strong vertical force can be produced.

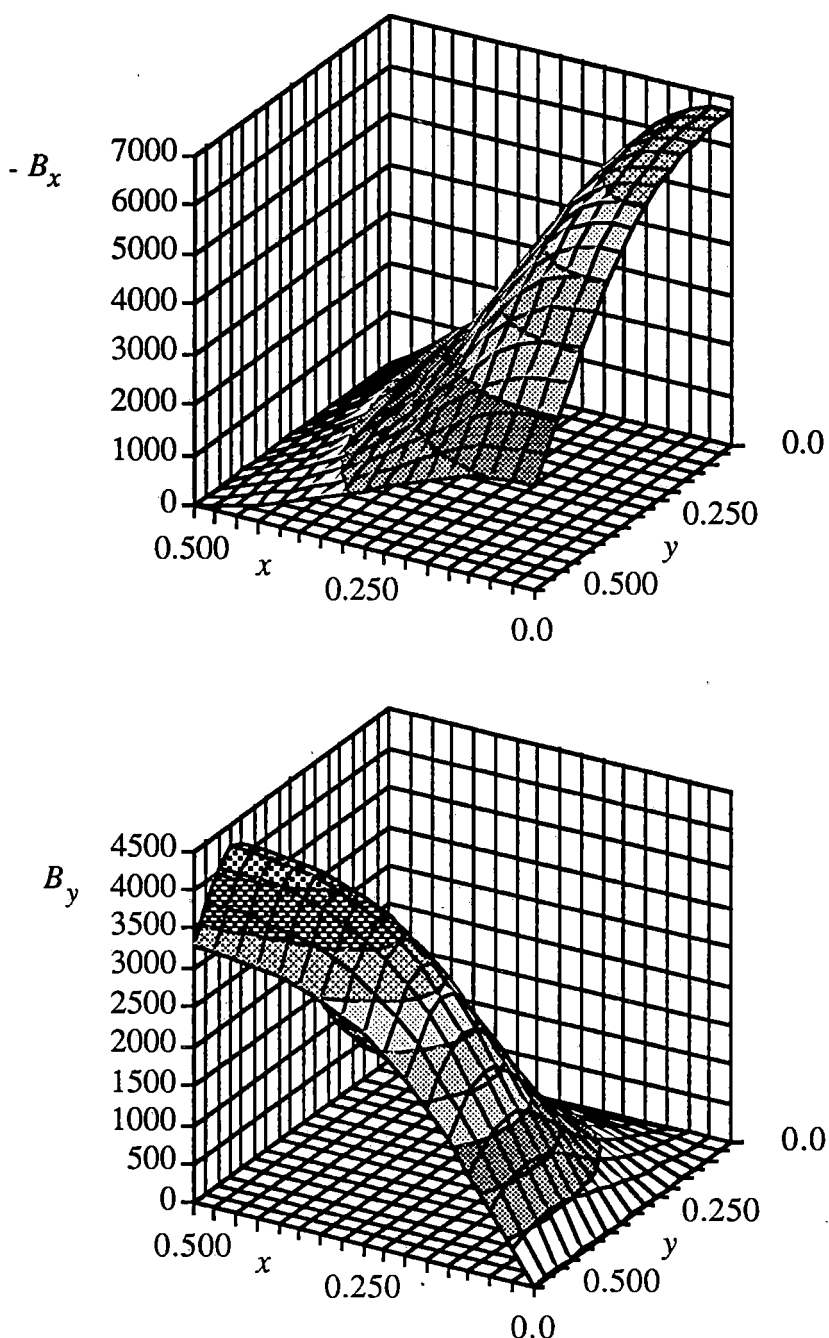


Figure 2.8.  $-B_x$  and  $B_y$  for same vehicle parameters as Figure 2.7.

### 2.3 Guideway winding

#### Design example

In order to illustrate the operation of an LSM, consider a particular example. The motor winding is assumed to have rectangular shape with simple end turns as shown in

Figure 2.9. The vehicle field is assumed to be as given in Figures 2.7-8 and the winding parameters are given in Table 2.2.

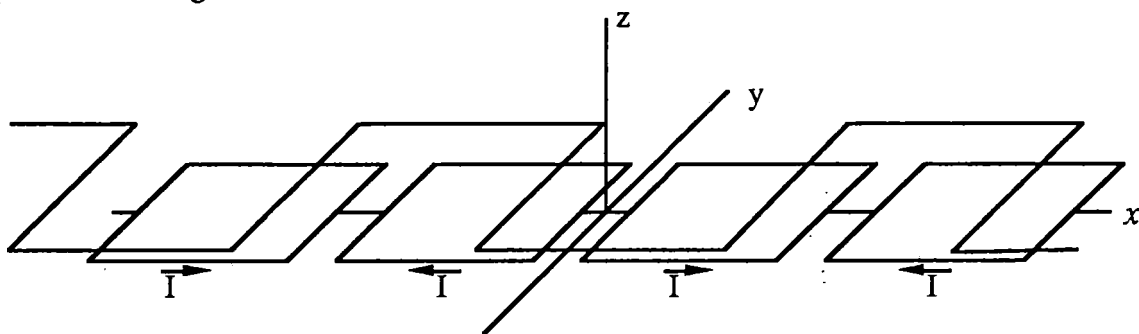


Figure 2.9. Model for computing motor voltage.

Table 2.2. Dimensions for LSM example.

Pole pitch	$p$	1.0 m
Winding width	$w_w$	1.0 m
Number of phases	$n_p$	6
Winding cross section area	$A_w$	400 mm <sup>2</sup>
Winding block length	$l_b$	2000 m

These parameters lead to field plots for different heights as shown in Figure 2.10 for the centerline,  $y = 0$ .

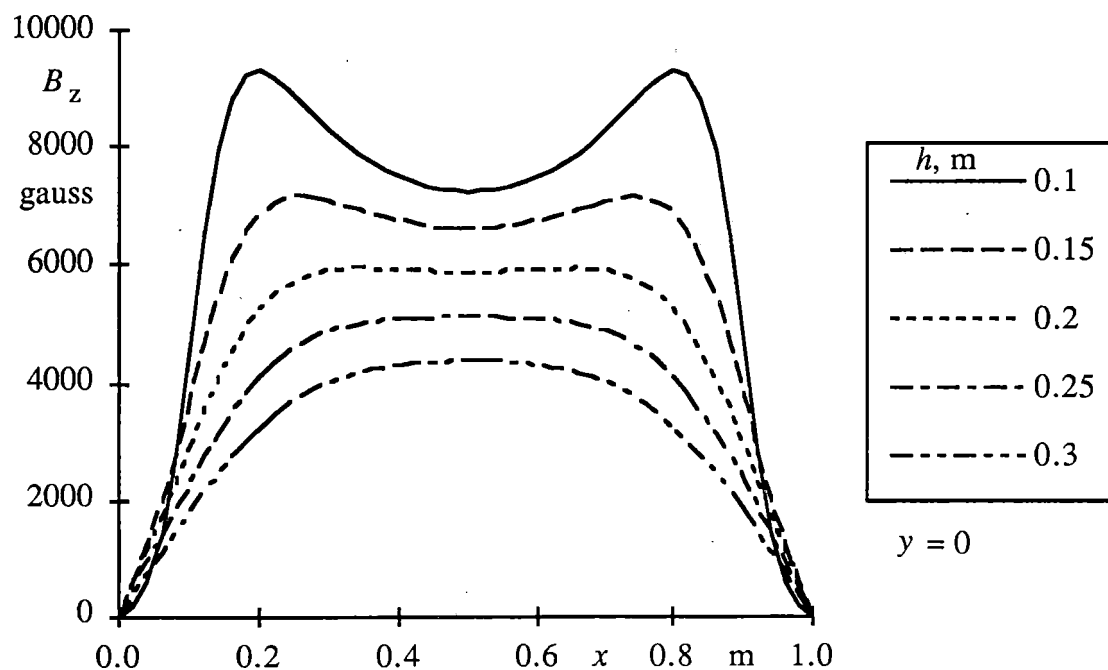


Figure 2.10.  $B_z$  vs.  $x$  for different  $h$  and  $y = 0$ .

If we use eight vehicle coils and compute the field in the center region there will be negligible difference from the field for an infinite array as long as the height  $h$  is less than about one half the coil width. In a later section, we consider the far field and the end effect.

The voltage waveform can be computed by determining the average value of  $B_z$  over the length of the transverse winding section and at a sequence of  $x$  values. The resulting plot is the shape of the voltage waveform. For the example the result is a waveform with a shape that depends on the height as shown in Figure 2.11.

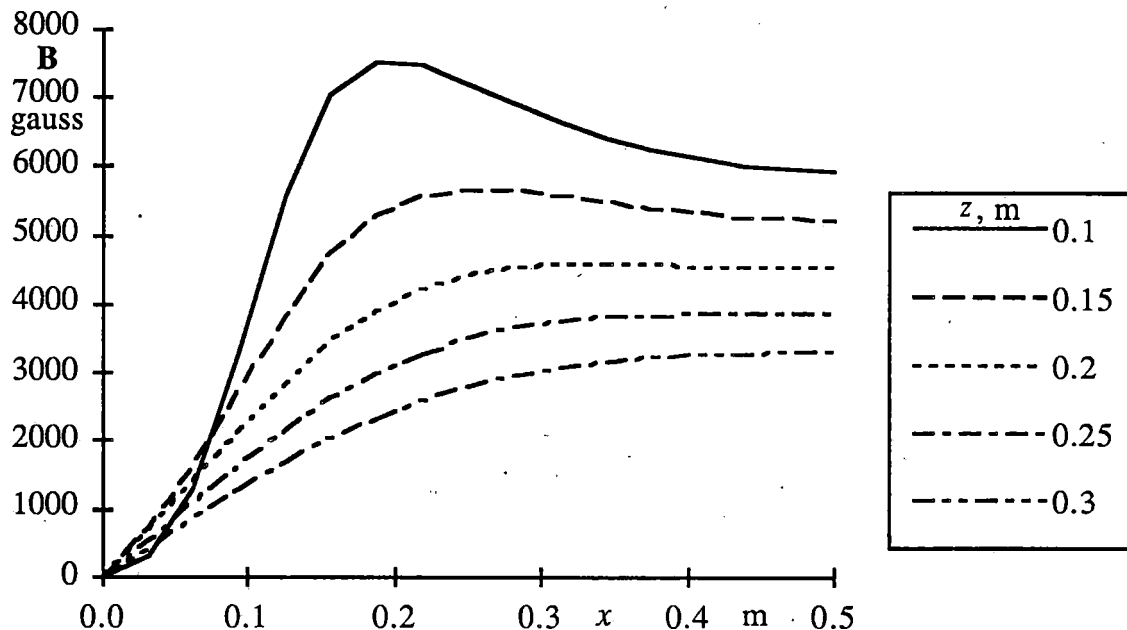


Figure 2.11. Average flux per pole for rectangular winding and for different heights.

A good way to analyze the motor voltage is by performing a harmonic analysis and representing the average field in the plane of the winding as a Fourier expansion in  $x$  and  $z$ . If the winding is long in the  $y$  direction, then the Fourier series can be approximated by Equation 2.6.

$$B_a(x, z) = \sum_{n=1,3,\dots} B_{an} e^{-k_n \pi n z / p} \sin(\pi n x / p)$$

$B_a$  is  $B_z$  averaged over the width of the winding (2.6)

$k_n$  are empirical constants with values  $> 1$

We can use this as an analytic approximation with  $k_{zn}$  adjusted to fit the data. Figure 2.12 shows a comparison of the computed harmonics with Fourier coefficients chosen to give a best fit to the computed data. The resulting  $B_{an}$  and  $k_n$  are given in Table 2.3.

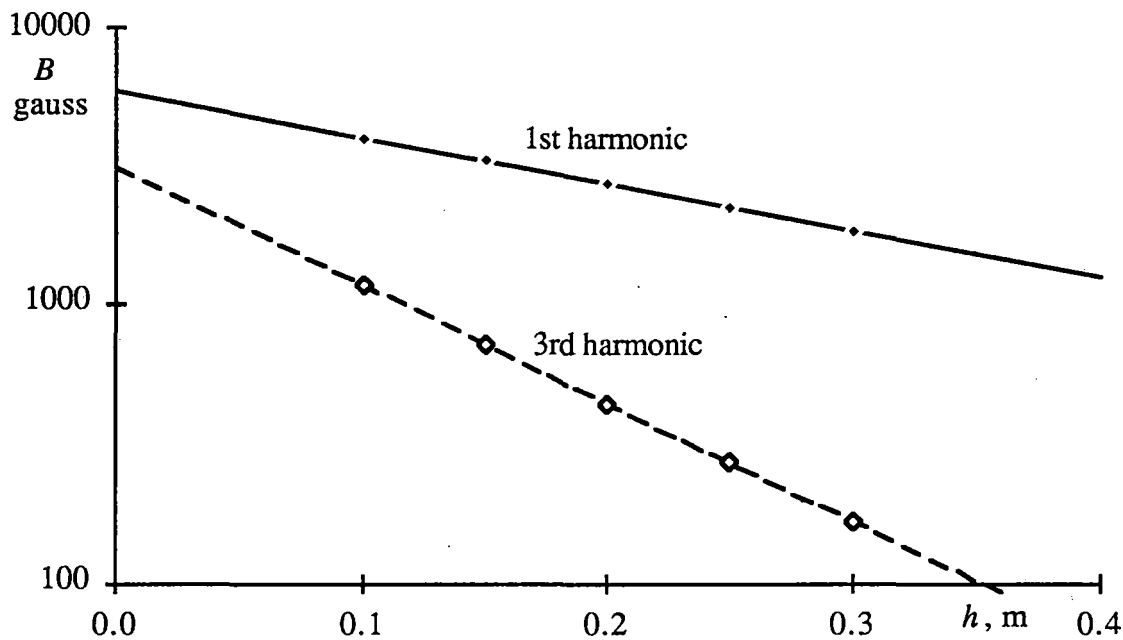


**Figure 2.12.** Amplitude of harmonics of  $B_a$  as a function of height. The straight lines are approximations from Equation 2.7 and the marks are calculated.

For this example the average flux can be modeled using the Fourier terms given in Table 2.3. The 5<sup>th</sup> harmonic is exactly 0 because the coil length was assumed to be  $0.8p$ . We could have chosen a coil length of  $2p/3$  to eliminate the third harmonic, but this would lead to less propulsive force. The 7<sup>th</sup> harmonic is less than 1.3 % for  $h > 0.2$  m.

**Table 2.3.** Fourier coefficients for approximations of Figure 2.10

$n$	$B_{an}$	$k_n$
1	5884	1.25
3	3065	1.03
5	0	...

The Fourier model fits extremely well and allows accurate analysis with minimum computational effort. For heights greater than about 20% of the pole pitch the only important harmonics are the first and third. With  $h = 0.2p$  the third harmonic is 16% of the fundamental.

### Three phase windings

A simplified drawing of a 3 phase winding is shown in Figure 2.13. The wavelength  $\lambda$  is the distance between successive peaks in the magnetic wave. It is also twice the pole pitch, which is the distance between successive magnetic poles. The winding width  $w$  is defined to be an effective width that is somewhat longer than the straight section to account for the flux linking the end turns; this part of the winding produces the propulsive force. The three phase currents are  $i_1$ ,  $i_2$  and  $i_3$ . The control of these currents is the key to controlling the vehicle, and is considered in Section 5.

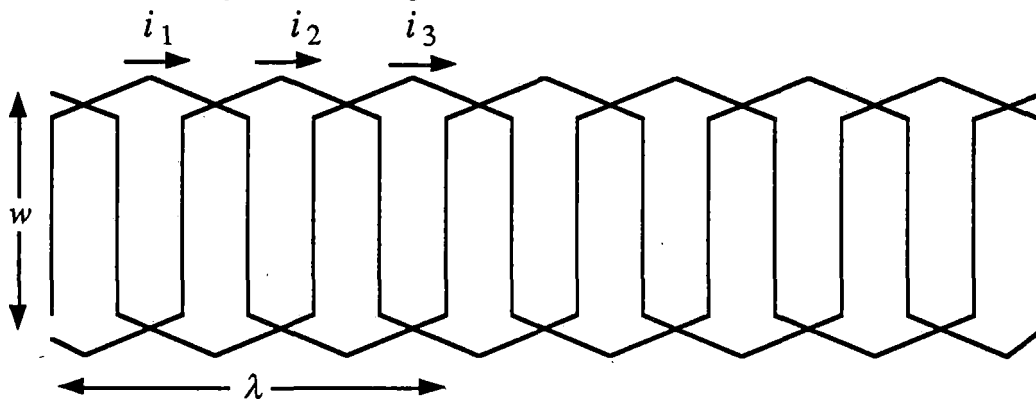


Figure 2.13. Simplified plan for a 3-phase guideway winding.

The wavelength should ideally be an order of magnitude greater than the gap between the vehicle coils and the guideway, but if it is too long the motor efficiency will suffer. Additionally, a long pole pitch would cause electromagnetic fields to extend greater distances from the vehicle. For many EDS designs the same magnets are used for suspension, guidance, and propulsion so it is not possible to optimize the pole pitch for a single function. Ultimately, for any national maglev system the pole pitch must be standardized, but before this is done it is essential to study the issue in detail, not only with respect to the initial design but, in so far as possible, to anticipate future evolution.

The width of the winding,  $w$  in Figure 2.13, need not be part of the guideway standard, and the vehicle magnet pole width could be less than the guideway pole width, but in practice the pole width probably has to be part of the standard.

### Winding impedance

To calculate the winding impedance accurately, the exact shape of the end turn must be considered, but very good accuracy can be achieved by assuming rectangular loops connected by two wire transmission lines as shown in Figure 2.14.

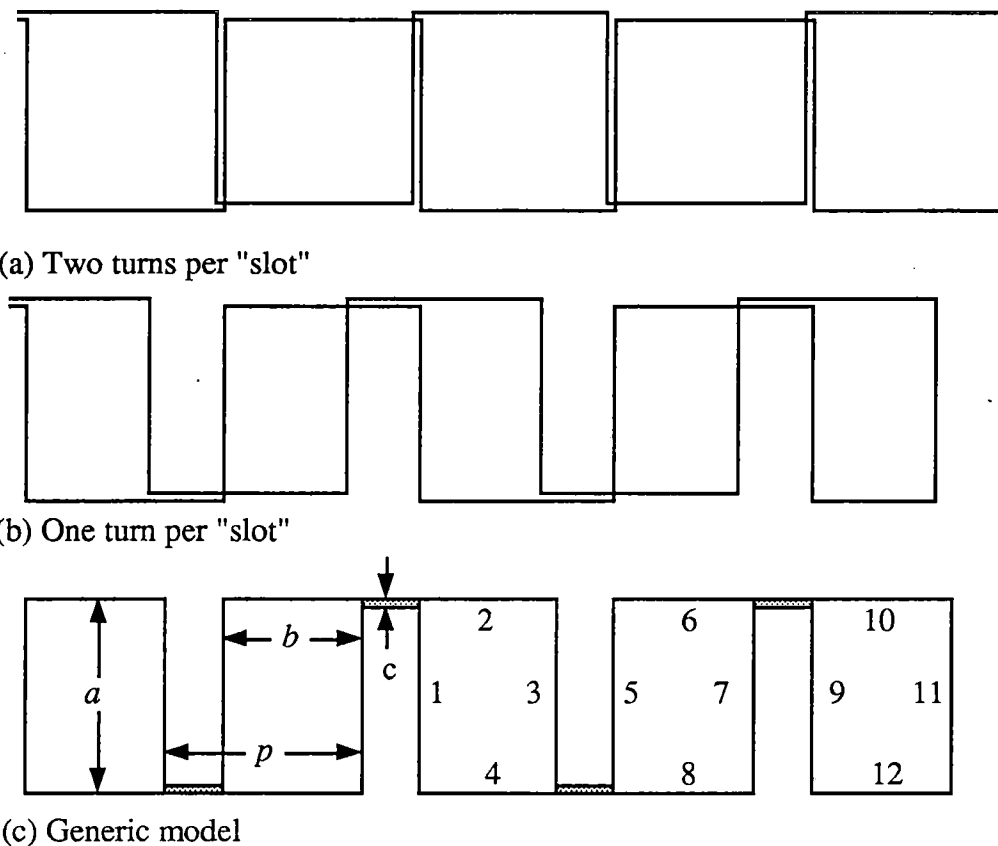


Figure 2.14. Inductance model of rectangular meander winding calculation.

### Inductance calculation

Figure 2.14 shows typical winding patterns for current flowing down one phase and back on another phase in the same three phase group. The winding loop creates a series of rectangular loops interconnected with closely spaced end turns. In the end turns the two conductors are in close proximity and act like a transmission line.

In order to compute the winding inductance we first compute the inductance of a single rectangular coil and then add the effects of mutual coupling to all of the other loops and the effect of the end turn transmission line. The transmission line model has no net coupling to the loops and the interaction between adjacent transmission lines is neglected.

The calculation proceeds by assuming the following:  $L_i$  is the self inductance of the  $i^{th}$  filament of wire,  $L_{ij}$  is the mutual inductance between the  $i^{th}$  and  $j^{th}$  filaments,  $L_{mi}$  is the mutual inductance between one loop and a loop  $i$  pole pitches away,  $L_{tl}$  is the inductance of the transmission line. If we assume the winding has infinite extent we proceed as follows to calculate  $L_{pp}$ , the inductance per pole of the complete winding.

$$\begin{aligned}
 L_r &= 2L_1 + 2L_2 - 2L_{1,3} - 2L_{2,4} \\
 L_{m1} &= 2L_{1,5} - L_{1,7} - L_{3,5} + 2L_{2,6} - 2L_{2,8} \\
 L_{m2} &= 2L_{1,9} - L_{1,11} - L_{3,9} + 2L_{2,10} - 2L_{2,12} \\
 L_{pp} &= L_r + L_u - 2L_{m1} + 2L_{m2} - \dots
 \end{aligned} \tag{2.7}$$

The factor of 2 for the mutual inductance between loops accounts for the coupling in both directions and the signs account for the direction of current flow; if the currents in two filaments are in the same direction then the mutual inductance increases the total inductance, otherwise it decreases it. Because the coils are rectangular there is no mutual inductance between an odd and an even filament.

The inductances are calculated using the terminology of Figure 2.15. Assume that a round wire with radius  $r$  and length  $l$  is spaced  $d$  from an identical wire. Then, assuming a permeability of  $\mu_0$  everywhere, the self inductance of a single filament,  $L_s$ , the mutual inductance between two filaments,  $L_m$ , and the inductance of a two wire transmission line are as given in Equation 2.8 [Ref. 1].

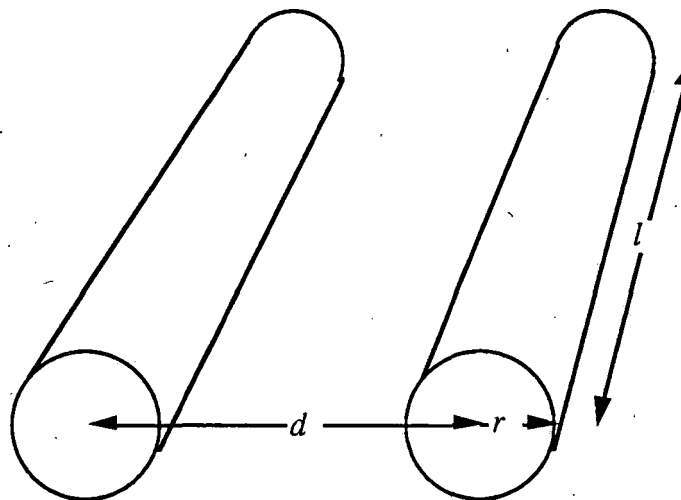


Figure 2.15. Transmission line model.

$$\begin{aligned}
 L_s &= \frac{\mu_0 l}{2\pi} \left( \ln\left(\frac{2l}{r}\right) - \frac{3}{4} \right) \\
 L_m &= \frac{\mu_0 l}{2\pi} \left( \ln\left(\frac{l}{d} + \sqrt{1 + \left(\frac{l}{d}\right)^2}\right) - \sqrt{1 + \left(\frac{d}{l}\right)^2} + \frac{d}{l} \right) \\
 L_u &= 2L_s + 2L_m = \frac{\mu_0 l}{\pi} \left( \ln\left(\frac{d}{r}\right) + \frac{1}{4} - \frac{d}{l} \right), \quad \frac{d}{l} \ll 1
 \end{aligned} \tag{2.8}$$

Table 2.4 gives an itemization of the inductances for a typical design according to the method described. Note that the self inductance term dominates and the negative effect of the mutual is approximately canceled by the remaining terms. Thus, for a very simple calculation we can simply add the self inductance terms.

Table 2.4. Calculation of typical winding inductance; units are microhenries per loop.

<u><math>2(L_1+L_2)</math></u>	1.10
<u><math>2(L_{13}+L_{24})</math></u>	-0.25
<u><math>L_{tl}</math></u>	0.1
<u>All else</u>	0.05
<u>Total <math>L_{pp}</math></u>	1.00

Because of the importance of the self inductance of the wire segments, it is desirable to use a design that minimizes this inductance. The self inductance of a straight section of wire is approximately inversely proportional to the perimeter of the wire. Thus, for a given cross section area a circular wire has the largest inductance and a wide, thin strip will have much less inductance. The best strategy is to make each phase conductor as wide and thin as possible.

The winding resistance is computed using equation 2.9. We use relatively fine strands of insulated wire to reduce eddy current loss, and to eliminate skin depth effects at the excitation frequencies used for propulsion. In a typical design the individual strands are 24 gauge wire with a diameter of 0.51 mm. Note that the stranding increases the outer dimensions of the cable and will increase the length somewhat because of the spiral twisting.

$$R = \frac{\rho\ell}{A}$$

where  $\rho$  is the resistivity of aluminum (2.9)

$\ell$  is the length of the conductor

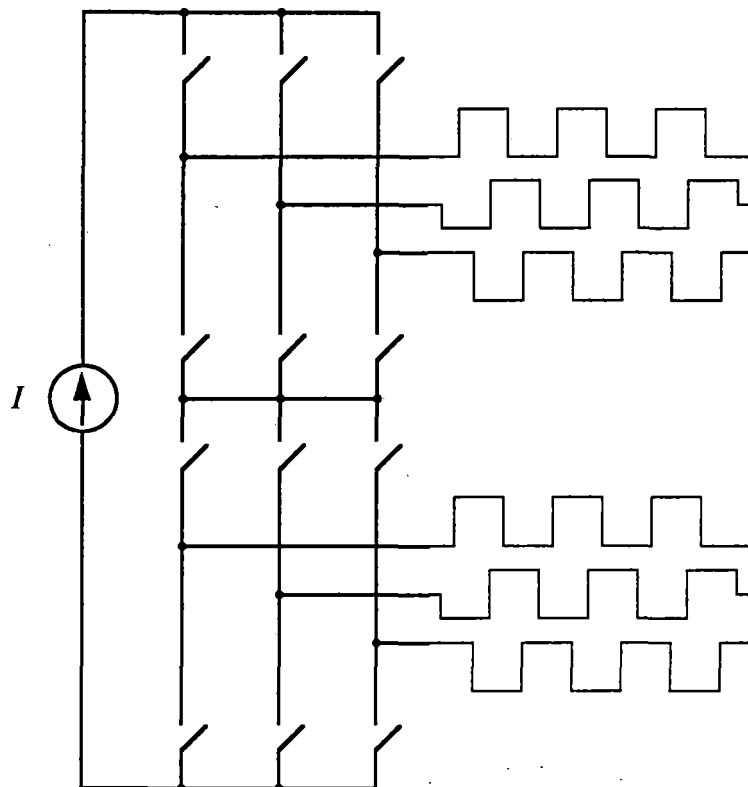
$A$  is the cross - sectional area of the conductor

Table 2.5 gives the key parameters for the motor example. Note that in this design there are 6 phase windings for each motor, so the total thrust and power output is 12 times the value for a single phase. The inductance is based on maximum use of inductance mitigation methods.

**Table 2.5.** Assumed motor parameters for one half of motor

<u>Parameter</u>	<u>value</u>	<u>units</u>
Block length	2,000	m
Pole pitch	1.0	m
Pole width	1.0	m
Winding resistivity (Al)	29	nohm-m
Wires per "slot" winding)	2	(i.e. round-trip phase
Wire length	8,000	m
Cable cross section area	0.0005	$m^2$
Winding space factor	85	%
Resistance per phase	0.55	ohms
Inductance per phase	2.5	mh
Wire density	2680	$kg/m^3$
Phase current, rms	500	amperes (235 A/cm <sup>2</sup> in Al)
Phases, port + starboard	12	
Power loss at $I_{max}$	1.6	Mwatt
Poles per vehicle; each side	24	
Cruise speed	135	m/s
Electrical frequency	67.5	Hz
Average B for winding	0.6	Tesla
Back voltage, rms	2700	volts
Maximum thrust	122	kN
Efficiency at max. thrust	91	%
Wire mass per phase	55	tonnes per km of guideway

## 2.4 Voltage and current waveforms



**Figure 2.16.** Six phase switching system for controlling the power flow to the windings.

In Figure 2.16 there are two 3-phase switch bridges, each controlling the current flow in a three phase group of windings. In a 6-phase LSM there are two distinct sets of 3-phase windings, the odd phases and the even phases, each group displaced longitudinally so as to create the effect of a single 6-phase winding. The switching is then displaced in time so that the upper and lower bridges are never switching at the same time.

Considering only one of the switching bridges, the currents in the corresponding 3 phases are approximately as shown in Figure 2.17. The current source is switched progressively from one phase to another, and with the finite current rise and fall times, caused by winding inductance, the current waveforms have a crude resemblance to 3 sine waves displaced  $120^\circ$  from each other. With a 3-phase bridge and symmetric control the lowest frequency harmonic is the 5<sup>th</sup>. However, in a favored inverter design there would be 6 single phase bridges in series, and in this case there could be a third harmonic component of current. Note that if there is a third harmonic of induced voltage, then for optimum efficiency there should also be a third harmonic of current.

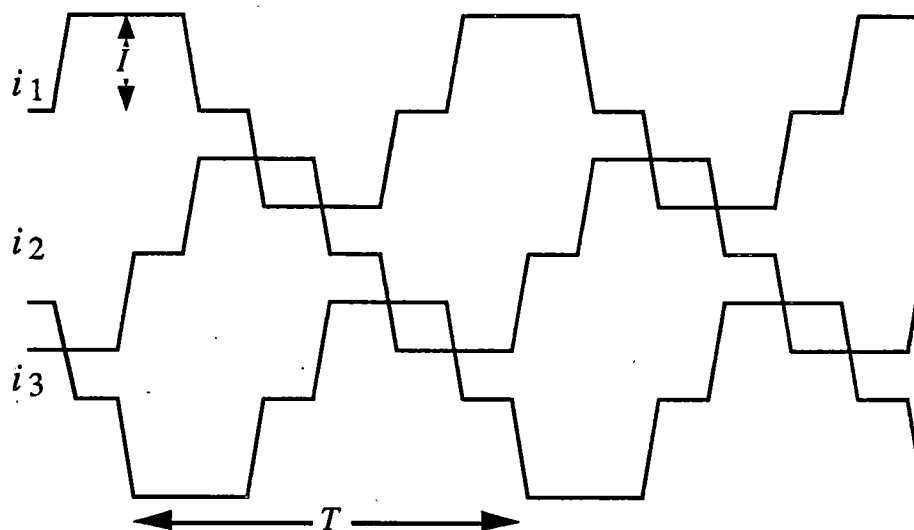


Figure 2.17. Typical currents for excitation of one 3-phase group.

The current requirements for the guideway windings depend on the shape and strength of the field produced by the vehicle magnets. The total thrust produced by a single winding is  $F = B l i$ , where  $B$  is the average magnetic field strength in the plane of the winding,  $l$  is the total effective length of the winding in a direction perpendicular to the direction of travel, and  $i$  is the winding current. For a given vehicle at a specified speed and acceleration, the force requirements and vehicle magnet strength will dictate a required winding current. For a national standard there must be a limit on the required winding current and voltage and the vehicle must provide the necessary  $B$  to achieve the thrust required to maintain the desired synchronous speed. The speed at each point on the guideway must be set by the system and continually monitored to ensure safe operation of vehicles with a close headway.

Note that longer vehicles will require somewhat less force per unit length of vehicle, but will require more thrust for acceleration and more power for cruise. One design problem is to devise a way to increase the power capability if vehicle length increases without requiring the initial installation to be too expensive, and without ever changing the guideway winding. This problem is common to all LSM designs, and to our knowledge no published paper has explained how existing systems will be upgraded to deal with the high voltages required to propel long vehicles. For example, the published Transrapid LSM design will work properly with up to 4 or 5 cars, but with 8 or 10 cars the winding voltage will exceed the insulation rating of the wire. If the wire insulation thickness is increased, then there will be less space for conductor and hence greater power loss in the winding.

## 2.5 End effects

Near the end of the array of vehicle coils the field will deviate from the values calculated previously. For example, if the vehicle has a long array of coils, then the field near the end of the array is as shown in Figure 2.18. The last pole has somewhat less field strength than the others, and there is some field beyond the last pole that will contribute useful force. As a result, the end effect is not too significant as far a propulsive force is concerned. The main importance of the end effect lies in its impact on the far-field, and this is discussed in Section 6.

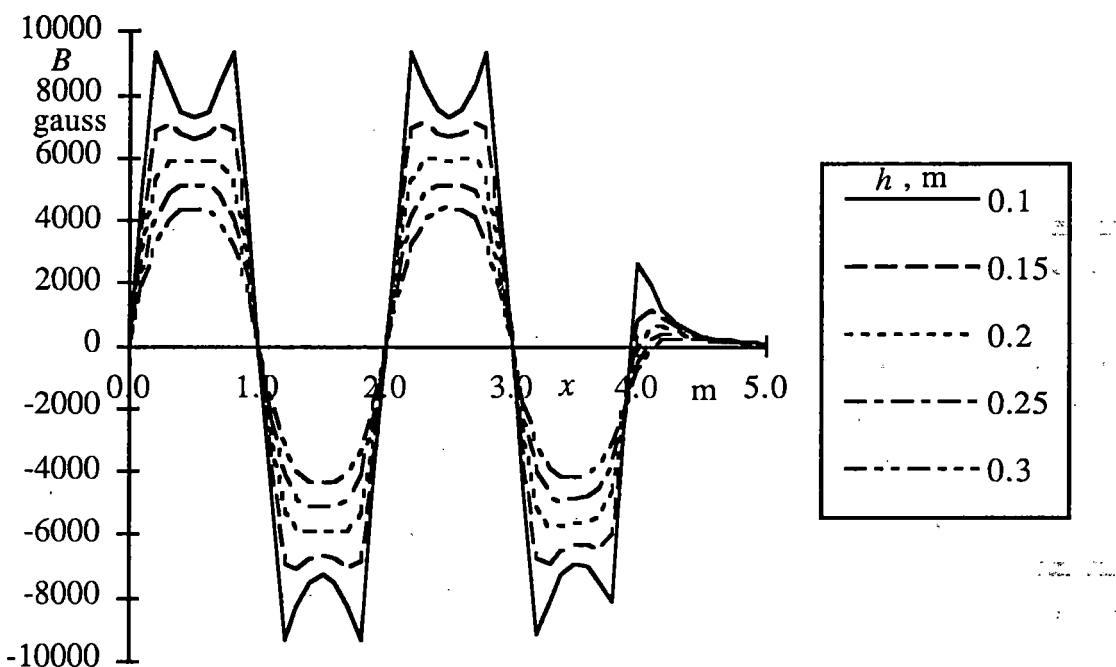


Figure 2.18. Field at end of array

## 2.6 Helical winding

### Alternative winding schemes

Rectangular windings have been used for almost a century for rotary and linear motors. This winding scheme uses transverse sections of the winding for propulsive and braking forces and the longitudinal sections, or end turns, develop transverse forces which are usually not of interest; one must, of course, insure that these forces do not produce undesirable effects. This rectangular winding method is well suited to rotary machines with a laminated steel core because the windings can fit in slots while the end turns wrap around the shaft.

For air core machines there is no need to fit windings in slots and it is difficult to find a good place for the end turns, so there is merit in pursuing alternative winding schemes. For an EDS LSM we would prefer a winding that is thin in the z direction so that the conductors can all be exposed to a high flux level. Prof. James Kirtley at MIT, and others, have pioneered the use of a "helical" winding for superconducting generators,. Now virtually all rotary superconducting machines use a helical winding. This winding scheme appears to be well suited for maglev for reasons that will be discussed.

A simplified comparison between a rectangular and a helical winding is shown in Figure 2.19. The helical winding intercepts less flux but the winding follows a shorter path and when a complete analysis is conducted [Ref. 3] the helical winding often comes out ahead. The helical winding has the added virtue of being thin so that it can be closer to the vehicle and hence in a region of higher magnetic flux density. This is particularly important with aluminum conductors because they require more volume for the same winding resistance.

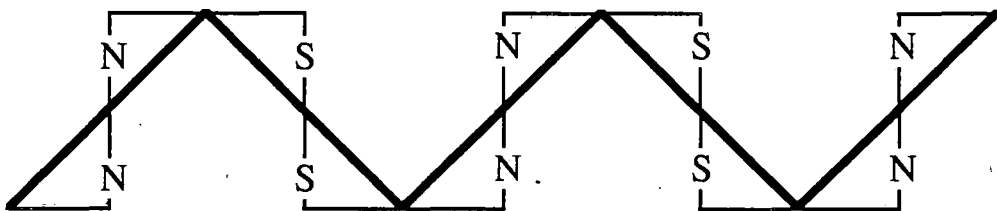
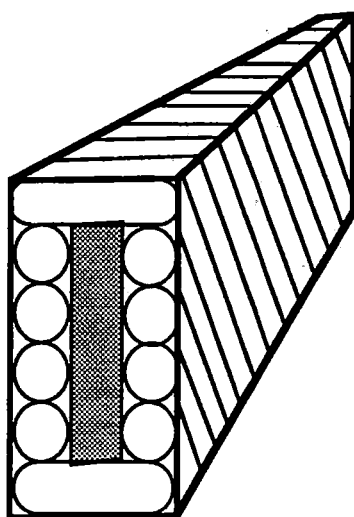


Figure 2.19 Comparison of helical winding (heavy) with rectangular winding.

### Construction of a helical winding

In order to picture how the helical winding is constructed, imagine that several wires are wound together in helical fashion in a single layer around a cylindrical core, and then the core is removed and the winding flattened. A perspective view is shown in Figure 2.20; the resulting structure resembles a braided belt. This winding would be fabricated in a factory and long lengths would be transported on a reel to the site for field installation.



**Figure 2.20.** Helical winding wound on an insulating core.

Figure 2.20 shows a winding with 10 conductors and as such it could be used with a 5 phase inverter, but the winding can be fabricated for almost any number of phases. It is important to remember that each conductor, shown as a round circle in Figure 2.20, is actually a Litz wire composed of many strands of fine wire so as to minimize eddy current losses due to the rapidly changing magnetic field produced by the moving vehicle. For inductance mitigation the Litz wire would be flat instead of round. Several companies have automated machines for making this helical Litz wire.

#### **Other virtues of the helical winding**

In addition to being a thin winding, the helical design has insulating virtues for high voltage applications. In the superconducting generator application it is envisioned that transmission line voltages can be generated directly by this winding. In our case we can limit the voltage between adjacent wires to about 5 kV while allowing up to 15 kV between non adjacent wires.

Another helical winding advantage is the reduced inductance of the winding. Although an LSM for EDS applications will have a lower inductance than a comparable winding for an EMS system, the inductance still creates problems for switching and inductance mitigation techniques are important.

#### **Series-parallel switching options**

The helical winding can be installed with almost any number of conductors. There is very little extra cost for a winding with more conductors, assuming a given total cross-sectional area. This allows the option of installing 12 phase windings and allowing adjacent phases to be connected either in series or in parallel. Rotary motors used for

propulsion have been switched in series/parallel combinations for many decades and the advantages are well known. We can allow higher motor current at lower speed when the induced voltage is low, and lower currents when the voltage is high. Transrapid uses a transformer to achieve a similar effect. At low speeds their controllers drive the windings directly while at high speeds they use a 2.5:1 transformer to generate the higher voltages that are needed for high speeds.

One possibility is to use the series connection at low speeds so that the LSM can be used to provide enough vertical force to provide full levitation at zero speed. Alternatively, the series/parallel connection could be used to allow a lower power inverter to give fairly good performance, exactly as Transrapid uses a transformer to provide this function.

## References and Bibliography

### Books

- 1 Grover, F. W., *Inductance Calculations*, Dover Publications, Inc., New York, 1946.
- 2 Boldea, I., Nasar, S. A., *Linear Motion Electromagnetic Systems*, John Wiley & Sons, New York, 1985.

### Papers and Reports

- 3 Kirtley, J. L., "Air-Core Armature Shape: A Comparison of Helical and Straight-With-End-Turns Windings," *Proceedings of SM100*, Zurich, Switzerland, August 27-29, 1991.

### **3 Electronic Power Conversion**

*The LSM requires high power electronics for converting fixed voltage and fixed frequency power from the utilities to variable voltage and frequency power for exciting the motor windings. It is preferable, though not essential, that the conversion be reversible in order to allow recovery of braking energy. The cost of the power conversion equipment is on the order of 10% if the guideway capital cost, so any design must make cost reduction a major issue. But fault tolerance and reliability are equally important. This section addresses these issues and describes the alternatives that seem most appropriate for maglev applications. A major focus is on methods of estimating and reducing cost.*

#### **3.1 Propulsion power requirements**

There are five major components of propulsion power requirements, listed here in order of importance:

- Aerodynamic drag;
- Power for acceleration due to a probable need for frequent acceleration and deceleration;
- EDS loss associated with induced currents in the guideway;
- LSM losses associated with resistance of the guideway LSM winding;
- Power loss in the transmission and conversion of power;
- Eddy current loss in conductors exposed to high and rapidly changing fields;
- Hotel power if this is provided by a linear generator, as with Transrapid TR07.

Table 3.1 gives a rough idea of the power requirements for level travel at different speeds for a vehicle capable of carrying about 120 passengers. This table assumes aerodynamic drag power varies as the cube of speed, eddy current loss is proportional to speed, power loss in the magnetic suspension is constant, and the linear motor losses are proportional to the square of motor thrust. Losses in the electronic converter will be about 4 % of the power output. There is an additional "hotel" power requirement of about 1 kw per passenger, and refrigeration power if there are is on-board refrigeration equipment; these power requirements are not included in the following discussion.

**Table 3.1.** Baseline power requirements for level travel for a typical 120 passenger vehicle designed for a nominal maximum operating speed of 135 m/s.

<i>Speed</i>	<i>m/s</i>	30	45	60	75	90	105	120	135	150
	<i>mph</i>	67	101	134	168	201	235	268	302	336
Aero. loss	MW	0.06	0.20	0.46	0.90	1.56	2.48	3.70	5.27	7.22
EDS loss	MW	0.63	0.63	0.63	0.63	0.63	0.63	0.63	0.63	0.63
Eddy loss	MW	0.01	0.02	0.03	0.05	0.07	0.09	0.12	0.15	0.19
<u>LSM loss</u>	MW	0.16	0.95	0.11	0.13	0.19	0.28	0.41	0.60	0.87
Total loss	MW	0.86	0.95	1.23	1.72	2.45	3.48	4.86	6.65	8.91
Energy/dist	kJ/m	28.8	21.2	20.5	22.9	27.2	33.2	40.5	49.3	59.4
	wh/s-km	65	48	47	52	62	76	92	112	135

A TR7 200 passenger vehicle is estimated to consume 4.2 Mw on a level guideway at 111 m/s (400 km/h). EMS consumes less power for suspension than EDS, but the aerodynamic drag can be greater because of the greater vehicle surface area associated with the wrap-around support structure.

We have assumed a top speed of 150 m/s (540 km/h, 336 mph) in order to allow continuous safe operation at 135 m/s (302 mph). With this design speed there will be enough extra capability to allow some variations with power supply, weather, partial failure, etc. We expect that a typical route will allow an average operating speed in the range 90 to 120 m/s (201 to 268 mph).

The minimum operating speed is zero, but for main line guideway operation we assume a normal minimum of 30 m/s. Some EDS designs will not operate at this low a speed except on wheels, and some will operate below 10 m/s. If low speed operation is possible the stations can be built with shorter acceleration and deceleration lanes.

The vehicle is assumed to be designed for one direction of travel, but reverse propulsion must also be possible at reduced speed.

There is an important compromise to determine the optimum LSM thrust capability. A typical vehicle requires between 40 and 50 kN of thrust for level cruise at 150 m/s. Figure 3.1 shows the net vehicle acceleration for different motor thrusts from -120 to 120 kN, where a negative thrust implies braking. Note that at speeds below about 75 m/s the magnetic drag dominates, so the total vehicle drag is relatively constant at about 0.04 g over a wide speed range. It appears that anything less than 120 kN thrust capability will not allow enough acceleration to accommodate varying guideway speed so as to accommodate terrain, wind and some performance degradation for unanticipated effects. This means the normal power rating of the inverter will be  $120 \times 150 = 18,000$  kilowatts. For the normal

maximum speed of 135 m/s and considering all of the losses, the inverter must provide about 6.6 megawatts for level cruise. In short, the power inverter should be sized for almost three times the power required for level travel at maximum operating speed. This may seem like an excessive over-rating, but anything less will lead to limited acceleration capability. If the guideway is level and straight, then a reduction in acceleration may be acceptable, but we will assume that the power converter should produce on the order of 10 to 20 megawatts in a frequency range of 20 to 100 Hz.

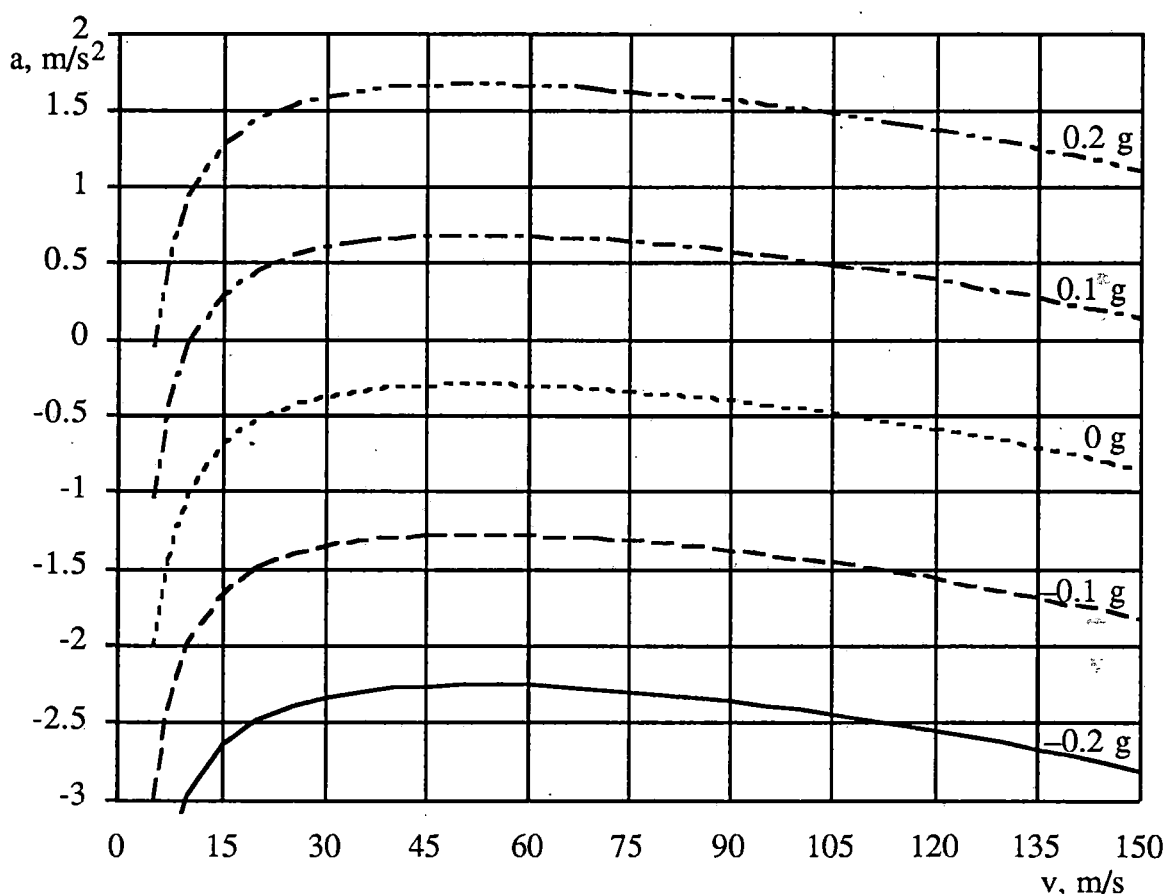


Figure 3.1. Acceleration vs. speed for various motor thrusts.

With the assumed 120 kN maximum thrust, and considering aerodynamic and magnetic drag, Figure 3.1 shows that the average acceleration capability is about  $1.6 \text{ m/s}^2$  except at the highest and lowest speeds. For braking the aerodynamic and magnetic drags add to the regenerative braking so 120 kN gives an average deceleration of about  $2.4 \text{ m/s}^2$ .

### 3.2 Semiconductor power switching devices

The key components in all power electronic circuits are the silicon power devices used to control the flow of power. At high power levels these are always operated in the

switched mode with a device either conducting substantial current with voltage drop of only a few volts, or operating with negligible current at voltages of several kilovolts. Following is a brief description of semiconductor power switching devices currently suitable for operating at megawatt power levels.

### Silicon-Controlled Rectifier Thyristor (SCR)

The thyristor, or silicon controlled rectifier, is available in a wider Volt-Ampere range than any other semiconductor switch. It is a 4-layer device that uses the PNPN structure to sustain very high currents once a gate signal triggers the device into the on-state. Its simplicity accounts for the fact that an entire 4 inch wafer can be used to build a single device and still achieve good yield. It depends on a mature, stable technology and is extremely robust. For example, a 3000 ampere thyristor may have a peak, 1/120 second surge rating of over 55,000 amperes.

The major disadvantage of the SCR is the need for external commutation circuitry, which can be extremely bulky, expensive, and lossy. Fast turn off devices now cost about the same as slower devices, but there are still serious speed limitations caused by the relatively slow commutation process.

### Gate Turn Off Thyristor (GTO)

A GTO is very similar to an SCR except that the gate can be used to turn the device off, so there is no need for expensive commutation circuitry and higher switching rates are possible. However, the GTO costs substantially more for several reasons:

- The device cost is 2 to 3 times higher than a comparable SCR because it requires many more processing steps.
- The gate drive circuitry is much more expensive. In order to turn off a given current, the gate drive may need to supply 20 to 25% of the conduction current with a 30 to 50  $\mu$ sec rise time.
- Unlike the thyristor, many types of GTOs cannot block reverse voltage, and thus there may be a need for auxiliary diodes in some circuits.
- Snubbers for a GTO application are stringent, and can account for a substantial portion of the losses.

In spite of its higher cost, the GTO has become widely used in the last few years, and has completely replaced the thyristor in some applications. For example, the new design for Transrapid power converters uses GTOs, as does the power circuitry in the German ICE high speed train. We believe that the GTO is the device best suited for use in inverters designed for use in a maglev system.

### MOS-Controlled Thyristor (MCT)

The MCT is a newer device that is not yet available in the highest power levels. It is similar to the GTO in allowing the gate to turn the device off, but the gate drive circuitry is much simpler. The MCT, like the SCR and GTO, has the advantage of relatively high efficiency as compared with transistor-like devices such as the Insulated Gate Base Transistor (IGBT) which is commonly used for lower power applications.

MCT modules currently exist which can block 3000 V and turn off 600 A, thus making them suitable for this power range, but fairly expensive. Although it is not known when MCTs will be commercially available for megawatt power levels, it will be relatively easy to replace GTOs with MCTs when such a change is appropriate.

### Other power switching devices

There are a number of other switching devices available, but none of them are suitable at present. The most likely candidate is the IGBT, but device researchers who believe very strongly in the future of the IGBT also believe megawatt level inverters are at least 5 years away. For lower power levels, and possibly for gate drive and hotel power applications, the IGBT and various types of transistors will be the components of choice.

### Device cost

Since the cost of the power switching devices gives a good indication of the cost of a complete inverter, it is instructive to examine the device costs. SCR devices, in a range of voltages with similar power ratings, have costs shown in Table 3.2. Here we see that the optimum design is for intermediate voltages and currents. The cost of the complete inverter is discussed later.

**Table 3.2.** Cost of SCRs, GTOs, and GTO gate drives.

(a) Inverter Grade, 1MVA Powerex SCRs (prices from Gerber Electronics).

<i>Volts</i>	<i>Amps</i>	<i>MVA</i>	<i>tq (us)</i>	<i>Part #</i>	<i>\$ @ 1</i>	<i>\$ @ 100</i>
1600	650	1.04	80	T72H164214DN	173.78	159.87
1400	700	0.98	40	T72H144544DN	137.30	126.32
1200	885	1.062	40	C477PB	137.16	114.30
1000	1000	1	40	C447P	173.58	159.61
800	1180	0.944	40	T82F087543DN	172.55	158.74

(b) Power frequency grade, 1MVA Powerex SCRs (prices from The Orion Group).

<i>Volts</i>	<i>Amps</i>	<i>MVA</i>	<i>tq</i>	<i>Part #</i>	<i>\$(1-24)</i>	<i>\$(100+)</i>
1400	750	1.05	200	T820-14-74 04dh	169.86	131.21
1200	900	1.08	200	T820-12-90 04dh	190.92	148.82
1000	1000	1.00	350	T9G0-10-10 03dh	196.52	152.54
800	1400	1.12	150	C451-N2	203.50	157.96
700	1500	1.05	150	C451-S1	128.10	128.10
600	1600	0.96	250	TA20-06-16 03dh	301.06	211.95
600	1800	1.08	250	TA20-06-18 03dh	349.92	246.35
800	1200	0.96	350	T9G0-08-12 03dh	183.15	142.16

(c) High voltage Powerex and GE SCRs (prices from The Orion Group).

	<i>A av</i>	<i>A rms</i>	<i>V pk</i>	<i>@100 pieces</i>
TA204014		1400	2200	4000 \$209.25
FT1500DV-80		1500	2350	4000 \$364.23
C784DD		1650	2950	4400 \$391.65

(d) Asymmetric GTOs and Gate Drives from Marconi (prices from MPS electronics).

<i>Volts</i>	<i>A rms</i>	<i>MVA</i>	<i>A ave</i>	<i>Part #</i>	<i>\$(1-10)</i>	<i>Gate Drive</i>	<i>\$(2-10)</i>
1300	310	0.403	200	DGT224SE13	108	GDU91-2	387
1800	625	0.945	335	DG386AP18	324	GDU91-201XX	387
2500	330	0.825	210	DG306AE25	225	GDU91-2	387
2500	620	1.55	395	DG386AP25	360	GDU91-201XX	387
4500	470	2.115	300	DG388AP25	864	GDU91-201XX	387
2500	1280	3.2	820	DG606AH25	990	GDU91-202XX	630
4500	1365	6.142	870	DG758BX45	1440	GDU91-203XX	720

### 3.3 Passive components

The major passive devices are resistors, capacitors, inductors, and transformers. It is not necessary to elaborate on the properties of these devices except for a few important observations relevant to requirements for maglev propulsion.

#### Power resistors

Power resistors are required to allow regenerative braking in case of power system failure. Power resistors may also be required for dynamic braking in emergency situations, but it may be possible to use the guideway winding resistance alone for this function.

#### Capacitors

Capacitors play a crucial role in all power electronics, particularly when the load has substantial inductive energy storage. The capacitor is used to store energy during transitions so that the switching devices due not have to dissipate substantial energy. For megawatt conversion the capacitors must store many joules of energy, and in this range the cost is roughly proportional to the energy storage. For example, in order to double the voltage rating the insulation thickness must be doubled, so the capacity is reduced by a factor of four for given capacitor dimensions (i.e. half the area of the metal electrodes and twice the thickness of the insulator). The parameters and cost for a specific GE non-polarized capacitor are given in Table 3.3.

**Table 3.3.** Parameters for a typical commutation capacitor

Part number	V peak	$\mu\text{f}$	A rms	\$@1500	\$/Joule
97F8625FC	1500	10	218	\$38.03	\$3.38

Other sizes of non-polarized capacitors have very nearly the same cost per unit energy storage. A typical application requires a capacitor with a capacitance of 100  $\mu\text{f}$ , a current rating of 500 amperes rms, and a voltage rating of 3000 volts. It would take a series/parallel combination of 40 of the capacitor described in Table 3.3 with a total cost of over \$1500. This cost may be greater than the cost of the associated semiconductor devices in an inverter.

#### Inductors

At low power levels it is common to use capacitors as the main filtering component with inductors used only at frequencies above the audio range. This is because large inductors that would be needed for low frequency application are relatively expensive and inefficient. However, the scaling laws imply that capacitor cost per unit energy storage

does not reduce with size but for an inductor cost does decrease with size. For example, if an air core inductor has an inductance  $L$  and resistance  $R$ , and all dimensions are doubled the ratio  $L/R$  will be quadrupled because it is proportional to the ratio  $\mu/\rho$  which has dimensions henries/m<sup>2</sup>. Thus, inductors can be used to store large amounts of energy at a lower cost per unit energy storage than capacitors, and this means that inductors can play a more dominant role at megawatt power levels.

At medium power levels we would use iron core inductors to store energy but at the highest power levels an air core inductor is preferable. One analysis [Ref. 6] indicated that:

An air core inductor is better if  $W > 37,000 \tau^{1.5}$

where  $W = LI^2/2 =$  maximum energy stored

$\tau = L/R =$  time constant.

As an example, a chopper for a 10 megawatt inverter might require an inductor with parameters given in Table 3.4.

Table 3.4. Parameters for an inductor in a 10 MW chopper.

L	0.05	Henry
R	0.1	ohm
I	800	A rms
W	16,000	J
$\tau$	0.5	s
$W\tau^{1.5}$	45,300	$J s^{-1.5}$

The implication is that an air core inductor would be somewhat less expensive, but an iron core inductor is definitely worth considering. An aluminum winding, air core inductor with these parameters would have a mass of about 250 kg, and a cost of about \$2500. A capacitor bank with the same energy storage capability would cost over \$54,000; this is an order of magnitude more expensive! The capacitor energy storage would be more efficient, but for converter applications the efficiency of this inductor is entirely adequate.

### Transformers

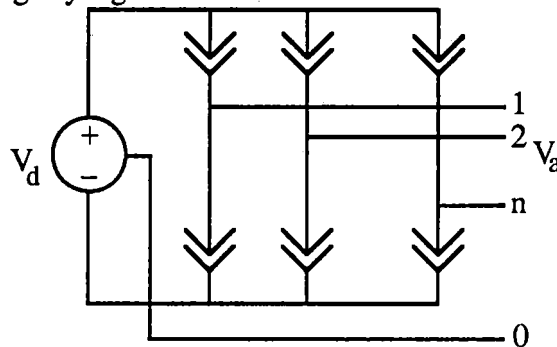
The transformer is another device commonly used in power electronic circuits. Like inductors, in larger sizes they are more efficient and less massive on a per unit power basis. However, they are still very expensive and require considerable space and related cooling and protective equipment. In general one should avoid too many levels of transformer and, when possible, use semiconductor devices instead. As a specific example, Southern California Edison obtained a quotation for a 25 MVA 3 phase transformer at \$500,000. Smaller transformers would be more expensive per unit MVA

rating, so for power and frequency ranges of interest we can assume that, roughly, large transformers cost on the order of \$20 per kVA.

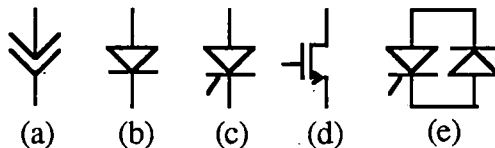
### 3.4 Inverter and converter modules

#### Generic inverter architecture

Virtually all high power dc to ac converters can be visualized in terms of the generic circuit shown in Figure 3.2. In these Figure we used a symbol that is a cross between a diode and a switch to signify a generic switch.



(A) Generic dc to ac  $n$ -phase converter.



(B) Typical switching devices.

Figure 3.2. A generic converter and examples of switching devices.

In Figure 3.2 the dc voltage source  $V_d$  is converted to an  $n$  phase voltage source  $V_a$  by means of  $2n$  switches indicated as polarized, generic switches. In an actual circuit the generic switch is replaced by a specific switching device such as the examples shown. Thus (a) in Figure 3.2 might be replaced by a simple diode (b), a thyristor (c), a Field Effect Transistor (d) or a GTO in parallel with a reverse diode (e). The type of switching device used will depend on the application, and passive devices, such as resistors and capacitors, may be added to control transients, but the basic topology is almost always the same. In Figure 3.2(A) there is an optional ground circuit shown as a connection from a mid-point in the dc source to a neutral terminal in the  $n$ -phase ac load. Note that power flow may be from dc to ac, from ac to dc, or both according to the nature of the switches and their controllers.

## Rectifiers

If the generic switch is replaced by a simple diode the result is the conventional rectifier. If it is replaced by a diode in parallel with a reversed GTO, as shown in Figure 3.3, it becomes a 4 quadrant rectifier if the GTO is triggered to turn on at the correct time.

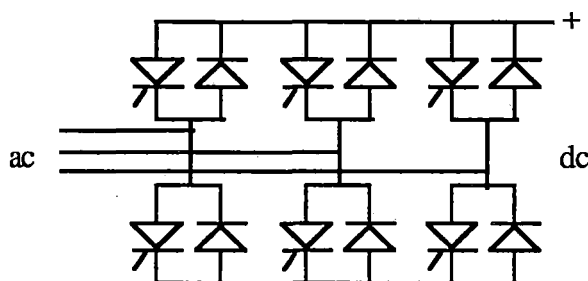


Figure 3.3. 4-quadrant rectifier.

At high power levels the simple 3 phase rectifier, commonly called a 6 pulse rectifier, does not provide a constant voltage or a good power factor for the transformer, so it is common to use two rectifiers in series. One of the series rectifiers is fed from Y-connected windings and the other from  $\Delta$ -connected windings, so that the result is a 12 pulse rectifier with very good regulation and power factor attributes. In some cases it is even worthwhile to build a 24 pulse rectifier.

## Voltage source inverter

One approach to finding a suitable topology for an inverter is to examine systems developed for other purposes. A good example is the electronic power system used in the German Intercity Express high speed train. This system uses a Voltage Source Inverter with Pulse Width Modulation (PWM) control and a fixed voltage dc link.

A simplified block diagram of the ICE system is shown in Figure 3.4. The ICE locomotive uses a transformer to reduce the catenary voltage of 15 kV, 16 2/3 Hz, to about 2500 volts, which is then converted to dc with four 4-quadrant rectifiers. This dc link is filtered with a parallel capacitor and series LC resonant circuit, tuned to 33 1/3 Hz, to produce a controllable dc voltage for four 3-phase Pulse Width Modulated Inverters.

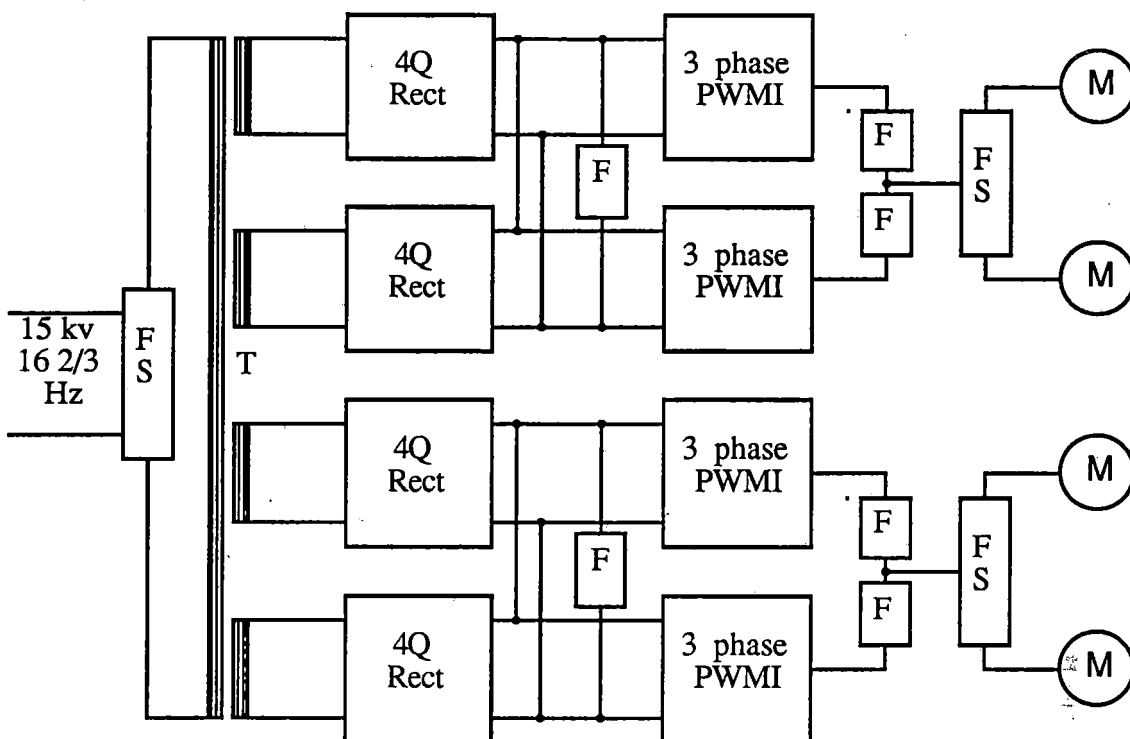


Figure 3.4. Rectifier and PWM voltage source inverter used on ICE locomotives.

In the new design the inverters use GTOs which, it is claimed, reduce the switching losses by almost a factor of 3 and save 3.5 tonnes of mass in the locomotive. The output of the inverter passes through suitable inductors and switches and is applied to 4 traction motors. Note that there is substantial fault tolerance so that the failure of any one component in the system will not totally disable the locomotive. Only the transformer is critical, and this is one of the more robust components.

Following are some of the advantages and disadvantages of a PWM voltage source inverter with a variable dc voltage source.

#### Advantages

- The output voltage as well as frequency may be controlled by a PWM scheme. This allows the use of a diode bridge rectifier at the input, which is less expensive, more reliable, and has better power factor than a phase controlled rectifier.
- Harmonic content is better than for a quasi-square wave inverter, and output frequency may be varied down to 0 Hz with minimal torque ripple. Also, selective harmonic elimination may be used to remove troublesome harmonics.
- Output frequency is only limited by switching losses or thyristor commutation, and output frequencies of over 200 Hz may be achieved.

#### Disadvantages

- While the high switching frequency reduces filter requirements, it also lowers efficiency because of switching losses.
- Regeneration to the ac supply requires additional hardware.

The ICE locomotives and Transrapid LSM propulsion systems were both built by Siemens, and share many attributes. The new system for Transrapid is being built with the same GTO modules used on the locomotive, and the system design approximates that for ICE, except with multiphase power input and the possibility of a variable voltage dc link.

### Current Source Inverter

A second major class of inverters is the Current Source Inverter (CSI) in which a current source is created with an inductor, thus providing a constant current over a switching interval, and switches are used to control the power flow to the individual phases. A typical 2-quadrant CSI is shown in Figure 3.5. Here the switching devices are thyristors which are commutated by capacitive coupling to adjacent phases. For regenerative operation the voltage source polarity is reversed and the current polarity unchanged.

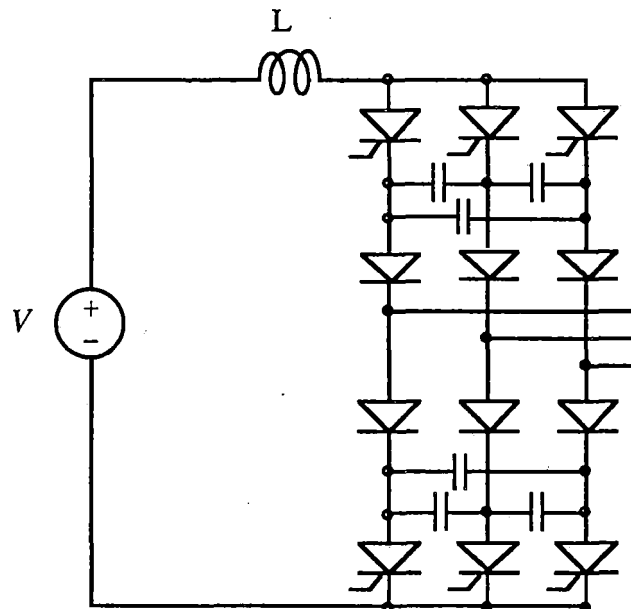


Figure 3.5. Quasi-Square Wave Current Source Inverter.

The CSI shown in Figure 3.5 uses an adjustable voltage source,  $V$ , to provide the input dc power, and an inductor,  $L$ , to maintain constant current over switching intervals. It can be a highly reliable solution in the megawatt power range, and its primary characteristics may be summarized as follows:

#### Advantages

- Commutation circuits are relatively simple (compared to a VSI), and sources indicate that commutation losses are relatively small [Ref. 2,5].

- Some sources [Ref. 2,3,5] indicate the commutation hold off times are long enough to permit inexpensive rectifier grade thyristors and diodes to be used, reducing the cost of the converter. The long holdoff times are the result of the need to oversize the commutation capacitors for voltage spike control.
- The CSI is known to be more rugged and reliable than a comparable voltage source inverter. Commutation failure is a non critical event for this converter, because shoot through is not an issue. Also, because commutation voltages respond to load currents, varying the rectifier output voltage does not affect commutation reliability, and the inverter responds well to sudden load changes [Ref. 5].

### Disadvantages

- The commutation capacitors for this type of system need to be matched to load parameters in order to control voltage spikes at the output. The size of these capacitors along with the link inductor tend to make this circuit somewhat bulky and expensive.
- At low frequencies (< 5 Hz), torque ripple may be a problem. However, this can be somewhat remedied by changing conduction patterns [Ref. 3,5].
- The upper output frequency is limited by the relatively slow commutation process.
- Without additional circuitry, this inverter cannot operate at no load since current is required for commutation.

Most of the negatives do not have a major impact on the LSM application for EDS, thus this topology may be a reasonable choice. For an EDS design the maximum electrical frequency will be in the range of 60 to 120 Hz, as compared with the 240 Hz value for Transrapid. Assuming there are either two motors or one motor with 6 phases, we can configure the circuit to use one inductor in series with two three-phase bridges as shown in Figure 3.6. The switching of the series sections is staggered so that only one is switching at any given time, so a smaller inductor is adequate. Also, this series design allows the power source to be taken directly from a medium voltage dc distribution system.

We can carry the series converter idea one step further by using a separate H-bridge for each phase, and putting all phases in series as shown in Figure 3.7. This topology is particularly convenient to use with a dc distribution system since the variable voltage dc source can be provided by a buck converter supplied directly by a 15 kV dc source.

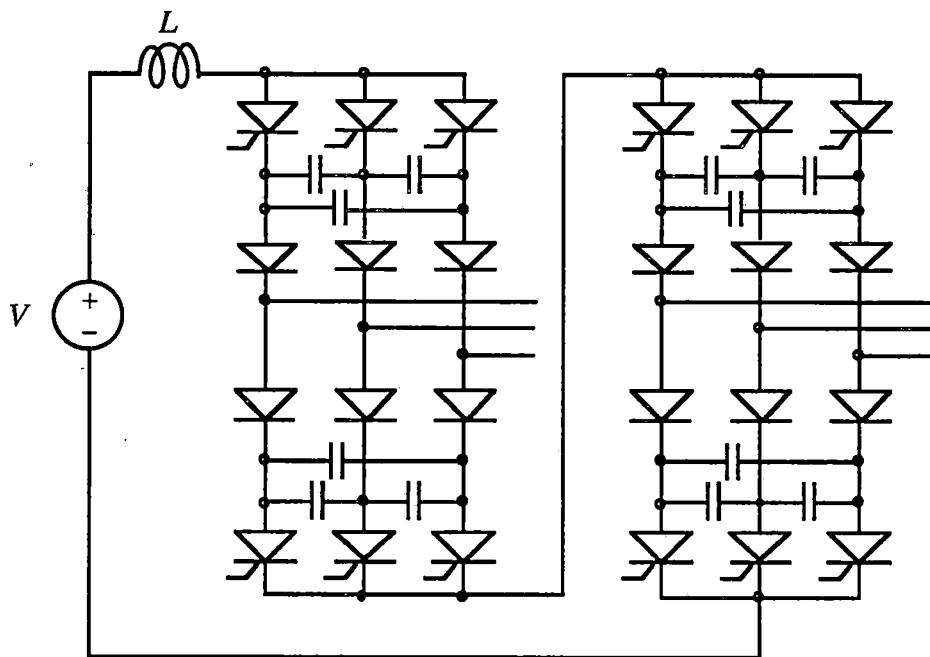


Figure 3.6. Series connected 6-phase CSI for an LSM.

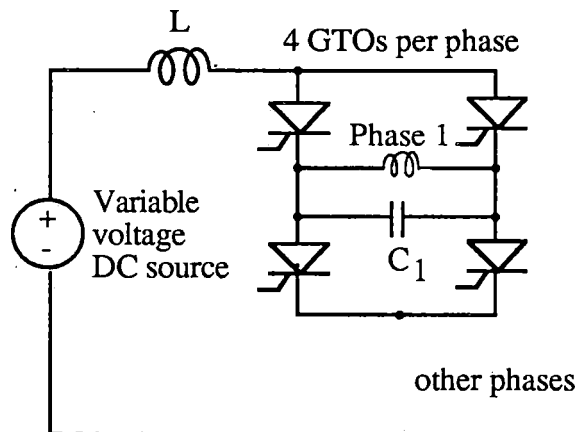


Figure 3.7. Series Current Source Inverter

### Cycloconverter

The MLU002 Japanese EDS maglev system used cycloconverters to generate power at up to 34 Hz. This very low frequency makes the cycloconverter feasible, though not necessarily optimal.

The cycloconverter is similar to the generic switch of Figure 3.2, but the input is multiphase ac and there are four switches from each phase of the input to each phase of the output. These switches directly convert ac line power to a different frequency, without going through a dc link. The elimination of energy storage elements makes this an economic solution at high power levels, but also leads to several drawbacks. While

cycloconvertors are widely touted for use at high power levels, they are typically used in naturally commutated applications, where forced commutation circuitry is not an issue.

Following are some of the advantages and disadvantages of a cycloconverter:

#### **Advantages**

- The elimination of energy storage elements reduces the converter size and cost.
- Regeneration is simple, and does not require any additional hardware, although bilateral switches are necessary in the first place.

#### **Disadvantages**

- Sources indicate that control is relatively costly and complex, making it only suitable for high power drives [Ref. 2,5].
- The cycloconverter fundamentally operates at less than unity power factor, and the power factor degrades as the output voltage is reduced.
- The supply current harmonics vary with output frequency and load, making them hard to filter.
- For some control schemes [Ref. 14], subharmonics may exist in the output voltage and input current. These harmonics are hard to filter out, and the output harmonics can cause significant torque ripple.

#### **Other alternatives**

In soft-switched architectures, switching losses are decreased by using a resonant or quasi-resonant auxiliary circuit to obtain a zero voltage and/or zero current switching opportunity for the main devices. These designs have not yet achieved major commercial success, and they do not appear to have any advantage in a maglev application.

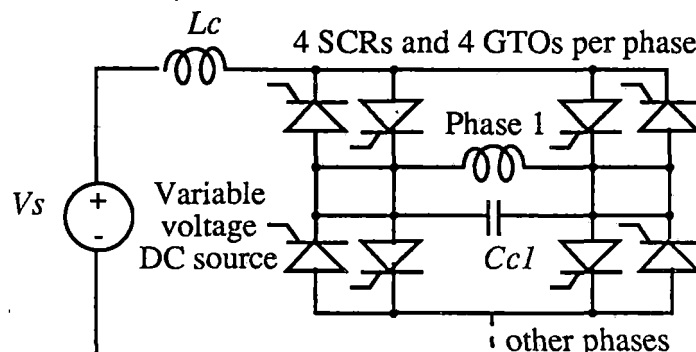
### **3.5 Commutation**

The relatively high inductance of the winding poses a major problem for the design of the inverter commutation circuitry. If the inductance is too high the CSI is probably not a good choice. As a rough measure, assume the waveform is sinusoidal and compare the voltage across the inductor at full load with the induced back voltage in the motor. If the inductive voltage is less than 1/2 the motor voltage, then a CSI is probably a good choice. If the inductive voltage is equal or larger than the motor voltage it is preferable to use a VSI. With a VSI it may be preferable to utilize an ac power distribution scheme in order to develop the low voltages and high currents required for the converters.

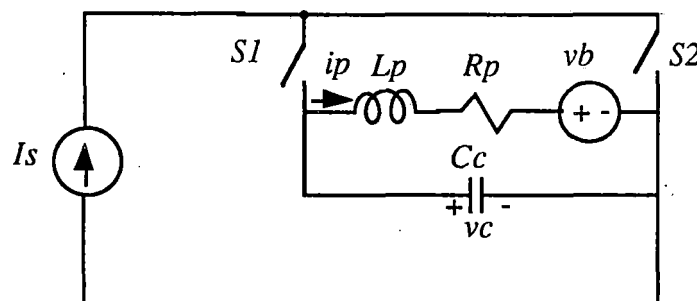
For EDS designs with reasonable care in reducing the winding inductance, the advantage of the series connected CSI is quite significant. It is then possible to use a dc power distribution system with lower overall cost because of the reduction in transformer and distribution line cost.

The commutation problem is aggravated since, for cost reasons, we do not wish to use a large enough capacitor to store all of the energy stored in the phase inductance. If the

inductance can be kept within reasonable limits, then a good option is to use 4 GTOs and a relatively small capacitor to commutate a bridge that uses 4 SCRs to perform the switching for a 2-quadrant inverter. A capacitor across the winding limits the voltage during switching and the GTO is "chopped" to prevent the voltage from getting too large during the transition. The turn-off is accomplished with the aid of natural commutation using the motor back voltage. The circuit and a simplified model are shown in Figure 3.8



(a) Series connected current source inverter.



(b) Simplified model of one phase for positive half-cycle.

Figure 3.8. 2-Quadrant, series connected CSI  
with GTO based power control and SCR based regenerative braking.

The circuit of Figure 3.8 can be simulated using the state variable representation given in Equation 3.1. The source  $i_1$  is either  $I_s$ , 0, or  $-I_s$ .

$$\begin{aligned} \text{S}_1 \text{ closed, } \text{S}_2 \text{ open: } s \begin{bmatrix} v_c \\ i_p \end{bmatrix} &= \begin{bmatrix} 0 & -\gamma_{C_c} \\ \gamma_{L_p} & -R_p/L_p \end{bmatrix} \begin{bmatrix} v_c \\ i_p \end{bmatrix} + \begin{bmatrix} 0 & 0 \\ -\gamma_{L_p} & 0 \end{bmatrix} \begin{bmatrix} v_b \\ I_s \end{bmatrix} \\ \text{S}_1 \text{ open, } \text{S}_2 \text{ closed: } s \begin{bmatrix} v_c \\ i_p \end{bmatrix} &= \begin{bmatrix} 0 & -\gamma_{C_c} \\ \gamma_{L_p} & -R_p/L_p \end{bmatrix} \begin{bmatrix} v_c \\ i_p \end{bmatrix} + \begin{bmatrix} 0 & \gamma_{C_c} \\ -\gamma_{L_p} & 0 \end{bmatrix} \begin{bmatrix} v_b \\ I_s \end{bmatrix} \end{aligned} \quad (3.1)$$

The results of simulating the circuit are shown in Figures 3.9 and 3.10.

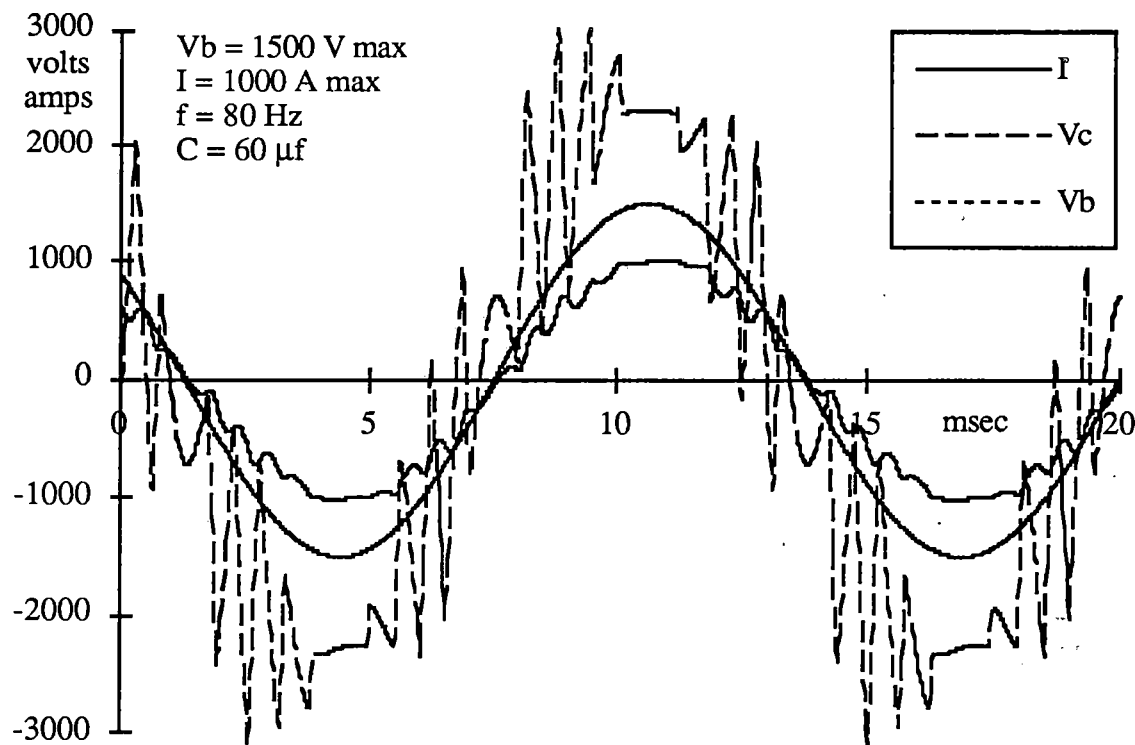


Figure 3.9. Simulated behavior of circuit of Figure 3.9.

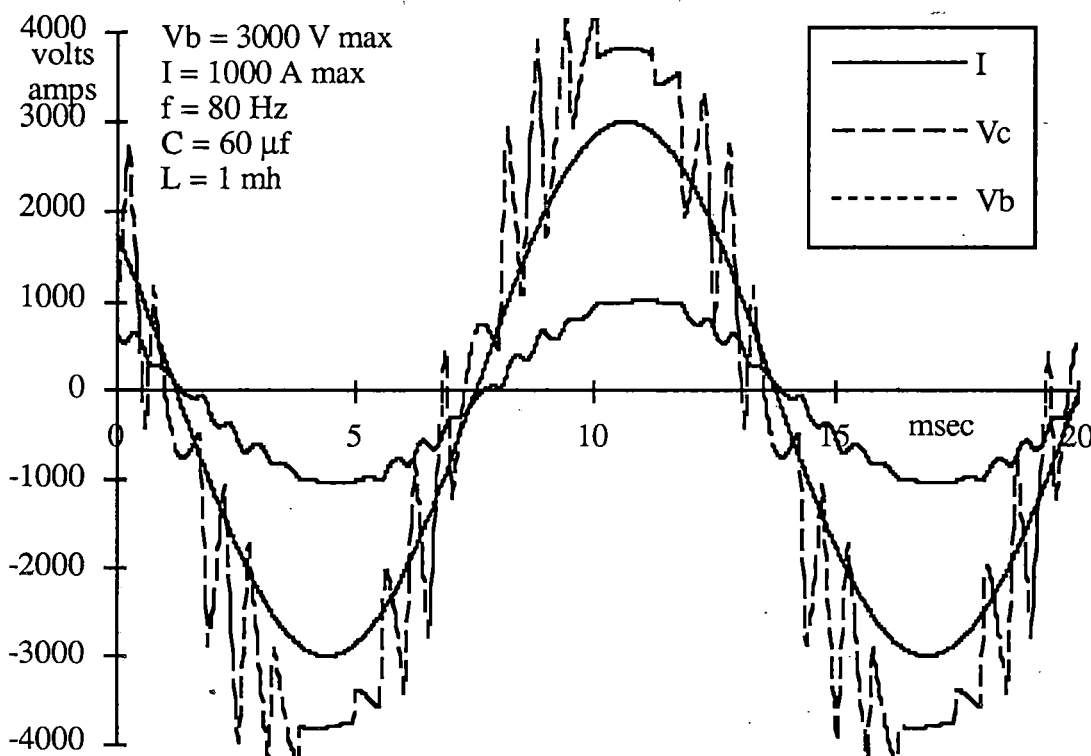
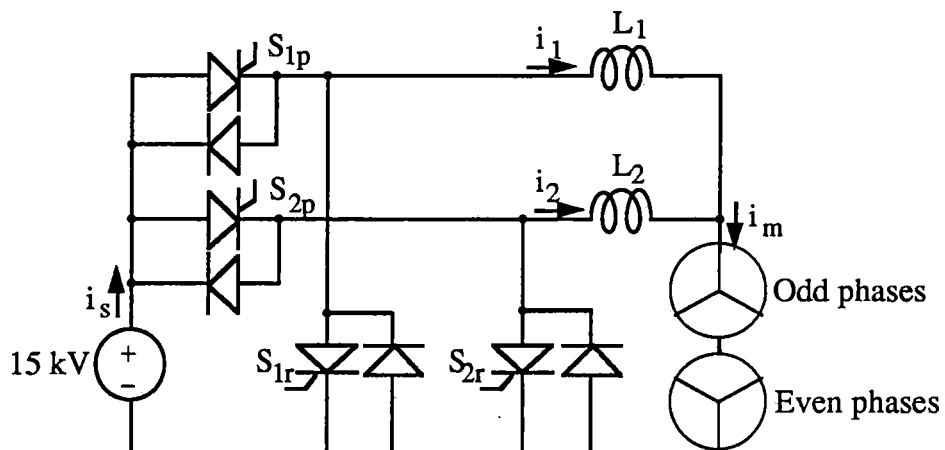


Figure 3.10. Same as Figure 3.9 except the back voltage is twice as large.

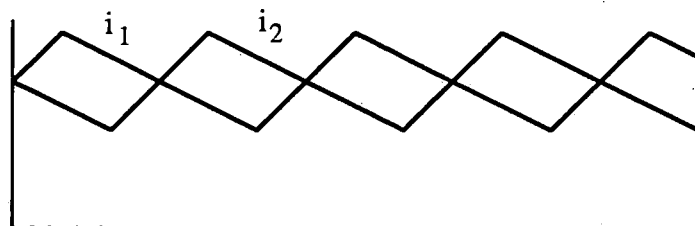
### 3.6 Chopper control

Our recommended design uses a dc power distribution bus to distribute power to the inverter stations. It is also the intention to use this dc bus for transmitting regenerated power from a braking vehicle to a vehicle which needs the power. By using a 30 kV bus it is possible to transmit power at least 30 km so the probability of finding a vehicle to absorb this power is relatively high. Note that although we use 30 kV, this is actually separate +15 kV and -15 kV voltages so the maximum voltage to ground is only 15 kV. If there are port and starboard motors, then one would be powered from +15 kV and the other from -15 kV. Alternately, if there is only one motor we would power half of the phases from each bus.

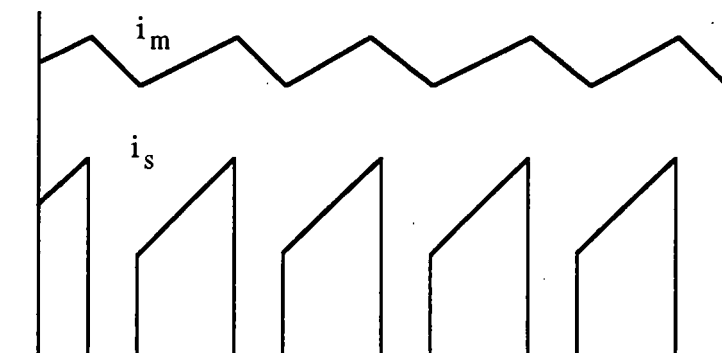
Figure 3.11 shows a two phase, two quadrant chopper. This design uses 2:1 interleaving to achieve the effect of a 2:1 step down transformer for reducing the 15 kV bus voltage to about one half that value for powering the series connected CSI. This interleaving has recently been studied in depth by Miwa [Ref. 51] and the principal conclusion is that interleaving can provide dramatic improvement in power control. Figures 3.9b and 3.9c shows typical waveforms and it is clear that large fluctuations in the current in each of the 2 inductors are added out of phase to produce relatively small current ripple in the output. The two inductors together do not need to store as much energy as the single large inductor that would be required without interleaving, and the peak input current is reduced by about a factor of 2.



(a) Two phase, two quadrant chopper



(b) Phase currents in power mode



(c) Source and motor currents

Figure 3.11. Two phase, two quadrant chopper.

### 3.7 Cost analysis

The cost per watt of power conversion circuitry does not decrease significantly as the total power capacity increases. For megawatt level converters the use of a few large power semiconductor devices creates problems because of the low yield for the large silicon area, and because of heat removal problems.

An important observation: In most megawatt level power conversion electronics the silicon power switching devices contribute only about 5% of the total cost. Silicon devices are likely to become better and less expensive, while other components are not likely to

become substantially less expensive. Thus the important design maxim: Use more silicon and less metal!

### Inverter cost

The cost of commercial motor drive inverters supplied by a number of manufacturers is given in Figure 3.12. These inverters have ratings from 75 to 750 kilowatts (100 to 1000 HP) and it is clear that at the lower end, where quantity production and competition are most extensive, the cost decreases somewhat with increasing power level. However, at the higher power levels the lack of a large market or extensive competition causes the specific cost to rise.

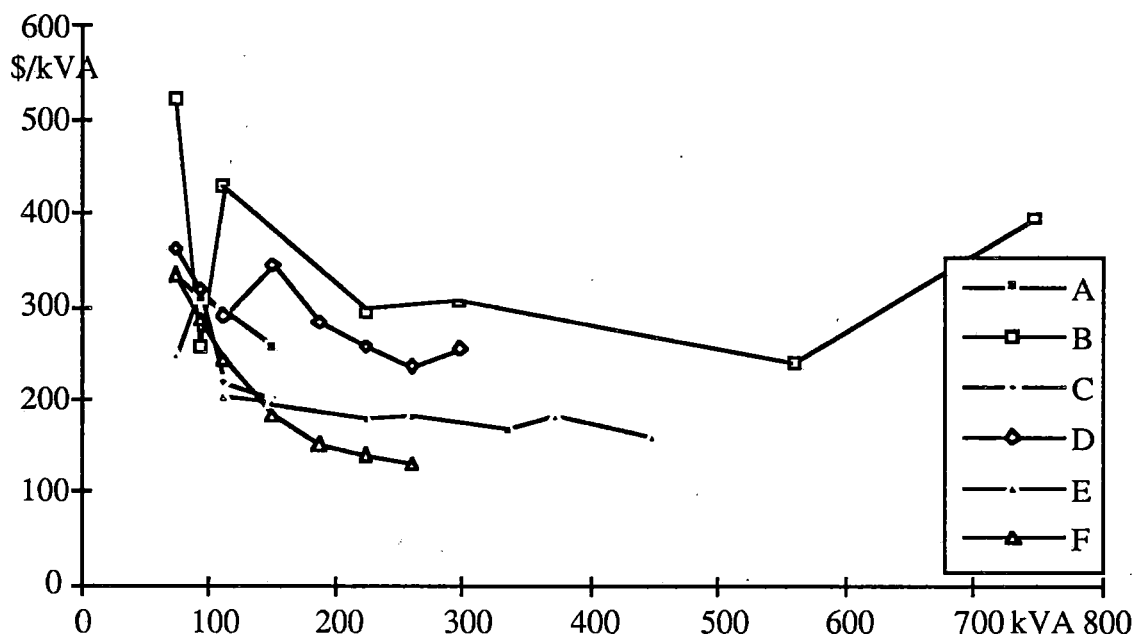


Figure 3.12. Inverter cost vs. power level for families of motor controllers.

As an independent check, an estimate of the manufacturing cost was made using a detailed cost analysis.

**Table 3.5.** Estimated cost for a 20MVA inverter including buck converter at input.

	<i>Num</i>	<i>\$/unit</i>	<i>\$</i>	<i>Tot \$</i>
Inverter, 6 1-phase bridges, 10 MW				32520
GTO, 2.5 kV, 1300 A rms	6	990	5940	
gate drive for GTO	6	630	3780	
thyristor, 3.2 kV 1300 A rms	48	200	9600	
gate drive	48	100	4800	
diode, 2.5 kV, 1300 A rms	24	100	2400	
snubber	30	100	3000	
heat removal components, 5 kW	30	100	3000	
Chopper, 2 phase, 2 quadrant, 15 kV, 700 A				36000
GTOs, 4 kV, 800 A rms	24	1000	24000	
gate drive for GTO	24	250	6000	
diodes, 3 kV, 650 A rms	24	50	1200	
snubbers	24	100	2400	
heat removal components, 5 kW	24	100	2400	
Inductors, air core, 800 A rms				8400
0.05 h, 0.1ohm, 560 kg	2	3400	6800	
heat removal equipment, 64 kW	2	800	1600	
Braking resistors				6000
1 Mw	12	400	4800	
heat removal equipment	12	100	1200	
Block switching				16800
thyristor, 3.2 kV 1300 A rms	24	500	12000	
gate drive	24	100	2400	
heat removal components, 5 kW	24	100	2400	
Sensing and control electronics				38800
Embedded control microprocessors	12	200	2400	
Communication facilities	1	10000	10000	
Zone control computer	1	20000	20000	
Position sensing	1	2000	2000	
Battery backup	1	2000	2000	
Disconnect switches	12	200	2400	
Miscellaneous				65000
building space, square meters	40	1000	40000	
mounting racks, furniture	1	5000	5000	
shipping and installation	1	20000	20000	
Total component cost				203520
spares			10%	20352
G&A, sales, manufac., eng'g			200%	447744
contingency			10%	67162
Total cost				\$738,778

### 3.8 References and Bibliography

#### General References and Review Papers

- 1 S. Bhowmik and R. Spee, "A Guide to the Application-Oriented Selection of AC/AC Converter Topologies," *IEEE Applied Power Electronics Conference*, Boston, MA, 1992, pp. 571-578.
- 2 B.K. Bose, "Adjustable Speed AC Drives - A Technology Status Review," *Proceedings of the IEEE*, Vol. 70, No. 2, February 1982, pp.116-135.
- 3 B.K. Bose, *Power Electronics and AC Drives*, Prentice-Hall 1986.
- 4 J.G. Kassakian, M.F. Schlecht, and G.C. Verghese, *Principles of Power Electronics*, Addison-Wesley, 1991.
- 5 B.L. Jones and J.E. Brown, "Electrical variable-speed drives," *IEE Proceedings*, Vol. 131 Pt. A, No. 7, September 1984, pp. 516--558.
- 6 Thornton, R, "Design Principles for Maglev," *IEEE Proceedings*, May, 1973, pp. 586-598

#### Topologies

- 7 K.E. Bornhardt, "Novel Soft-Switched GTO-Inverter Circuits," *IEEE-IAS Conference Proceedings*, 1990, 1990, pp. 1222-1227.
- 8 P.H. Chappel, R.M. Davis, and R.J. Blake, "Operating principles for hidden-link convertor drive," *IEE Proceedings*, Vol. 131 Pt. B, No. 6, November 1984, pp. 237-244.
- 9 N.S. Choi, J.G. Cho, G.H. Cho, "A General Circuit Topology of Multilevel Inverter," *PESC 91 Record*, Boston MA, August 1991, pp. 96-103.
- 10 R.W. Dedoncker and J.P. Lyons, "The Auxiliary Quasi-Resonant DC Link Inverter," *PESC '91 Record*, pp. 248-253.
- 11 R.W. Dedoncker and J.P. Lyons, "The Auxiliary Resonant Commutated Pole Convertor," *IEEE-IAS Conference Proceedings*, 1990, 1990, pp.1228-1235.
- 12 D.M. Divan and G. Skibinski, "Zero Switching Loss Inverters for High Power Applications," *IEEE-IAS Conference Proceedings*, 1987, 1987, pp. 627-634.
- 13 J. Holtz, S. Stadtfeld, and P. Lammert "An Economic Very High Power PWM Inverter for Induction Motor Drives," *European Conference on Power Electronics and Applications*, Brussels, Belgium, 1985, pp. 3.75-3.80.
- 14 P.D. Ziogas, S.I. Khan, and M.H. Rashid, "Some Improved Force Commutated Cycloconverter Structures," *IEEE 1984 Industry Applications Society Annual Meeting*, 1984, pp. 739-748.

#### Existing systems and performance data

- 15 E. Abel, J.L. Mahtani, R.G. Rhodes, "Linear Machine Power Requirements and System Comparisons," *IEEE Transactions on Magnetics*, Vol. MAG-14, No. 5, September 1978, pp. 918-920.
- 16 R. Friedrich, K. Freimann, and R. Leistikow, "The Power Supply and the Propulsion System of the Transrapid 06 Vehicle - Result of Trials," *IEEE International Conference on Maglev and Linear Drives*, Vancouver Canada, May 1986, pp. 243-249.
- 17 R. Friedrich, K. Freimann, and R. Leistikow, "The Long Stator Propulsion System of the Transrapid - Development Prospects Until Service Maturity," *IEEE International Conference on Maglev and Linear Drives*, Vancouver Canada, May 1986, pp. 171-180.

- 18 S. Saijo, S. Kioke, and S. Tadakuma, "Characteristics of Linear Synchronous Motor Drive Cycloconvertor for Maglev Vehicle ML-500 at Miyazaki Test Track," *IEEE Transactions on Industry Applications*, Vol. IA-17, No. 5, Sept/Oct 1981.
- 19 S. Suzuki, Y. Hikasa, K. Suzuki, Y. Hosoda, S. Yamoka, and N. Takada, "Power Supply to Drive HSST - EXPO '86," *IEEE International Conference on Maglev and Linear Drives*, Vancouver Canada, May 1986, pp. 251-256.
- 20 S. Tadakuma, S. Tanaka, H. Inoguchi, Y. Tanoue, H. Ikeda, and S. Kaga, "Consideration on Large Capacity PWM Inverter for LSM Drives," *Int. Power Electron. Conf (IPEC) Record*, Vol. 1, April 1990, pp. 413-420.
- 21 S. Tadakuma, S. Tanaka, K. Miura, S. Inokuchi, and H. Ikeda, "Fundamental Approaches to PWM Control Based GTO Inverters for Linear Synchronous Motor Drives," *IEEE 1991 Industry Applications Society Annual Meeting*, 1991, pp. 847-853.
- 22 G. Weigner, "GTO Convertors for Electric Rail Traction," *Translation of an article from Glasers Annalen*, Vol. 113, No. 6/7 (1989), pp. 259-272.
- 23 R. Wlodyka, "Power Characteristic Comparisons of AC Traction Inverter Systems," *IEEE-IAS Conference Proceedings 1979*, 1979, pp. 355-369.

#### Devices, Snubbers, etc.

- 24 K. Bornhardt "Switching Behaviour of a Pulse-Commutated GTO," *Third Intl. Conf. on Power Electronics and Variable Speed Drives* (IEE Conf. Publ. 291), 1988, pp. 83-86.
- 25 S. Bowes, and R. Bullough, "Optimal PWM microprocessor-controlled current-source inverter drives," *IEE Proceedings*, Vol. 135, Pt. B, No. 2, March 1988, pp. 59-75.
- 26 S. Bowes, and R. Bullough, "PWM switching strategies for current fed inverter drives," *IEE Proceedings*, vol. 131, Pt. B, No. 5, Sept 1984, pp. 195-202.
- 27 J. Holtz and S. Salama, "Megawatt GTO-Inverter with Three-Level PWM Control and Regenerative Snubber Circuits," *PESC 88 Record*, April 1988, pp. 1263-1270.
- 28 A. Mertens, H. Skudelny, P. Caldiera, and T. Lipo, "Characterization of GTOs Under Different Modes of Zero Current Switching," *PESC 91 Conference Record*, 1991, pp. 444-452.
- 29 H. Patel, and R. Hoft, "Generalized Techniques of Harmonic Elimination and Voltage Control in Thyristor Inverters: Part I - Harmonic Elimination," *IEEE Transactions on Industry Applications*, Vol. IA-9, No. 3, May/June 1973.
- 30 J. Pascal, G. Coquery, and R. Lallemand, "Increasing Frequency using GTO in Gate-Assisted-Turn-Off Mode," *Third Intl. Conf. on Power Electronics and Variable Speed Drives* (IEE Conf. Publ. 291), 1988, pp. 87-90.
- 31 B. Passerine, S. Tenconi, and M. Zanbelli, "High Power GTOs Characteristics: A Comprehensive Review," *IEEE 1984 Industry Applications Society Annual Meeting*, Oct 1984, pp. 920-922.
- 32 S. Tenconi, M. Zambelli, L. Malesani, and P. Tenti, "The Reverse Blocking GTO as a Very Fast Turn-Off Thyristor," *Proc. of IEEE-IAS Ann. Meeting*, 1986, pp. 377-383.
- 33 B. Williams and P. Palmer, "Drive and Snubber Techniques for GTOs and Power Transistors - Particularly for Inverter Bridges," *Power Electronics and Variable Speed Drives* (IEE Conf. Publ. No. 234), 1984, pp. 42-45.

**Current-Source Inverter Technology**

- 34 S. Biswas, B. Basak, S. Sathiakumar, and J. Vithayathil, "A New Three-Phase Current Source Inverter with Flexible PWM Capability," *IEEE Transactions on Industry Applications*, Vol. IA-23, No. 5, Sept./Oct. 1987, pp. 921-926.
- 35 S. Bowes, and R. Bullough, "Novel PWM Controlled series-connected current-source inverter drive," *IEE Proceedings*, Vol. 136, Pt. B, No. 2, Mar. 1989, pp. 69-82.
- 36 Y. Chung and G. Cho, "New Current Source Inverters with dc-Side Commutation and Load-Side Energy Recovery Circuit," *IEEE Transactions on Industry Applications*, Vol. 27, No. 1, Jan/Feb 1991, pp. 162-171.
- 37 D. Dewan, S. Rosenberg, N. Nicholson, "Comparison of Single Phase Current Source Inverter Configurations," *IEEE-IAS Conf.Proc.1975*, 1975, pp. 783-789.
- 38 M. Hombu, S. Ueda, and A. Ueda, "A Current Source GTO Inverter with Sinusoidal Inputs and Outputs," *IEEE Transactions on Industry Applications*, Vol. IA-23, No. 2, March/April 1987, pp. 247-255.
- 39 T. Lipo, and L. Walker, "Design and Control Techniques for Extending High Frequency Operation of a CSI Induction Motor Drive," *IEEE Transactions on Industry Applications*, IA-19, No. 5, Sep/Oct 1983, pp. 744-753.
- 40 Y. Murai, and T. Lipo, "High Frequency Series Resonant DC Link Power Conversion," *IEEE-IAS Conference Record*, 1988, pp. 648-656.
- 41 Y. Murai, H. Nakamura, T. Lipo, and M. Aydemir, "Pulse-Split Concept in Series Resonant DC Link Power Conversion for Induction Motor Drives," *IEEE Industry Application Society Annual Meeting*, 1991, pp. 776-781.
- 42 S. Nonaka, and Y. Neba, "A PWM GTO Current Source Converter-Inverter System with Sinusoidal Inputs and Outputs," *IEE Transactions On Industry Applications*, Vol. IA-25, No. 1 Jan/Feb 1989, pp. 76-85.
- 43 R. Palanappian, "Voltage Clamping Circuits for CSI/IM Drives," *IEEE Transactions on Industry Applications*, Vol. I-21, No. 2, Mar/Apr 1985, pp. 429-447.
- 44 M. Showleh, W. Masowskim and V. Stefanovic, "An Exact Modeling and Design of Current-Source Inverters," *IEEE Industry Applications Society Annual Meeting*, 1979, pp. 439-457.

**Parallelized /Distributed Power Conversion**

- 45 M. Honbu, Y. Matsuda, K. Miyazaki, and IY. Jifuku, "Parallel Operation Techniques of GTO Inverter Sets for Large AC Motor Drives," *IEEE Industry Applications Society Annual Meeting*, 1982, pp. 657-662.
- 46 J. Kassakian, "High Frequency, High Density Converters for Distributed Power Supply Systems," *Proceedings of the IEEE*, Vol. 76, No. 6 June 1988 (invited).
- 47 J. Kassakian, "High Frequency Switching of Distributed Conversion in Power Electronic Systems," *Proceedings of the 6th Conference of Power Electronics an Motion Control*, Budapest, Hungary, 1990h.
- 48 T. Kawabata, and S. Higashino, "Parallel Operations of Voltage Source Inverters," *IEEE Transactions on Industry Applications*, Vol. 24, No. 2, March/April 1988.
- 49 S. Okuma, K. Iwata, and K. Suzuki, "Parallel Running of GTO PWM Inverters," *PESC '84 Conference Record*, 1984, pp. 111-120.
- 50 F. Petruzziello, P. Ziogas, G. Joos, "A Novel Approach to Parallelizing of Power Converter Units with True Redundancy," (PESC, APEC, or IAS), 1990, pp. 808-813.
- 51 B. Miwa, "Interleaved Conversion Techniques for High Density Power Supplies," MIT Ph.D Thesis, May, 1992.

## 4 Power Distribution

*The power distribution system accepts power from electric utility operated high voltage transmission lines and distributes this power at lower voltages to the electronic power inverters. This section describes power distribution alternatives for an LSM propulsion system including the option of distributing energy that is regenerated from braking vehicles. Among the issues discussed are reliability, flicker, harmonic power generation, and fault tolerant design. This section also discusses methods of estimating the cost of delivered energy.*

### 4.1 Overview

The power distribution system will normally have the generic form shown in Figure 4.1. Substations located every 20 to 50 km convert 3-phase, high voltage utility power to lower voltages suitable for distribution. The power distribution can be either dc or 3 phase ac with typical voltages in the 15 to 33 kV range. Power is distributed along the guideway to wayside inverters which generate variable voltage, variable frequency power for the LSM. This power system is similar to ones used for conventional electrified rail and does not pose any problems that have not been addressed in that context.

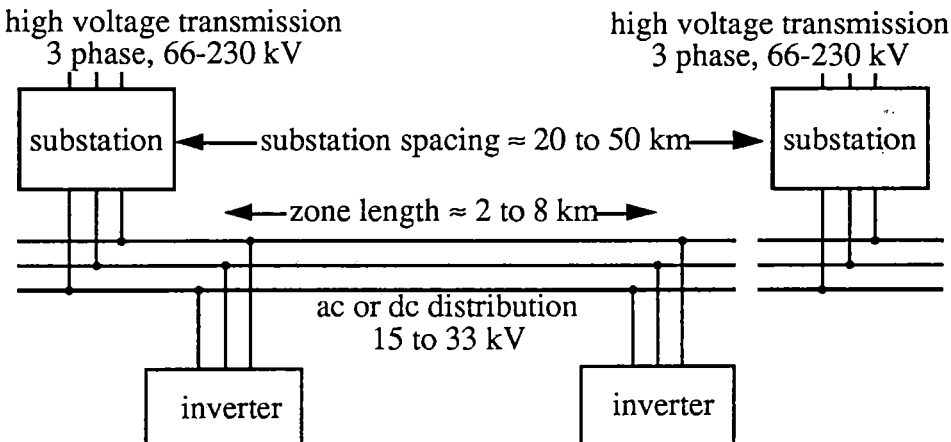


Figure 4.1. Generic power distribution system.

The choice of transmission line voltage is based on availability and power requirements. Lower transmission voltages are preferable because they lead to lower cost substations. Transmission voltages less than 66 kV will not normally have enough capacity for a high speed maglev system, and even 66 kV systems may be inadequate for reasons to be discussed. Voltages over 230 kV will lead to very high substation cost and should be avoided unless the maglev substation can share facilities with other power users.

The choice of distribution voltage is based on power levels and distribution distances. Most high speed rail systems use 25 kV, the exception being the German ICE which uses 15 kV because of a 1912 decision. The German Transrapid maglev design is based on a 20 kV, 3 phase distribution system that is common in Germany. U.S. studies have arrived at voltages in the 30 kV range as more suitable for U.S. maglev.

The substations contain transformers, circuit breakers and equipment for disconnection, switching, protection and control. For dc distribution the substations also include a rectifier, and there are options as to whether the rectifier can regenerate power into the utility system and as to whether there is a dc voltage control capability.

The detailed design decisions will be based on required power levels and headway distances. As an example, if the vehicles can operate with headways as short as 4 km and each vehicle requires about 6 MW average power, then a 2-way system will require 3MW per km. If the substations are spaced at 25 km, then the maximum average power per substation is 75 MW. Because of statistical fluctuations in headway and power levels, the maximum power averaged over several minutes will be less than this value, but the instantaneous peak power could be significantly larger.

## 4.2 Utility issues

Conventional electric trains are single-phase loads, while proposed maglev systems have the advantage of being balanced three-phase loads. This avoids a difficult load balance problem, but maglev still has all of the other utility problems associated with electrically propelled rail systems. These include power regeneration hazards, periodic power fluctuations (i.e. flicker), harmonic generation, and power flow. Evaluation of these issues is required to verify that they do not adversely affect the utility power systems.

### Regeneration into the utility grid

Recovering of energy from decelerating vehicles is done in many electric rail systems, such as the German ICE and the San Francisco BART systems. In low speed transit applications there is almost always a vehicle near enough to absorb the regenerated power. A typical design allows power to be returned to the overhead catenary or third rail whenever the generated voltage is less than 110% of the normal supply voltage. When voltages exceed 110% of the nominal level, dynamic braking resistors are used to dissipate the excess power. A very similar system seems ideal for a short headway maglev system. With the dc distribution option it is relatively inexpensive to distribute regenerated power, and with a 30 kV bus the power could be transmitted as far as 30 to 50 km.

With large vehicle headway, such as proposed by Transrapid, in conjunction with their larger vehicles, the headway is on the order of the substation spacing so there may be no power distribution along the guideway. Regenerating energy back into the transmission system is an option that can save Transrapid significant energy. However, since they are using ac distribution there could be serious utility problems unless there is specific provision to protect the utility system when the transmission line can not absorb the power without exceeding a voltage limit. The regeneration may also create excessive harmonic power and flicker.

With small headway systems there will typically be several vehicles powered from a single substation, so the regeneration can be limited to providing power to neighboring vehicles. This is particularly convenient with dc distribution and it may preclude the need for substation rectifiers with 4-quadrant capability.

### Periodic power fluctuations

Momentary fluctuation in transmission line voltages, or "flicker," causes irritating fluctuation in electric lighting connected on a utility system. All electrically propelled rail systems can create flicker problems as the vehicles accelerate, decelerate, and possibly regenerate power into the utility grid. In order to reduce flicker to acceptable levels, utilities have created requirements for loads that are subject to large and frequent changes. All electrically propelled rail systems must meet these flicker constraints.

Power fluctuation is important primarily because it can produce visual changes in electric lighting, so the flicker specification is related to how rapidly the maglev load varies, and how big a change it produces in transmission line voltage. When the power is extracted from a 220 kV transmission line there is very little effect because the maglev load is a small fraction of the total load, but for 66 kV transmission voltages the problem is more serious. The measure of acceptability is related to the ratio of the load current to the short circuit current of the transmission system. Although flicker is well understood, maglev has more potential to produce flicker than any existing utility load.

Southern California Edison has created Planning Guidelines for flicker and these are shown in Figure 4.2. For a maglev system with reasonable traffic density the flicker frequency will be on the order of a few hundred "dips" per hour, so the voltage flicker must be less than about 1 %. With the possibility of a single vehicle producing fairly rapid changes from -10 MW to +20 MW, the need to reduce flicker to 1% may require the use of 110 kV power lines.

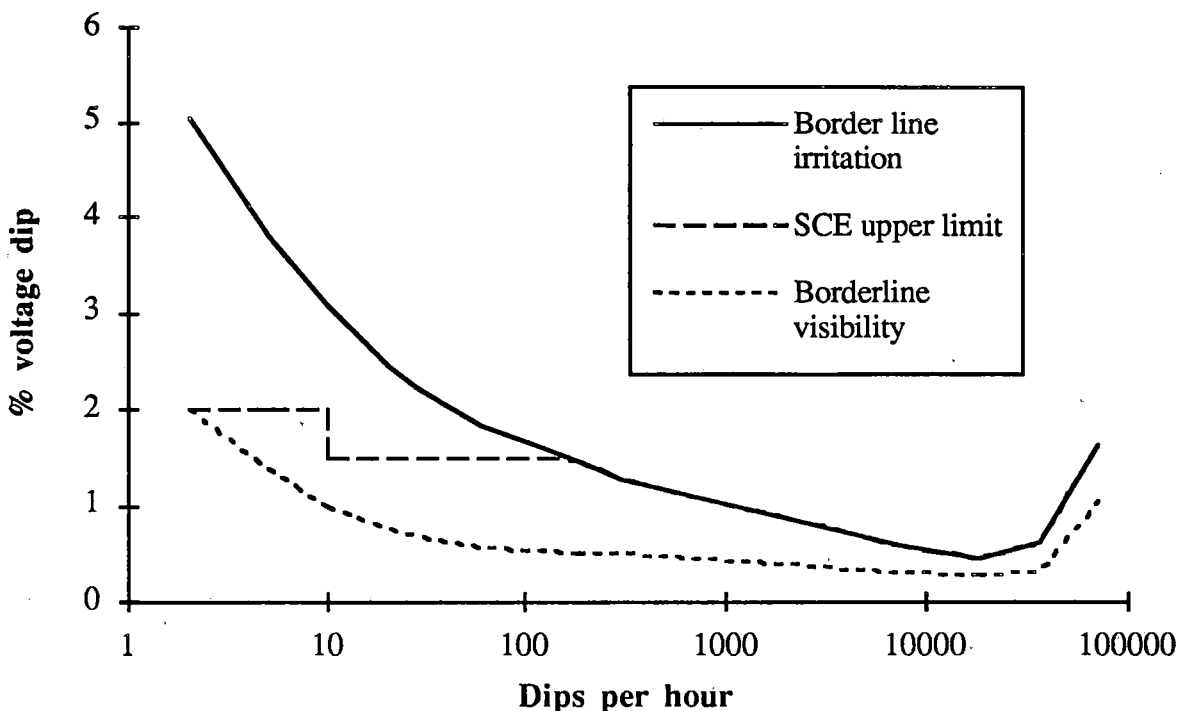


Figure 4.2. Flicker guidelines for Southern California Edison loads.

Large headway systems, such as Transrapid, will have more trouble meeting flicker guidelines because there are larger load changes and no one substation will be powering more than 2 or 3 vehicles at any one time, so there is less averaging. This may necessitate the use of 110 kV or higher transmission line voltages. With smaller vehicles and shorter headway it is conceivable that one could enforce "cooperation" between neighboring vehicles so that only a small number of vehicles in one region will accelerate rapidly at the same time.

### Harmonics

Any variable speed motor can create power at frequencies other than the power distribution frequency. The other frequencies can be harmonics of the power system frequency, such as 120 or 180 Hz for a 60 Hz system, or they can be entirely different frequencies, often related to the motor speed or the switching frequency of the motor controller. Higher frequencies can usually be removed by proper design of the power electronics or addition of filter circuits, but the generation of power frequency harmonics requires special consideration.

As an example of harmonic generation, Figure 4.3 shows the output voltage of an n-pulse rectifier assuming sinusoidal voltage sources connected to ideal diodes. The

waveform shown is for a 6-pulse rectifier; for example, this could be the output from a full-wave, 3-phase bridge. The output voltage can be represented as the sum of dc plus harmonics of the power line. For a  $n$ -pulse rectifier the harmonics generated are multiples of  $n$  times the power line frequency. For 60 Hz power and a 6-pulse rectifier the harmonics are 360 Hz, 720 Hz, etc.

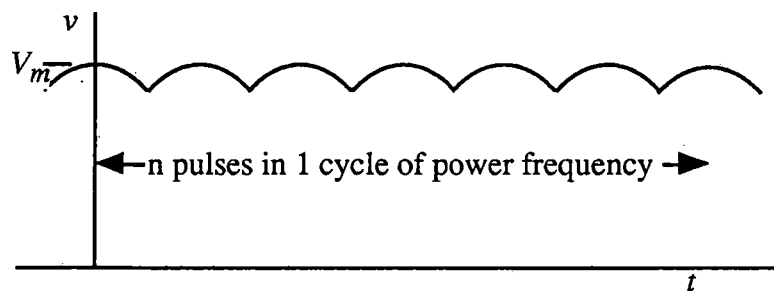


Figure 4.2. Voltage waveform for an  $n$ -pulse rectifier.

Table 4.1 gives the ratio of the rms voltage of all of the harmonics to the total rms voltage. For pulse numbers greater than 6 the ac harmonic power is inversely proportional to the square of the pulse number. Note that if the load is not a resistance, then the power in the harmonics is not necessarily proportional to the rms harmonic voltage. Also, if the transformer and rectifier circuits have a finite resistance and inductance, these impedances can create additional harmonic power.

Table 4.1. Percent rms voltage of harmonics as a function of the pulse number.

$n$	total harmonic %
4	8.79
6	4.00
8	2.27
12	1.02
18	0.45
24	0.25

In most applications a 12 pulse rectifier produces adequately low harmonic power. This type of rectifier is readily constructed by stacking two 3-phase 6-pulse rectifiers in series. Both rectifiers are powered from the same transformer, but one of the rectifiers uses a Y connected secondary and the other uses a  $\Delta$ -connected secondary. This leads to a reasonably efficient use of the transformer, and is an established practice in providing high power dc, such as for transit applications.

It is possible to construct a rectifier with silicon controlled rectifiers instead of diodes, and then control the firing time to control the output voltage. This scheme is effective in regulating voltage and is not much more expensive than a diode rectifier. Unfortunately, it can reduce the power factor by a significant amount and it may be necessary to use substantial filtering to eliminate the effects of the harmonics.

### Power flow

In the distribution system of Figure 4.1 it is possible for power to flow from one transmission line to the other through the distribution circuit. This power flow poses serious problems to the utilities and must usually be avoided. There are known circuit breaker schemes for providing protection, but these could impose reliability problems on the maglev system. One of the virtues of dc distribution with diode rectifiers is that it is inherently impossible for power to flow from one transmission line to another through the dc link. With a dc link there does not appear to be a need for regeneration into the utility grid, so this seems to be an ideal solution to both the power flow and regeneration problems.

### 4.3 Power distribution examples

This section provides an overview of various existing and proposed scenarios for power distribution for high speed rail and maglev.

#### AC distribution for high speed rail

The first experiments with electric trains were done by Mr. Siemens in Germany in the late 1800s. Early designs used a variety of power distribution schemes, including 3-phase overhead catenary systems with three pantographs for power pickup. An electric vehicle with 3-phase pickup set a speed record of 60 m/s (134 mph) in 1903. The early attempts to use induction motor drives gave way to designs using series dc traction motors with mechanical commutation. The variety of early designs led to a variety of power distribution systems, and the lack of uniformity had a serious impact on the growth of electric powered rail systems. As a result, in 1912 Germany standardized on a 15 kV, 16 2/3 Hz distribution system, and this is used throughout Germany today, even though it is far from an optimum choice for modern propulsion. The power is generated by a special railroad power system.

The German Inter City Express locomotives each have a 4.5 MVA transformer and a single phase rectifier that produce a dc voltage of 2800 Vdc for the electronic inverters. Because of the low frequency, the transformer weight is 10 tonnes and constitutes 10% of the weight of the locomotive. When trains enter and leave Germany they must change

locomotives because most other European countries have a different standard. Some of the newer locomotives have power electronic systems that can accommodate a range of power sources, so the lack of a common standard is becoming less significant. When all locomotives are equipped with dual power capability Germany may well change to a higher voltage, higher frequency distribution system.

For the French TGV and most new high speed European rail systems the power distribution is at 25 kv, 50 Hz single phase. The use of single phase power is mandated by the use of a single catenary with rail return. The large single phase load produced by electrified rail can create severe unbalance on the otherwise balanced 3-phase utility power distribution system. It also requires unsightly overhead power distribution lines. Recent proposals for new electrification of U.S. rail from New Haven to Boston are planned to use a new type of catenary tower with less objectionable environmental impact.

Japan has both 50 Hz and 60 Hz utility systems. When they built the Shinkansen high speed rail system they made the decision to use 60 Hz throughout. This entailed the use of large rotary power converters in regions of the country where 50 Hz was the utility power frequency. The existing and proposed extensions to Shinkansen use 25 kV, single phase 60 Hz power.

### AC distribution for maglev

For maglev with ac distribution the substations include:

- Three-phase transformers that convert utility transmission voltages to lower voltages suitable for distribution;
- Three phase ac distribution lines that are underground or mounted in the guideway, and deliver the ac power to the inverter stations;
- Associated circuit breakers and disconnects that protect both the electric utility and distribution system from faults;
- A control system that monitors and controls the various parts of the system.

For the Transrapid design the proposed distribution uses 20 kV, 3 phase, 50 Hz with transformers and rectifiers that produce 2.6 kv dc at the inverter stations. Recent U.S. System Concept Designs have proposed similar systems, typically with 33 kV, 60 Hz power distribution and a second set of transformers located at the inverter stations.

### DC distribution for maglev

For maglev with dc distribution the substations include:

- Transformers that convert utility transmission voltages to lower voltages suitable for driving rectifiers;
- 12-pulse rectifiers that create dc power for distribution along the guideway;
- Distribution lines that are underground or mounted in the guideway, for delivery of the dc power to the inverter stations;

- Associated ac circuit breakers and disconnects that protect both the electric utility and distribution system from faults;
- A control system that monitors and controls the various parts of the system.

There is merit in having dc circuit breakers for the distribution system but, because dc breakers are not readily available and are expensive, it is worth considering systems that do not require dc breakers. For example, one can use dc disconnects and momentary activation of the ac circuit breakers to turn the power off before the disconnects are activated. Alternately, it might be possible to use solid-state circuit breakers with the ac breakers used as a last resort in case of extreme failure conditions. Ultrahigh-voltage dc transmission systems have successfully avoided the use of dc circuit breakers.

#### 4.4 A dc distribution system

Figure 4.3 shows a maglev utility substation for a dc distribution system. This is particularly appropriate to an EDS system with short headway vehicles and high acceleration and deceleration capability:

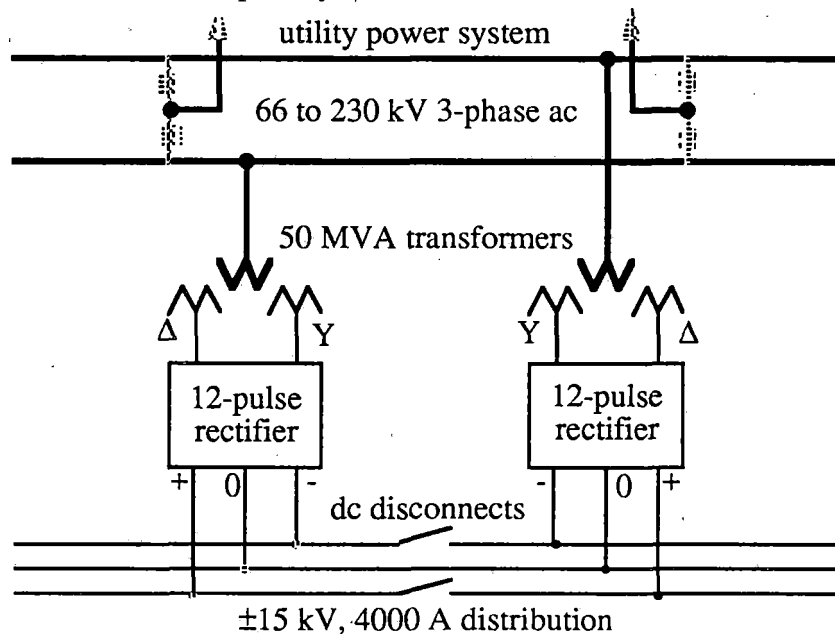


Figure 4.3. Maglev dc substation (courtesy of Southern California Edison).

The substation depicted in Figure 4.3 is based on a load of 75 MVA with 30 kV dc distribution. The dc bus includes a mid point ground return so that the load can use the + and - voltage buses as separate supplies provided the load is approximately balanced. This type of 3-wire bipolar system is now common in dc transmission systems.

### Fault tolerant considerations

A fault tolerant design philosophy must be used to ensure reliable operation in spite of many types of failures of individual parts of the system. Typical fault tolerant features are shown in Figure 4.3 and itemized below.

- The control system allows reduced power operation in case of failure of any part of the system. At times of peak load the reduced power may require the vehicles to slow down or accelerate less rapidly, but the guideway capacity need not be reduced so the slow down affects only a few kilometers of the guideway. At times of reduced guideway loading, and for most types of failure, there would be no reduction in operating speed. Monitors on the transformer and rectifier can allow some overload as long as temperature and current limits are observed. For example, in cold weather the transformers will be able to operate indefinitely at higher than rated power.
- There are two parallel connected transformer and rectifier modules at each utility substation. A failure in either module does not prevent the system from continued operation at reduced power. In this case the neighboring power stations pick up the additional load with a modest increase in power loss on the dc distribution system.
- The dc distribution cables are mounted in the guideway or buried underground so they are not exposed to severe weather conditions and hence are less subject to failure.
- The transformer and rectifier modules are standardized so that mobile spares can be located at appropriate intervals along the guideway. This method is used for existing utility transformers, and it is fortuitous that a 50 kVA, 3-phase transformer can be carried on a flat bed trailer so that a reasonably rapid installation of a spare is possible.
- The dc distribution uses +15 kV and -15 kV with a neutral ground return. In case of a failure in either the plus or minus power bus the system can operate at reduced power and speed using the other power bus.
- The multiple power feed for the guideway distribution systems prevents a power interruption of at any one of the substations from halting operation. The only effect is reduced power availability, and thus a possible need for reduced speed operation.
- The normal design does not use a battery backup for the dc distribution power, but in regions where power outages are unusually common it is possible to install battery backup modules. In some cases it may be desirable to install cogeneration peaking power, and excess power could be sold to the utilities at times of high demand but could also provide emergency power backup. Operating statistics for most utilities indicate that the probability of failure of two adjacent power line interconnects will be extraordinarily rare, on the order once every 5 or 10 years for failures of more than a few minutes. This excludes power interruption due to extreme weather conditions which would cause the maglev system to be shut down even if there was no power failure.
- Circuit breaker protection on the ac side of the transformers allows the system to clear most types of faults, such as ones due to lightning, and will allow the isolation of sections that can not be cleared so as to avoid shutting down the entire maglev system.

### 4.5 Cost analysis

#### Capital cost

Southern California Edison did a study of the cost of providing a utility interface for a maglev system connecting San Diego to Sacramento with a spur to San Francisco. The

results of this study led to an estimated cost of approximately \$2,700,000 to \$2,800,000 per mile for a 640 mile installation. This cost was 53.5% for new maglev substations, 13.5% for additions at existing substations, and 33% for transmission and subtransmission line work. The cost included all components shown in Figure 4.3 but did not include the cost of the dc distribution system.

SCE estimated the cost of the dc power distribution system with results as shown in Table 4.2.

Table 4.2. Cost of dc power distribution.

	<u>Underground</u>	<u>Overhead</u>
Cable:	Power Ground Return	2000 KCM Cu 1033 KCM Al
<u>Cost</u>	<u>\$1000/mile</u>	<u>\$1000/mile</u>
Construction	390.0	26.0
Material	568.0	182.0
Home office	48.0	10.4
Contingency	96.0	20.8
<u>Construction overhead</u>	<u>276.0</u>	<u>59.8</u>
Total cost, \$1000 per mile	\$1378.0	\$299.0

Summary: for underground installation the total estimated power system cost is about \$3,100,000 per mile or \$1,930,000 per km. At least \$670,000 km can be saved by using overhead power lines, but it may be possible to mount the dc bus on or in the guideway and achieve the advantage of underground installation without the high cost.

#### Power cost

There is a 3 to 1 variation in power cost from one region of the country to another, and each region distributes the charge differently. As a guide to typical cost, Table 4.3 lists the ratio of kWh usage to total cost for large industrial customers. This table includes the lowest cost state, Kentucky, and the highest cost state, Hawaii, as well as states in which early maglev systems are most likely to be built. For a maglev system that owns the substations and distribution facilities, and assuming a vehicle consumes 5 to 10 MW for level cruise power, it may be possible to reduce the cost an additional 20% below the values given in Table 4.3. If utilities own the substations and have to install new power plants to provide power for a maglev system, the cost could be substantially higher.

**Table 4.3.** Average power cost for large industrial users by state.

<i>State</i>	<i>\$/MWh</i>
Kentucky	33
Wisconsin	42
Texas	45
Maryland	47
Illinois	48
Ohio	49
Florida	51
Pennsylvania	59
California	62
New York	72
New Jersey	74
Massachusetts	80
Connecticut	81
Hawaii	108

Assumptions: 10 MW demand, 5,000 MWh/month usage.

Source: Based on Edison Electric Institute's Typical Bills, from *Plants, Sites and Parks*, Sep/Oct '92, Vol. 19, No. 6.

### **Cost of delivered electric energy**

Most utilities are expected to be willing to offer a large customer a choice as to who owns the substations and distribution facilities. If the utility owns and operates this equipment, they would increase the electric power charges to cover the amortized capital cost. In the case of SCE, the electric cost per kWh would be about 40% less if the maglev system operator owned the substations and distribution system and purchased the power in bulk directly from the transmission lines.

The ownership decision will ultimately be based on the most favorable overall economics, but in estimating cost one should be careful to separate the equipment cost from the base cost of electricity as delivered from the transmission lines. In most parts of the country the cost of bulk power is expected to be in the range \$40 to \$60 per MWh. A heavily used system could have 500,000 vehicle passages per year on each km of guideway. With a 5 MW consumption at 125 m/s the total power usage would be 6,700 MWh per year per km. Therefore, the power usage cost would be between \$230,000 and \$400,000 per km per year. Assuming a power system cost of \$1,500,000 per km and 10 % interest and amortization, the capital cost would add about \$22 per MWh to the cost of electricity. Thus, a good median estimate for electric energy delivered to the inverters is \$75 per MWh.

Assuming a vehicle consumes an average of 5 MW at 125 m/s and carries 110 passengers, the electric consumption is 0.100 kWh per passenger km. At a cost of \$0.075 per kWh; the electric cost is about \$0.008 per passenger km. If one assumes this as the operating cost, then there is no additional cost associated with the power distribution system. Alternatively, one could assume a power cost of \$0.05 per kWh and an additional capital cost of about \$1,500,000 per km.

## References and Bibliography

### Books

- 1 ICE: High-tech on rails, Rahn, T., Hochbruck, H., & Moler, F. W., Hestra-Verlag, 1991.
- 2 Straszak, A., Tuch, R., Eds., *The Shinkansen High-Speed Rail Network of Japan*, Proceedings of an IIASA Conference, June 27-30, 1977, Pergamon Press, New York, 1980.
- 3 Power Systems Harmonics, Textbook, Arrigallaga, Bradly, J., Bodger, P. S., John Wiley & Sons Ltd., 1985.
- 4 Heinrich, Klaus & Kretzschmar, Rolf, Editors, *Transrapid Maglev System*, Hestra-Verlag Darmstadt, 1989 (ISBN 3-7771-0209-1).
- 5 Principles of Power Electronics, Kassakian, J. G., Schlecht, M. F., & Verghese, G. C., Addison Wesley, 1991

### Papers

- 6 IEEE Guide for Harmonic Control and Reactive Compensation of Static Power Converters, ANSI/IEEE Standard 519-1981.
- 7 Unbalance and Harmonic Studies for the Channel Tunnel Railway System, Barnes, R., Wong, K. T., IEE Proceedings Paper, Part B: Electric Power Applications vol. 138, No. 2, March 1991, pp 41-50.

## 5 Control

*The control system is a critical part of the LSM because it affects many system attributes, including safety, reliability, fault tolerance, efficiency, and passenger comfort. Control of a synchronous motor depends critically on position sensing, and multiple position sensing schemes are mandatory. This section discusses all of these issues and describes a novel position sensing scheme that shows promise for high accuracy and reliability and low cost. There is also a discussion of observer based control, the preferred scheme for enhancing performance and improving efficiency.*

### 5.1 Overview

The motor primary is driven by an inverter that produces a magnetic field pattern that moves along the guideway as a traveling wave. The velocity and position of the traveling wave are determined by the frequency and phase of the currents in the motor windings. The interaction of the traveling magnetic field pattern produced by the winding currents with the field produced by the vehicle coils produces forces that propel and, in some cases, lift and/or guide the vehicle.

A synchronous motor produces a net force only when the stator and rotor fields are stationary with respect to one another. Without the use of damper windings, a stable synchronization of the stator and rotor fields can be accomplished only if rotor position and velocity information are utilized by a controller to derive and produce the correct currents in the stator windings.

The control is best done by an observer based control system that continually compares the speed and position of the motor with a prediction based on a mathematical model of the propulsion system. This observer allows the system to provide more precise control and to follow a predefined velocity profile that takes account the known attributes of the route, such as hills, turns, and expected wind velocity. An observer based control also allows the system to detect any deviations from normal behavior that may require special attention.

### 5.2 Position Sensing

A closed loop control scheme requires a sensor to determine the position of the vehicle. Some control systems require a rotor velocity sensor, others derive velocity information from repeated sensing of position. Rotary synchronous motors often utilize optical shaft encoders or hall-effect sensors, but the cost of placing optical or hall-effect position sensors along the entire length of the maglev guideway is prohibitive.

In addition to sensing position, several "sensorless" position sensing schemes have been proposed for use in rotary machines. These schemes rely on sensing the voltage induced in the stator windings by the moving magnetic field of the rotor. This "back EMF" is substantial when the rotor velocity is large, and reliable sensing is possible. However, when the rotor is moving slowly, or is stationary, the back EMF is small and masked by voltage drops in the winding impedance. While it is theoretically possible to operate without induced voltage sensing, this does not seem to be a wise choice.

### Proposed position sensor

It is preferable to have a position sensing system that will operate reliably at slow vehicle speeds. A proposed position sensing concept is pictured in Figure 5.1. An inductor and its driver are located in the vehicle. The inductor is driven with a current  $I_L = I_c \sin \omega_c t$  which links a flux  $\lambda = \Phi_0 \sin \omega_c t$  with the three stator winding phases located in the guideway. The amount of flux linked by each of the stator phases varies as a function of vehicle position. Figure 5.1 is drawn with the vehicle in the position that links the maximum possible amount of flux with stator phase A; define this position as  $\theta = 0$ .

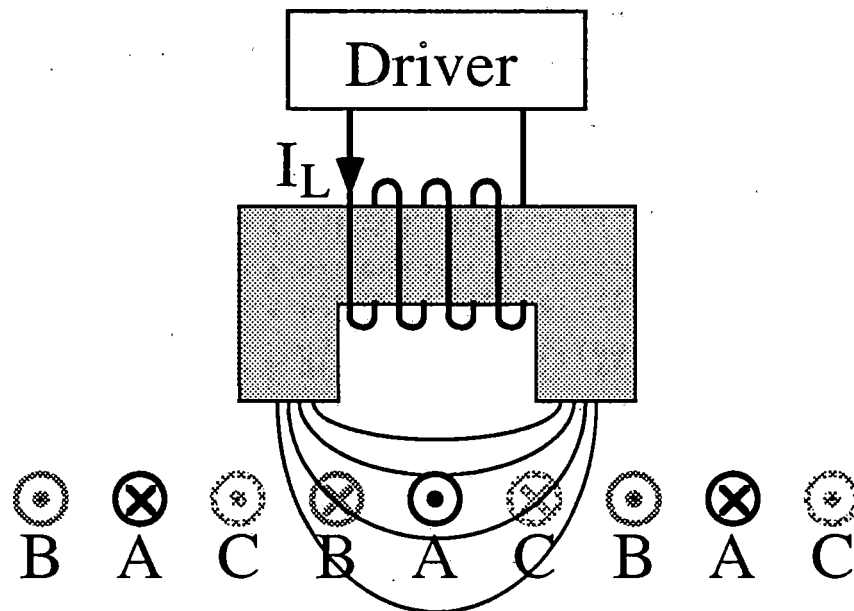


Figure 5.1. Position Sensing Pictorial.

Note that each of the induced phase voltages represents a signal at the carrier frequency  $\omega_c$  amplitude modulated by the cosine of the position  $\theta$  (or  $\theta$  shifted by  $\pm 2\pi/3$ ). The frequency of the carrier is chosen to be much higher than the frequency of position variation. Figure 5.2 shows a plot of the modulated signal for a the vehicle accelerating from a stationary state at position  $\theta = 0$ .

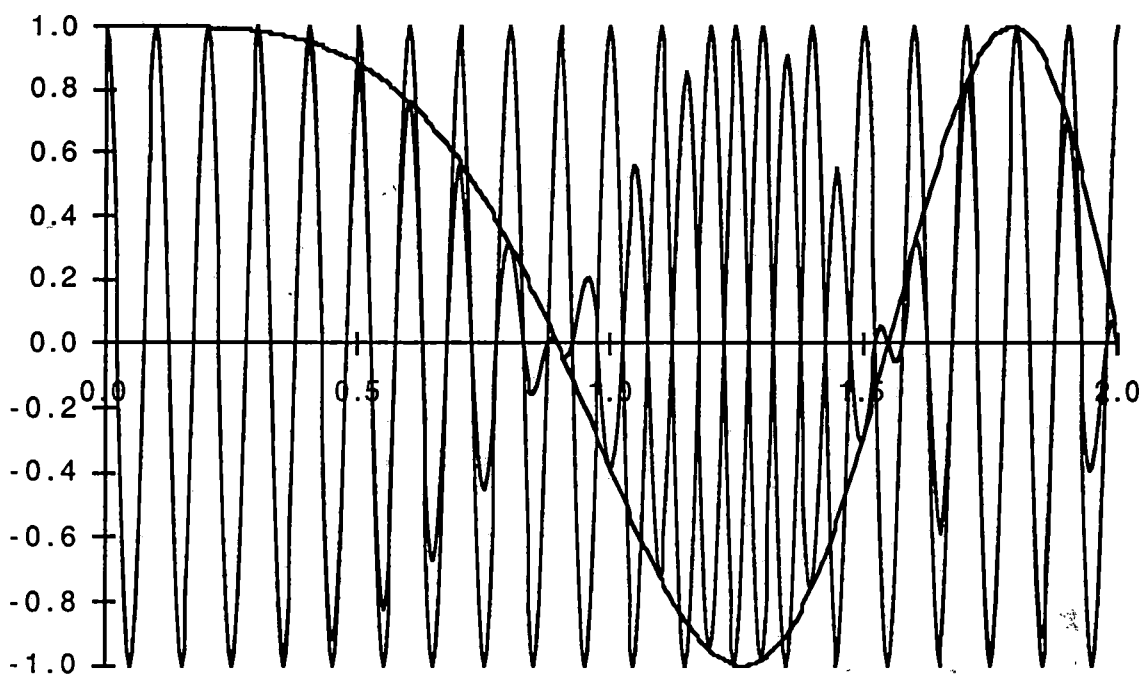


Figure 5.2. Modulated carrier sensing signal for an accelerating vehicle.

A block diagram of the system to extract the position information from the modulated carriers present on the stator phase windings is shown in Figure 5.3. Each phase voltage is first sent through a band-pass filter centered at the carrier frequency to reject signals other than the position information. A synchronous demodulator extracts the envelope waveform from each modulated carrier, and an A/D converter digitizes the envelopes. An algorithm implemented in the microprocessor determines the position of the vehicle by finding the value of  $\theta$  that best solves the nonlinear system equations relating the envelope waveforms to  $\theta$ .

The synchronous demodulators must be clocked at the carrier frequency. Since an unmodulated carrier is not explicitly available, the carrier frequency must be reconstructed from information contained in the modulated carriers. This reconstruction is accomplished by phase locking an oscillator to the sum of the squares of the modulated carriers. The oscillator frequency is divided by two to obtain the reconstructed carrier. Note that this reconstructed carrier may be either in phase or  $\pi$  radians out of phase with the original carrier. This half-cycle uncertainty is not resolvable without additional information from the modulating circuitry. A simple method of providing this additional information may be realized by occasionally blanking the carrier for exactly one cycle. The demodulating circuitry detects the blank carrier cycle with a threshold detector and resets the  $\div 2$  circuit, thus ensuring the proper phase relationship between the actual and reconstructed carriers.

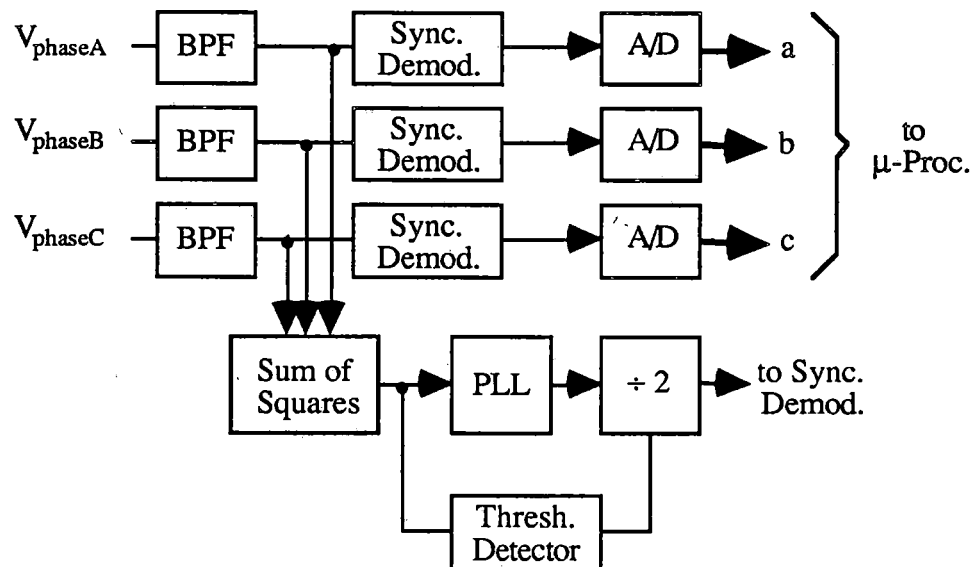


Figure 5.3. Block diagram of demodulator.

This position sensing scheme has been built and tested with a 1/50 scale model LSM propelling a wheeled vehicle with a permanent magnet field. The sensing scheme has been found to be so precise that minor perturbations of the winding can be detected. When used with a winding that has uniform spacing, the vehicle position relative to the magnetic field can be detected with about a  $1^\circ$  tolerance.

### 5.3 Observer based control

#### Velocity Control Loop

The velocity control loop for the system is shown in a block diagram form in Figure 5.4. The structure of this control loop is quite similar to a speed control loop for a dc motor system. The Proportional Integral (i.e. PI) compensator, the observer, and the commutation algorithm are all implemented on a microcontroller. The digital implementation allows sophisticated features such as adaptive control and parameter estimation.

The desired velocity profile  $v_{cmd}$  is a function of position in order to allow speed changes for hills, turns and stations, as well as for weather and traffic conditions.

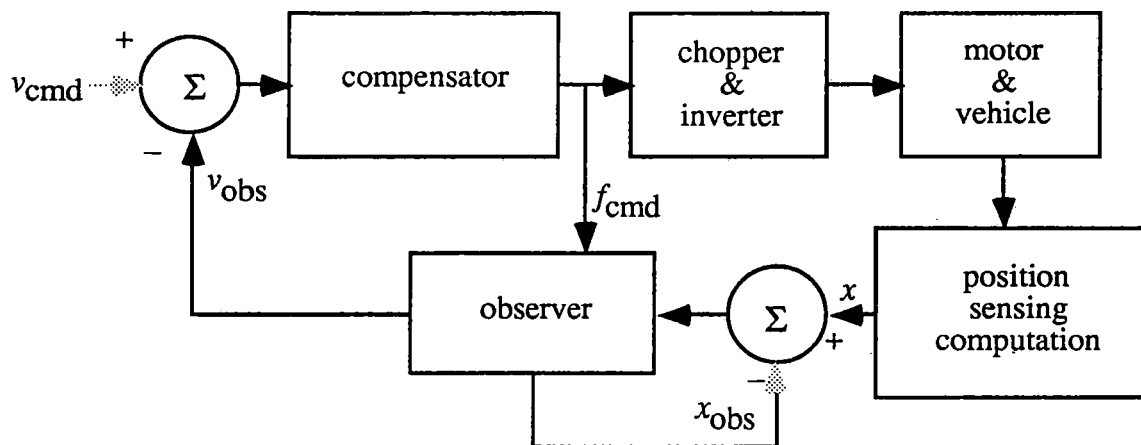


Figure 5.4. Block diagram of velocity control loop.

### Zone Switching

A guideway zone consists of a section of track approximately 4 kilometers in length, a set of power inverters to drive the track windings, and a controller. Control of the vehicle must be passed from one zone controller to the next when the vehicle crosses a zone boundary. With reference to Figure 5.5, this hand-off of control is accomplished in the following manner.

When the vehicle reaches position  $X$ , controller  $A$  notifies controller  $B$  of the approaching vehicle. Controller  $B$  synchronizes its inverter drive signals to controller  $A$  (i.e. controller  $A$  acts as a master, controller  $B$  as a slave). Thus the track windings in zone  $B$  carry current waveforms identical to the corresponding windings in zone  $A$ .

As the vehicle reaches position  $Y$ , controller  $B$  assumes the role of master, with controller  $A$  as its slave.

When the vehicle is entirely within zone  $B$ , at position  $Z$ , controller  $B$  relieves controller  $A$  of its role as a slave. Controller  $A$  shuts down the drive to its track windings.

Additional position sensing hardware may be included at zone boundaries to ensure sufficient knowledge of position information to allow a smooth transition across zone boundaries.

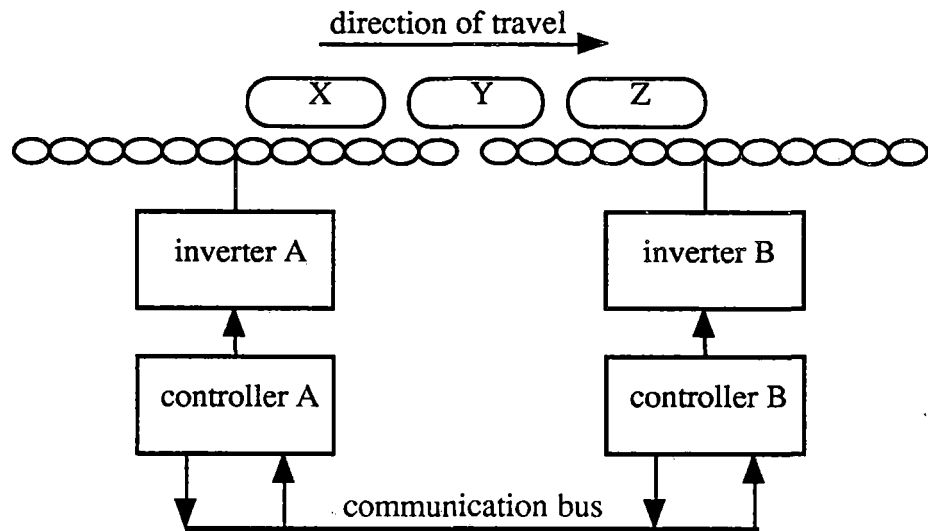


Figure 5.5. Zone switching pictorial.

## References

- 1 Sepe, R., *Adaptive Control of a Permanent Magnet Synchronous Motors*, MIT Ph.D Thesis, September, 1990.
- 1 Luenberger, D.G., *Introduction to Dynamic Systems*, John Wiley & Sons, Inc., 1979.

## **6 Far Fields and Shielding**

*The vehicle magnets for an LSM will create magnetic fields that extend significant distances from the vehicle. These remote fields can create a number of problems, particularly for designs with large magnetic gaps and no ferromagnetic path for the flux to follow. This section develops approximate models that provide a good understanding of how the design can be adapted to minimize the impact of the far field and to provide shielding.*

### **6.1 Far field analysis**

The far field can be calculated by methods discussed previously, but there are simpler methods that are more appropriate for conceptual design studies involving far field effects and their mitigation.

#### **A Bessel Function approximation**

A good approach is to model the vehicle magnets as an array of small magnetic dipoles which can then be approximated with a Fourier series. This model, shown in Figure 6.1, is equivalent to representing the field of the vehicle coils as an array of coils which have negligible extent in the  $y$  direction but have the correct dipole moment. Since the dipole moment dominates the far field behavior, this model can give good results. The trick is to use a Fourier series representation because the higher harmonics have very little effect on the far field.

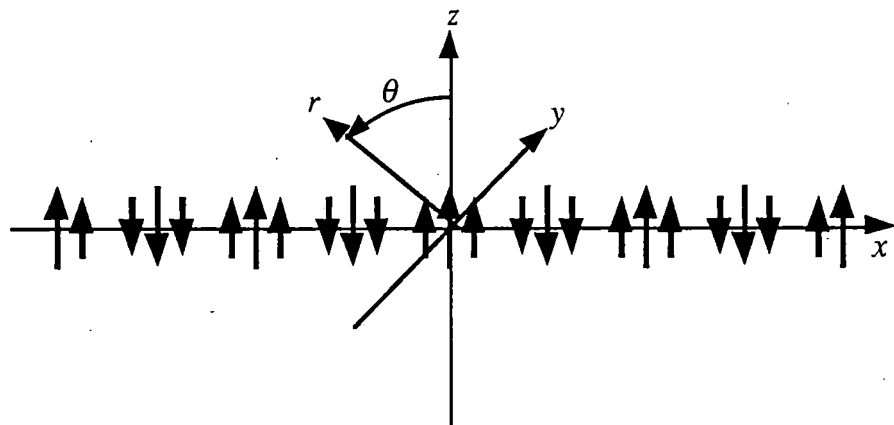


**Figure 6.1.** Dipole array model for far field calculation.

The assumed problem is to calculate  $|\mathbf{B}|$  in the  $y = 0$  plane. The same methodology can be used to calculate the field in all of space, but that more complex problem is not considered here. The fields are calculated in the cylindrical coordinate system  $x$ ,  $r$ , and  $\theta$ .

as shown in Figure 6.1. Note that  $x$  is used instead of  $z$  as the linear axis in order to avoid confusion with  $z$  in the rectangular coordinate system used previously.

For large  $r$  the fields can be approximated with the Bessel Function approximation given in Equation 6.1. In this equation the coefficient  $k_\phi$  is calculated to match the computed field for a very long array.

If  $r > p / \pi$  then:

$$\phi = \frac{\mu_0}{4\pi} k_\phi \sum_{n=1,3,\dots} m_n \left( \frac{n\pi}{p} \right)^2 \sqrt{\frac{p}{n\pi r}} e^{-n\pi r/p} \left( 1 + \frac{a_1 p}{n\pi r} + \dots \right) \cos(n\pi x / p) \cos(\theta) \quad (6.1)$$

$m_n$  is the  $n^{\text{th}}$  harmonic of the Fourier representation of the dipoles,

$$k_\phi = 1.017.$$

Equation 6.1 can be simplified by neglecting all Fourier harmonics except the first, because the higher harmonic fields attenuate very rapidly. A less accurate, but adequate approximation is to neglect all but the leading term in the polynomial in  $1/r$ . To calculate  $|\mathbf{B}|$  use classical field theory on the simplified form of Equation 6.1, with the result shown in Equation 6.2.

for  $y = 0$  replace  $z$  by  $r$  and  $\cos\theta$  by 1, then:

$$\begin{aligned} B_z &= -\frac{\partial \phi}{\partial r} \approx \frac{\mu_0 m_1}{4\pi} k_\phi \left( \frac{\pi}{p} \right)^2 \left( \frac{1}{2z} + \frac{\pi}{p} \right) \sqrt{\frac{p}{\pi z}} e^{-\pi z/p} \cos(\pi x / p), \\ B_x &= -\frac{\partial \phi}{\partial x} \approx \frac{\mu_0 m_1}{4\pi} k_\phi \left( \frac{\pi}{p} \right)^3 \sqrt{\frac{p}{\pi z}} e^{-\pi z/p} \sin(\pi x / p), \\ B_y &= -\frac{1}{z} \frac{\partial \phi}{\partial \theta} = 0. \end{aligned} \quad (6.2)$$

For  $r \gg p / 2\pi$ :

$$|\mathbf{B}| \approx \frac{\mu_0 m_1}{4\pi} k_\phi \left( \frac{\pi}{p} \right)^3 \sqrt{\frac{p}{\pi z}} e^{-\pi z/p}.$$

Equation 6.2 predicts that the far field attenuates as  $e^{-\pi z/p} / \sqrt{z}$ . This exponential dependence on  $z$  is much faster than is possible with simple multipoles and makes the field strength surprisingly small at distances only  $2p$  from the field magnets. The field also attenuates exponentially in the  $y$  direction, and for a given  $r$  the field is usually less for  $y \neq 0$  than it is for  $y = 0$ .

### Example of far field calculation

In order to apply this method to the example in Section 2, we first perform a Fourier analysis of the field array. The coil length and width were 80% of  $p$ , so the harmonic components are:

$$m_n = 4 \int_0^{0.4p} 0.8pI_f \cos(n\pi x / p) dx = \frac{3.2p^2 I_f}{n\pi} \sin(0.4n\pi)$$

$$m_1 = 0.9687, m_3 = -0.1996, m_5 = 0, \dots$$
(6.3)

Figure 6.3 shows a comparison of the Bessel approximation with the calculated field for the example of Figure 2.6. The array for the example had 8 coils, with parameters in Table 2.1. The  $x = 0$  position is in the middle of the array where there is only an  $x$  directed field, and the position  $x = 0.5$  is where there is only a  $z$  directed field. If the magnet array had infinite length then the field at both of these locations would have the same far field magnitude, but for  $z$  greater than 2 they diverge because of the finite length of the vehicle array.

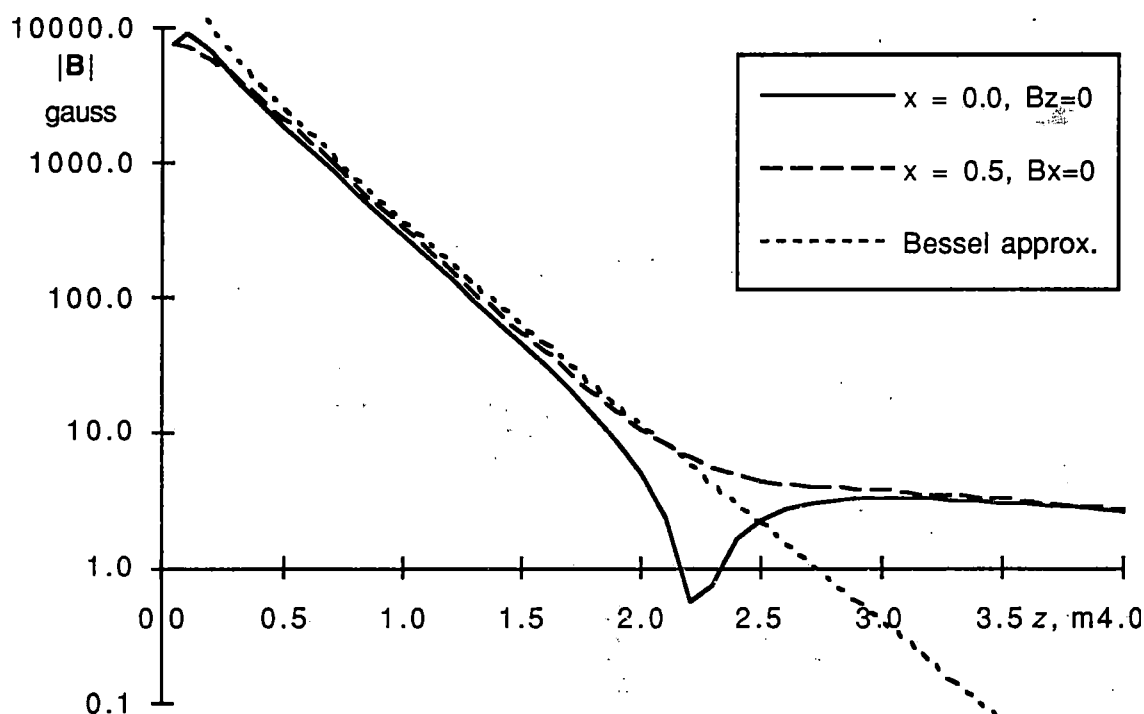
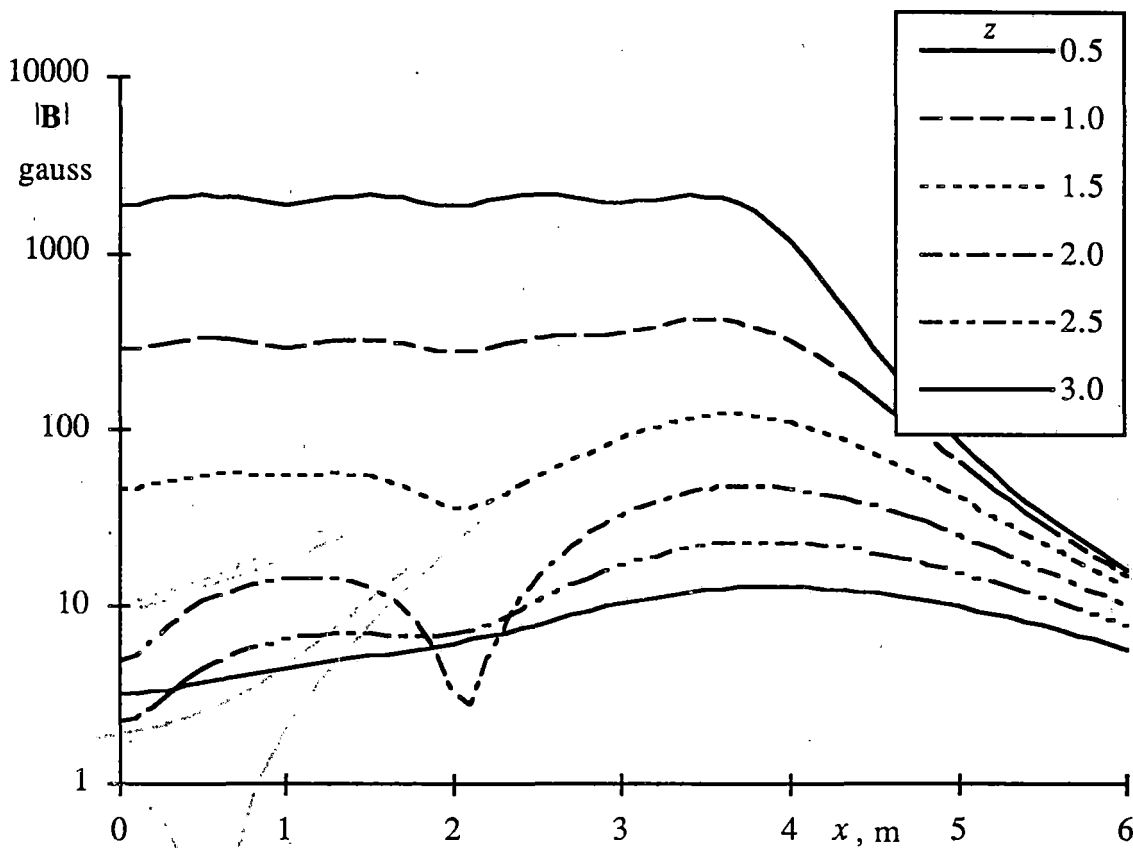


Figure 6.2. Comparison of fields for example of Figure 2.7 with approximations.

For distances up to  $2.2p$  the Bessel approximation is good enough for shielding calculations. At larger distances the fact that there were only eight coils in the example causes the field to have nulls and plateaus, and to be larger than the approximation. Although  $|B|$  has a complex spatial dependence, it depends primarily on the distance from the line of dipoles.

## 6.2 End effects

The field predicted by Equations 6.1 and 6.3 falls off very fast and it encourages one to believe that the undesirable effects of this field can be minimized by making  $p$  as small as possible and using a spacing of at least  $2.2p$  between the magnets and people. Unfortunately, this simple approach neglects the very important end effect. Even if magnets run the full length of the vehicle, at some point they end and the field for a given  $z$  can be an order of magnitude larger at the end of the dipole array. This effect is indicated by the plot of Figure 6.3.



**Figure 6.3.** Far fields near end of array for same example as Figure 6.2  
 $x = 0$  is location of middle of 8 coil array with a pole pitch of 1 meter.

Figure 6.3 shows the field as a function of  $x$  for different  $z$  for the same example as Figure 6.2. The field has a surprisingly complex set of peaks and valleys, but the important conclusion is simple and shown graphically in Figure 6.4. This Figure is a plot of the field as a function of  $z$  for different  $x$ . It shows that for  $z > 2p$  the field at  $x = 3.5$  is 4 to 5 times larger than at  $x = 0.5$ . The field at  $x = 3.5$  can be predicted quite accurately using a magnetic dipole model. We observe that the field of a magnetic dipole, described

by vector  $\mathbf{m}$ , is as given in Equation 6.4. This field falls off as  $1/z^3$ , or much more slowly than that of an array of dipoles. To find the field above the last dipole in a long array we observe that half of the dipole field is almost canceled by the field of the array to one side, but there is no array on the other side to cancel the remaining dipole field. Thus the actual field is almost exactly that of a half strength dipole. To find the approximate field for  $x = 3.5$  in Figure 6.4, compute the field above a current loop carrying 250,000 ampere turns and having an area of  $0.8^2$  square meters, or  $|m| = 160,000 \text{ A}\cdot\text{m}^2$ . The field from this dipole is shown in Figure 6.4 and it is clear that it accurately describes the far field for large  $z$ , at least until the fact that the array is of finite length causes the field to fall off much more slowly.

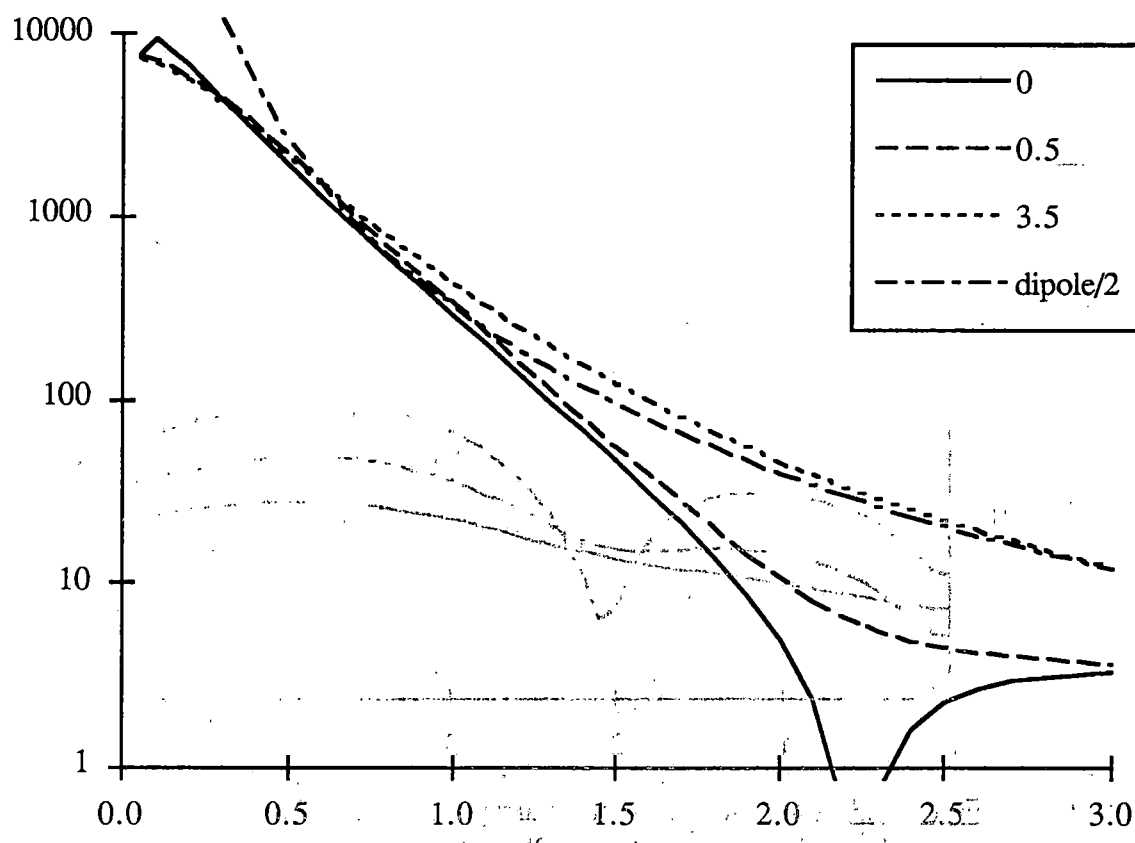


Figure 6.4. Far field for dipole array of Figure 6.1.

$$\mathbf{B} = \frac{\mu_0}{4\pi} \nabla \left( \mathbf{m} \cdot \nabla \frac{1}{r} \right)$$

$$B_r = \frac{\mu_0}{4\pi} \frac{2|\mathbf{m}| \cos \theta}{r^3}$$

$$B_\theta = \frac{\mu_0}{4\pi} \frac{|\mathbf{m}| \sin \theta}{r^3}$$
(6.4)

### 6.3 Mitigation techniques

There are two solutions to reducing the impact of the field produced by the vehicle magnets: remove sensitive equipment and people from this region, or reduce the effect.

This section considers the various possibilities for reducing the impact so that moderately close spacing of people and magnets is possible.

#### Reduce the pole pitch

One of the easiest ways to reduce the far field is to reduce the pole pitch so that the field falls off more rapidly. This has the disadvantages of requiring higher frequencies for propulsion, increasing eddy current loss in the propulsion winding, and requiring either more ampere turns in the magnets or a closer spacing between vehicle coils and guideway windings. Although there is no way to determine an optimum pole pitch without considering many system attributes, various maglev designers have converged on a pole pitch in the range 0.5 to 2.0 meters. It appears that a good strategy is to pick a pole pitch that is about 5 times the vehicle coil-to-guideway winding spacing, and to keep this spacing as small as possible.

#### Taper the fields for the end magnets

If a long array of magnets is used the field may be sufficiently low except in the regions near the end magnets. We can reduce the end effect by tapering the field strength of the end magnets. Figure 6.5 shows the field for the same example used in Figure 6.4 except that the 2 end coils have 250,000 ampere turns while the middle 6 coils have 500,000 ampere turns. This tapering decreases the maximum field by about a factor of 3 with only a 12.5% reduction in motor thrust. More gradual tapering of field strength near the end of the magnet array can be used to achieve an almost perfect cancellation of the excess field, but this will lead to substantially less propulsive force for the motor.

#### Use longer arrays

In the example used to illustrate the far field, there were only 8 vehicle magnets with the result that for  $z > 2p$  the field did not follow the Bessel approximation. If the array

had been longer, the field would continue to drop for larger  $z$ , so it is clear that a larger number of coils is desirable from the point of view of reducing the far field. An additional advantage of long arrays is the fact that tapering the strength of the end magnets does not produce as large a percentage reduction in motor thrust.

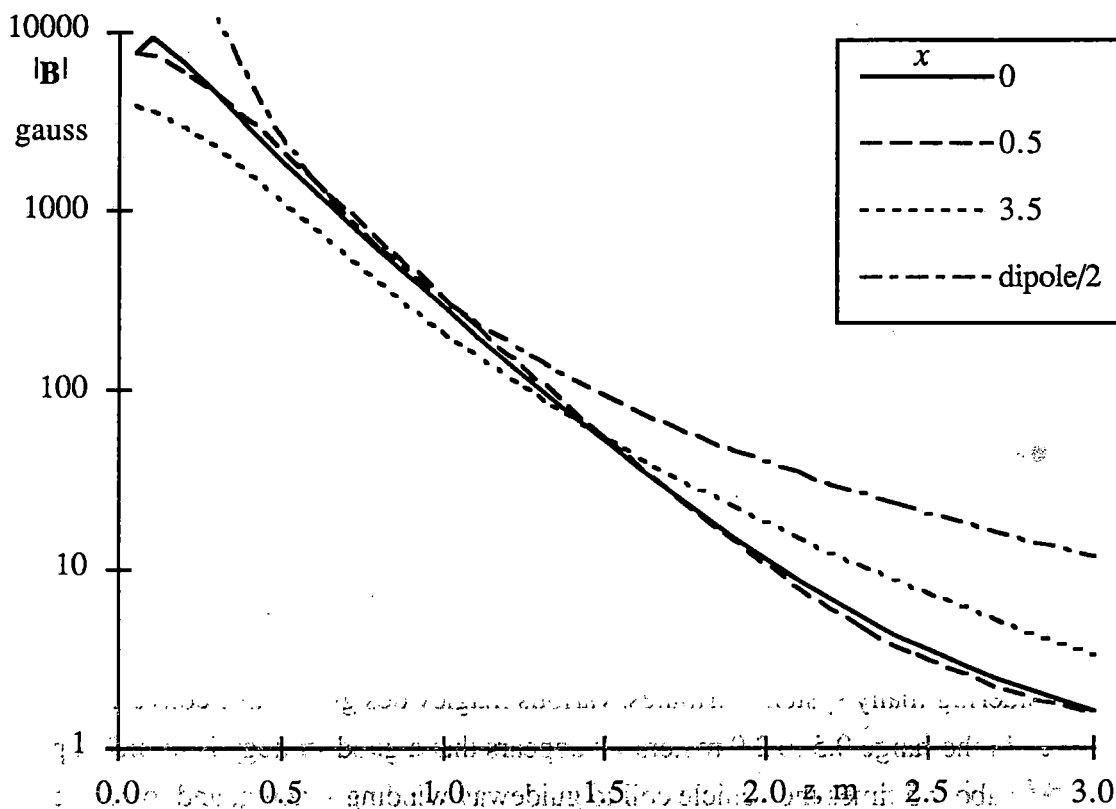


Figure 6.5. Same field as Figure 6.4 except the end magnets have 50% of the ampere turns of the other magnets.

### Use flux canceling designs

If there are port and starboard field magnets, then there is a possibility of achieving some reduction in far field by proper phasing of the two sets of magnets. This method is only effective if the two rows of vehicle coils are within about  $2p$  of each other, but it can lead to a factor of 2 reduction in the peak field strength in the passenger cabin.

A much larger improvement is possible if each row of field coils is replaced by two closely spaced and oppositely phased coils. This configuration is, in effect, a replacement of magnetic dipoles by quadrupoles. It will not change the form of the Bessel Function approximation, but it will reduce the amplitude of the coefficients. This design will probably lead to heavier and more expensive vehicle magnets, but it may be preferable to alternative field reducing techniques.

### Use active shielding

If it is necessary to reduce the passenger cabin field to flux levels less than about 5 to 10 gauss, then it may be necessary to use active coils under the floor of the vehicle. These coils can be located and excited in such a way as to cancel most of the field. In some of the System Design Concept Studies this active shielding was shown to be capable of providing at least an order of magnitude field reduction. The trick is to place these coils as far from the vehicle coils as possible so that the field created by the active coils can be as small as possible; locating the coils directly under the floor is a good idea.

If the flux to be shielded is no more than 5 or 10 gauss, then active shielding requires only modest increases in vehicle mass and power requirements. This method tends to be much more unwieldy if it is required to cancel fields of 50 to 100 gauss. Thus active field cancellation should only be included after implementing other field reduction techniques..

### References

#### Books

- 1 Grover, F. W., *Inductance Calculations*, Dover Publications, Inc., New York, 1946.
- 2 Stratton, Julius, *Electromagnetic Theory*, McGraw Hill Book Co. Inc., New York, 1941.

**PROPERTY OF FRA  
RESEARCH & DEVELOPMENT  
LIBRARY**

Linear Synchronous  
Motors for MAGLEV,  
FRA, NMI, Richard D Thornton,  
Systems

Linear Synchronous Motors for MAGLEV, US DOT,  
FRA, NMI, Richard D Thornton, 1993-11-Advanced  
Systems

142  
SNEAD CO 192356 1993-11-Advanced Systems